mtwardowski@fau.edu
http://www.fau.edu/hboi/ocean_optics

Light Scattering in Water

Mike Twardowski

Harbor Branch Oceanographic Institute

Ft. Pierce, FL

Brief Background…

PhD	Oceanography, Biophysics – University of Rhode Island (Percy Donaghay)	1998
Postdoc	Environmental Optics Fellowship – Oregon State University (Ron Zaneveld)	1998-2000

CURRENT POSITIONS

Director, Center for Marine Applied Technology and Engineering (C-MATE)	2021-present
Professor, *Harbor Branch Oceanographic Institute, FAU*	2015-present
Affiliate Professor, *Ocean Engineering, FAU*	2017-present
President, *Sunstone Scientific LLC*	2017-present
Senior Engineer, *SEACORP Inc.*	2015-present

FORMER POSITION

Director of Research and Vice President, *WET Labs, Inc.*	2000-2015

- Ocean optics research: basic and applied
- Sensor development: fundamental optics, imaging systems
- Modeling: radiative transfer theory, imaging and visibility
- NASA PACE Science Team
- Bioluminescence

“Lex Groovius”

BIOSOPE, led by Villefranche (2004)

Radiative Transfer in the Ocean

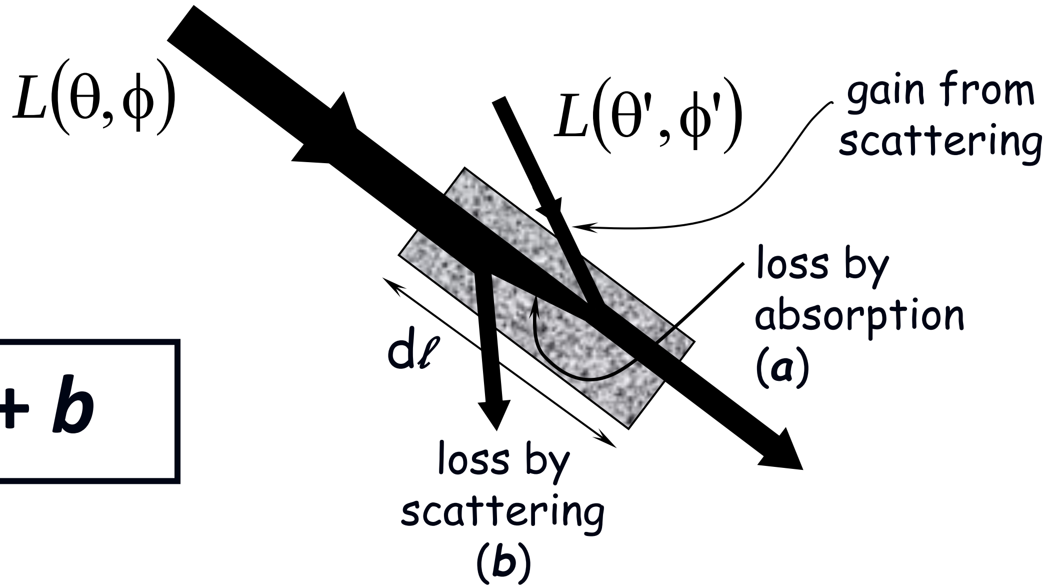

$$\boxed{c \equiv a + b}$$

Inherent Optical Properties (IOPs)
Depend only on substances in water
[Attenuation (c), Absorption (a), Scattering (b), and related subfractions]

Apparent Optical Properties (AOPs)
Depend on substances in water AND *ambient light field*
[Reflectance (R), Diffuse attenuation (K), and related parameters]

Volume Scattering Function (VSF) defined

$$\beta(\theta) = \frac{dI(\theta)}{EdV} = \frac{W \cdot sr^{-1}}{W \cdot m^{-2} \cdot m^3} = m^{-1} \cdot sr^{-1}$$

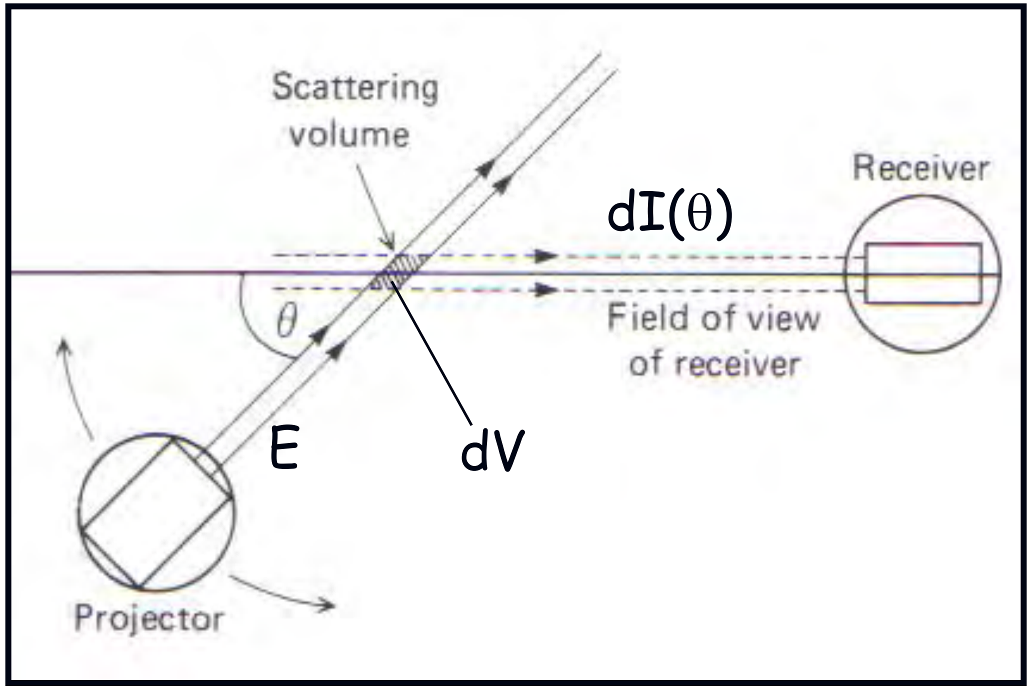

$dI(\theta)$ radiant flux in direction $d\theta$ ($W\ sr^{-1}$)

dV elemental volume (m^3)

E incident irradiance ($W\ m^{-2}$)

Typical VSF

*Log Scale ~10^7 Dynamic range

*Very steeply forward peaked

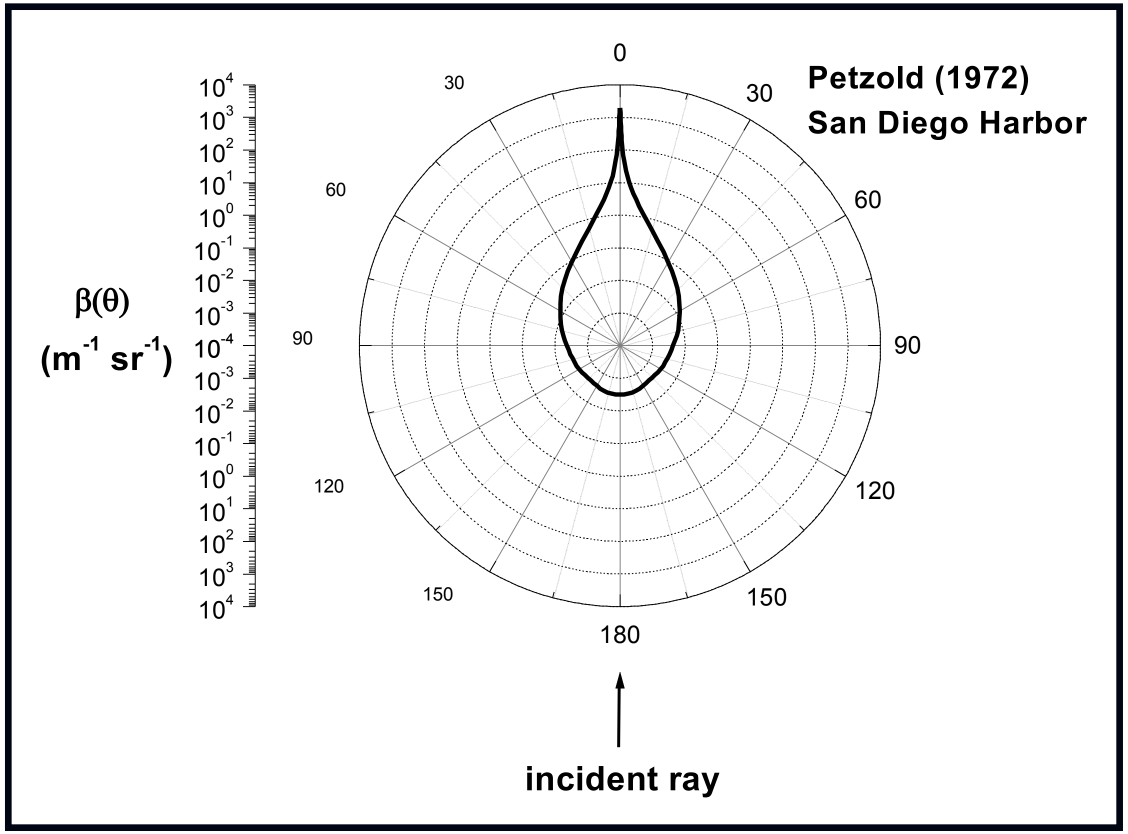

Scripps Pier, 2008

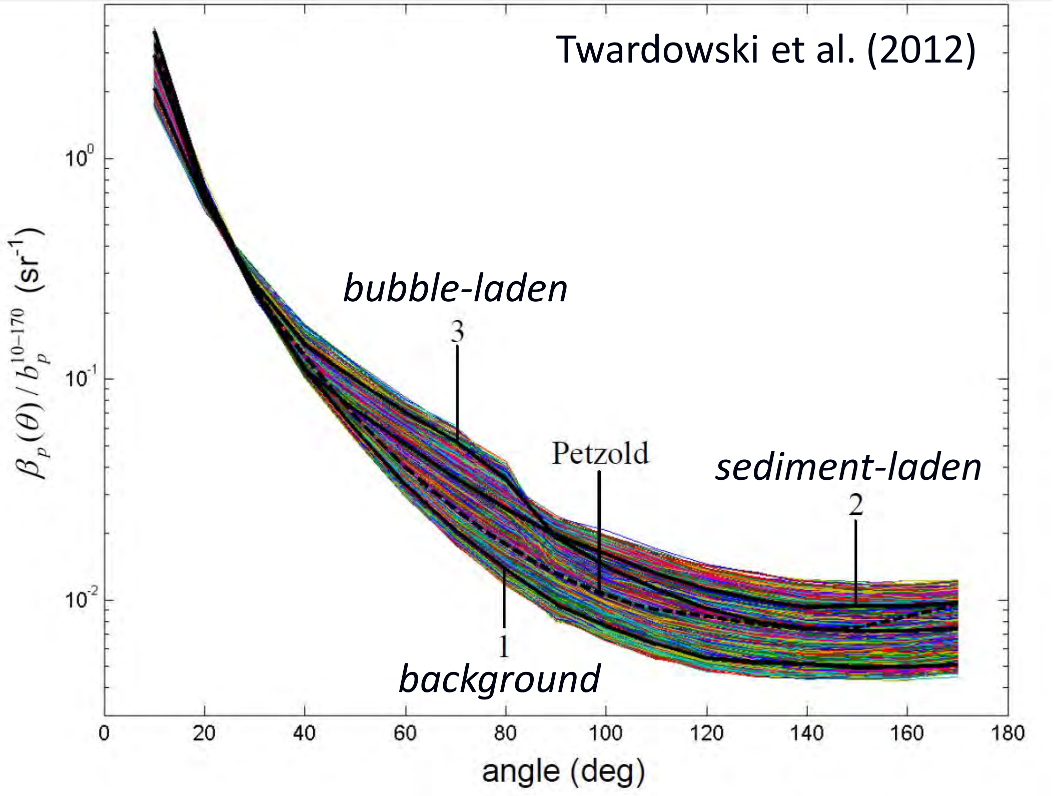

Typically, only ~0.3-3% of scattering (b) is backscattering (b_b)
(however, in clear waters, b_w can increase this %)

VSF integration to obtain *b*

$$b = 2\pi \int_0^{\pi} \sin(\theta)\beta(\theta)d\theta$$

Assuming azimuthal symmetry

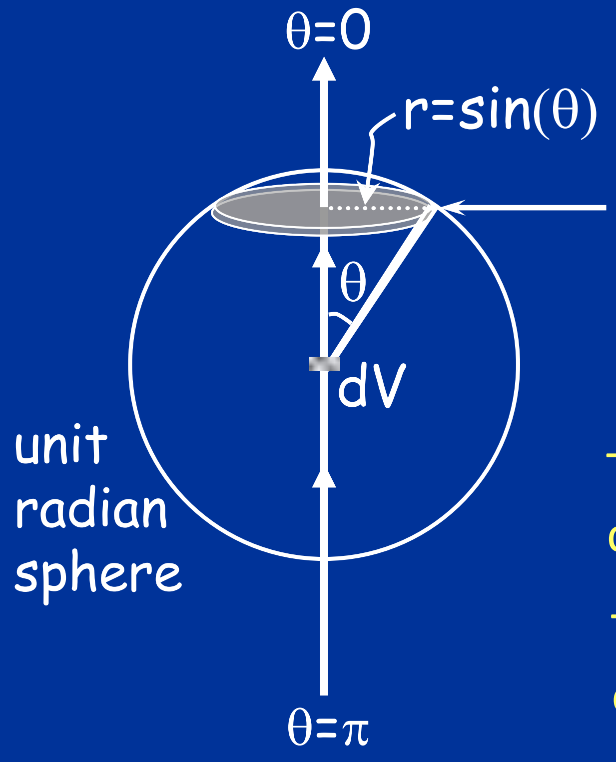

perimeter = $2\pi r$

solid angle, $d\omega = 2\pi r\, d\theta = \underline{2\pi \sin(\theta) d\theta}$ (sr)

The $2\pi\sin(\theta)$ effectively "weights" contribution of β to b

The contribution of β to b is zero at $\theta=0$ and $\theta=\pi$, even though β is nonzero

Scattering components

Can partition with respect to constituent components…, e.g.:

$$b_t(\lambda) = b_w(\lambda) + b_p(\lambda)$$ units m^{-1}, possible to further partition b_p …

Also with respect to angular distribution:

$$b_x = 2\pi \int_i^j \sin(\theta)\beta(\theta)d\theta$$

<u>Total scattering</u>
set $x = t$
$[i, j] = [0, \pi]$

<u>Forward scattering</u>
set $x = f$
$[i, j] = [0, \pi/2]$

<u>Backscattering</u>
set $x = b$
$[i, j] = [\pi/2, \pi]$

Primary scattering components in water

- Pure seawater (molecular)
- Turbulence (i.e., refractive index discontinuities)
- Particles… may be partitioned for different types
- Bubbles

Other scattering properties from VSF

Phase function:

$$\tilde{\beta}(\theta) = \frac{\beta(\theta)}{b}$$

units (sr^{-1})

Backscattering ratio:

$$\widetilde{b_b} = \frac{b_b}{b}$$

unitless

Asymmetry parameter (mean cosine):

$$g = \langle \cos(\theta) \rangle = 2\pi \int_0^{\pi} \tilde{\beta}(\theta)\cos(\theta)\sin(\theta)d\theta$$

If symmetric around 90°, g = 0

If highly skewed g → 1

unitless

VSF Measurement Considerations

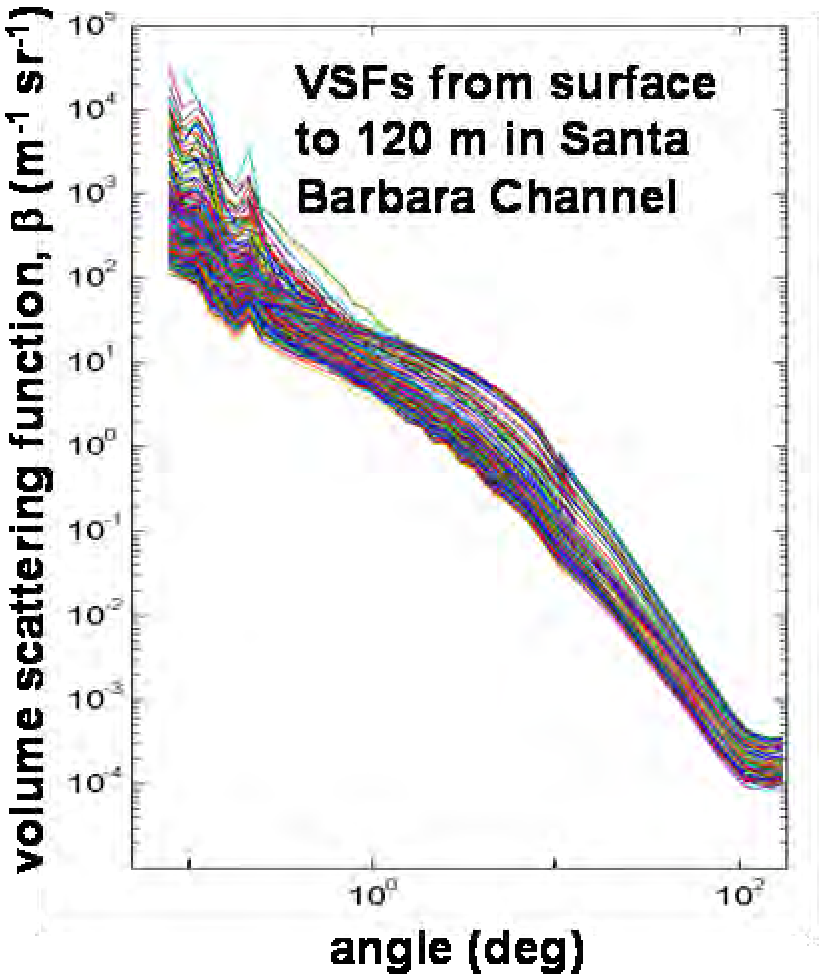

- 6+ orders of magnitude variation in intensity from the near-forward to backward in single VSF
- several orders of magnitude natural dynamic range in intensity at any single angle
- rapid temporal variability in particle fields in surface waters
- rejecting ambient light is challenging at surface, particularly for low scattering signals in the backward
- calibration without absolute "standard"
- Errors can grow at higher turbidities and pathlengths

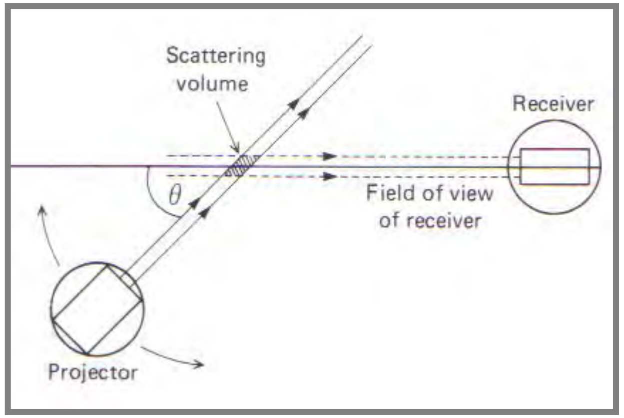

Measuring the VSF: MASCOT (HBOI-FAU)

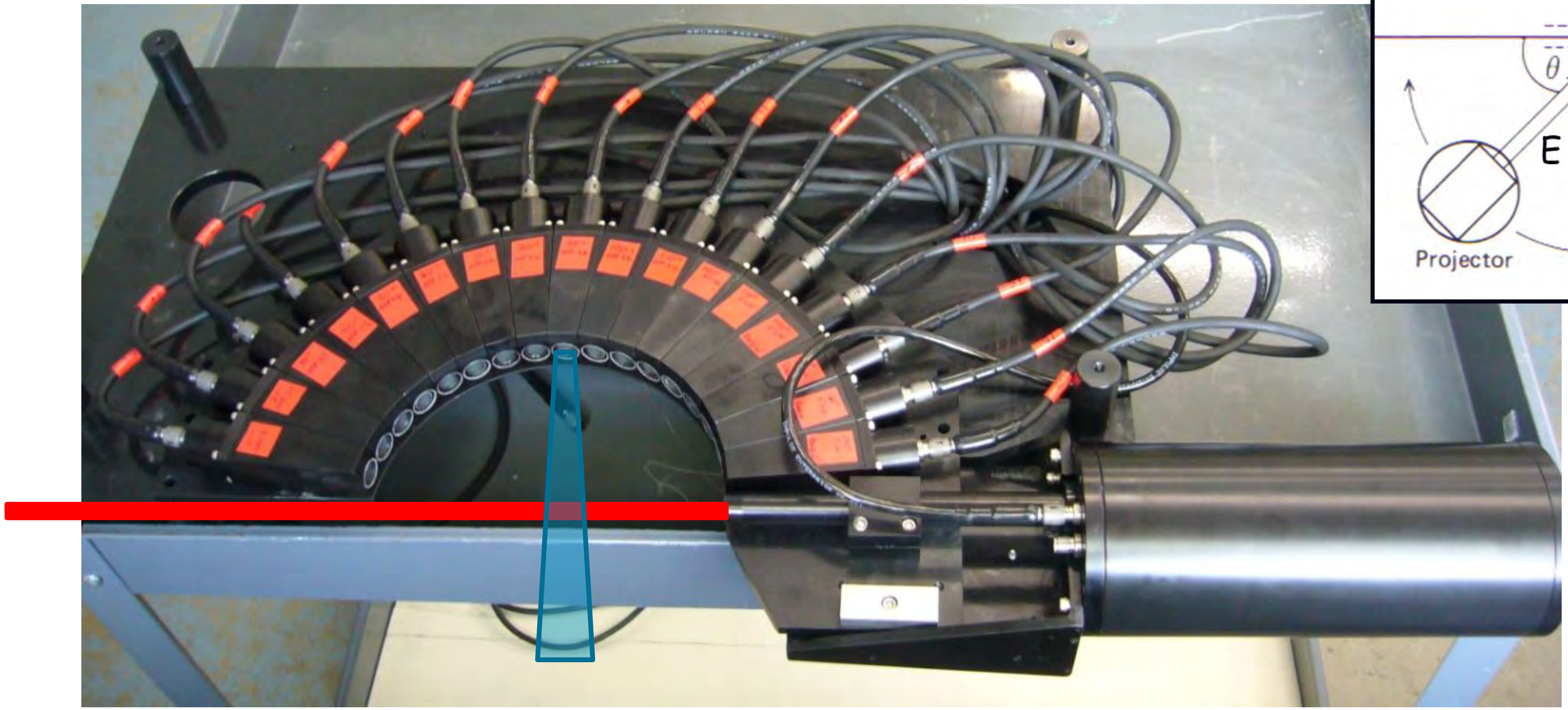

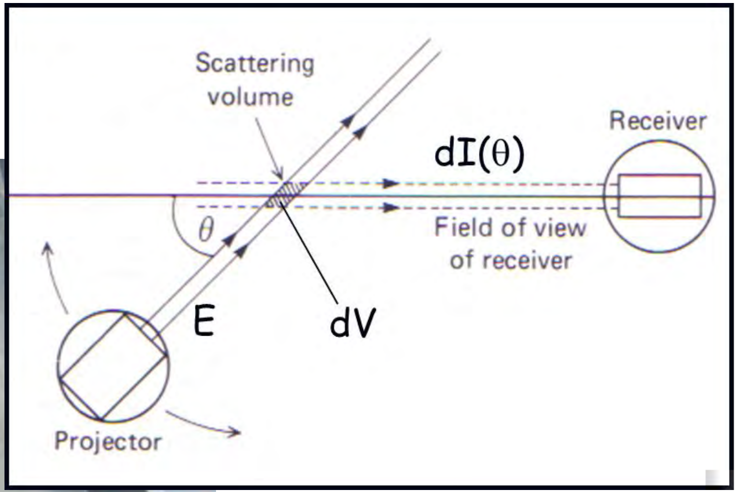

- Measures VSF from 10°(10°)170°
- 0.8-5° detector FOVs
- 20 Hz sampling rate
- Wedge depolarizer on source

LISST-100X (Sequoia Scientific)

near-forward scattering (diffractometry)

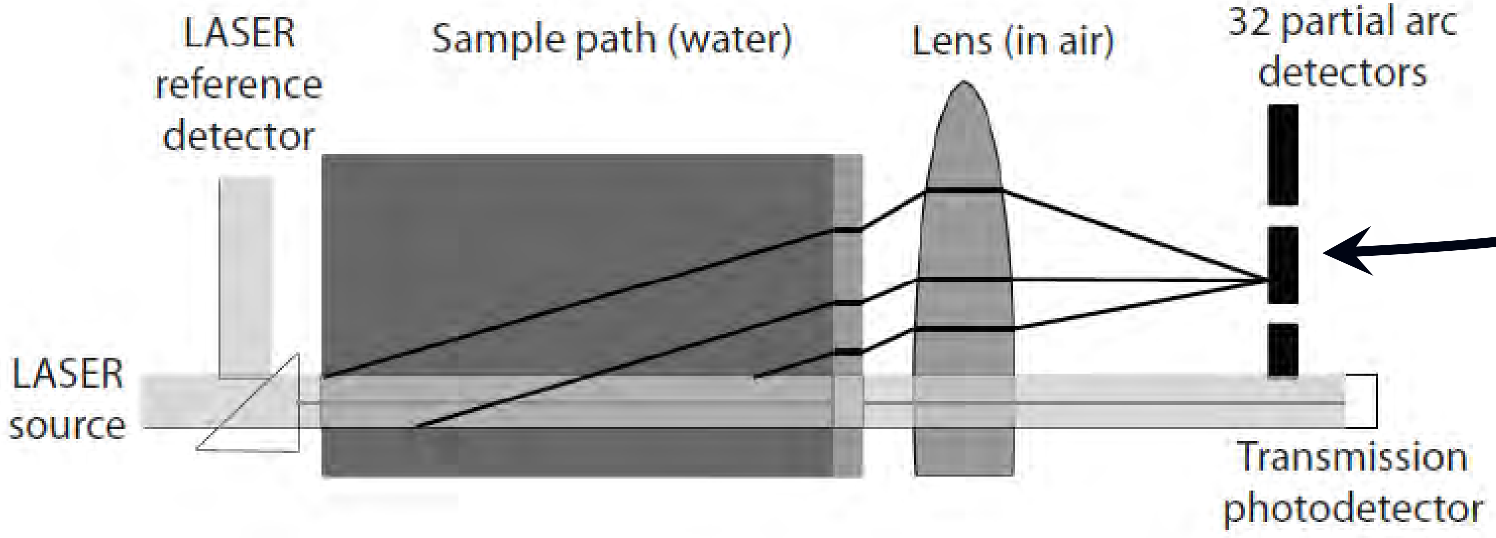

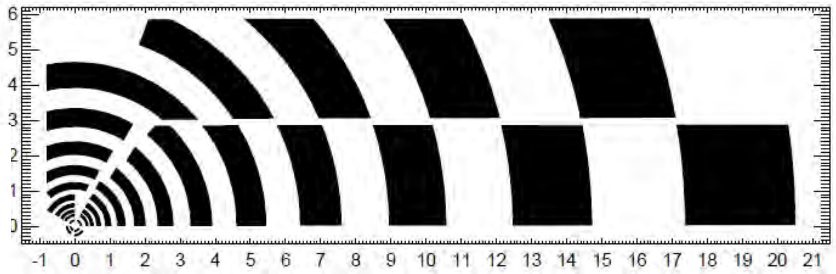

LISST-VSF (Sequoia Scientific)

Full volume scattering function (and linear pol)

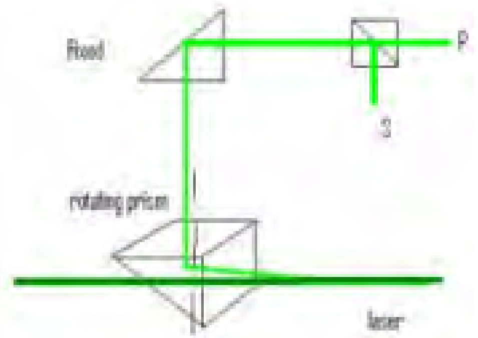

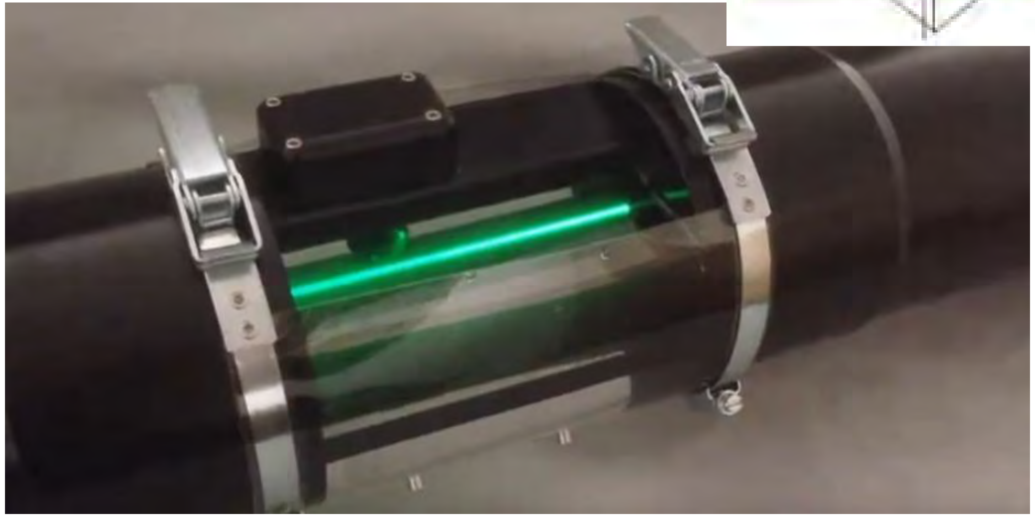

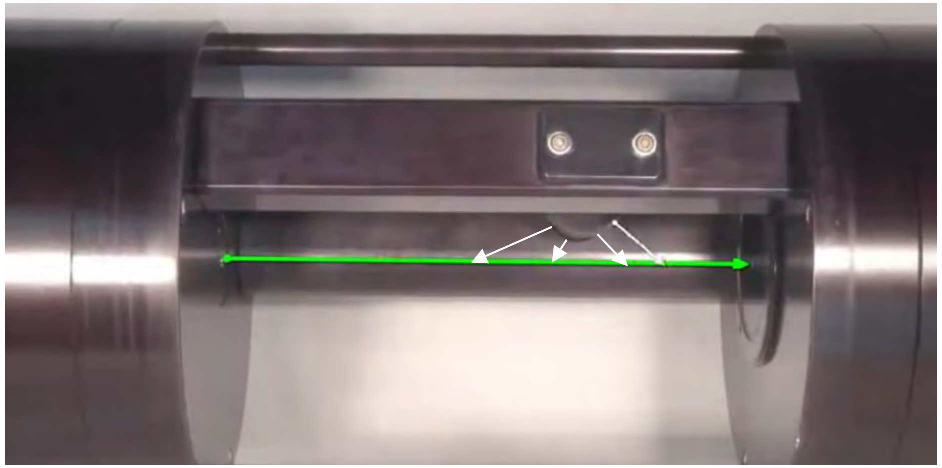

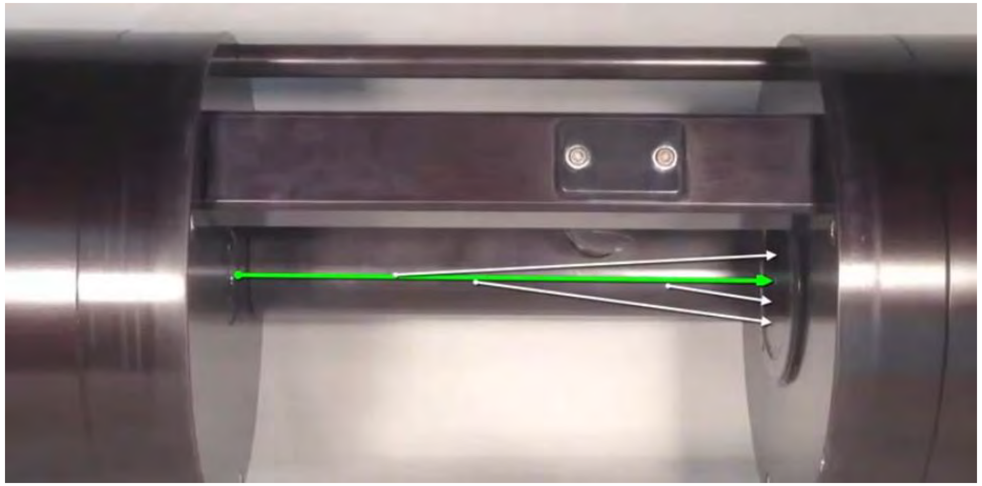

https://www.youtube.com/watch?v=E4wt5lLhUK8

Hyper-bb (Sequoia Scientific)

Hyperspectral $\beta(135°)$ from 430 to 700 nm

I-VSF
Helmholtz-Zentrum Geesthacht (HZG)

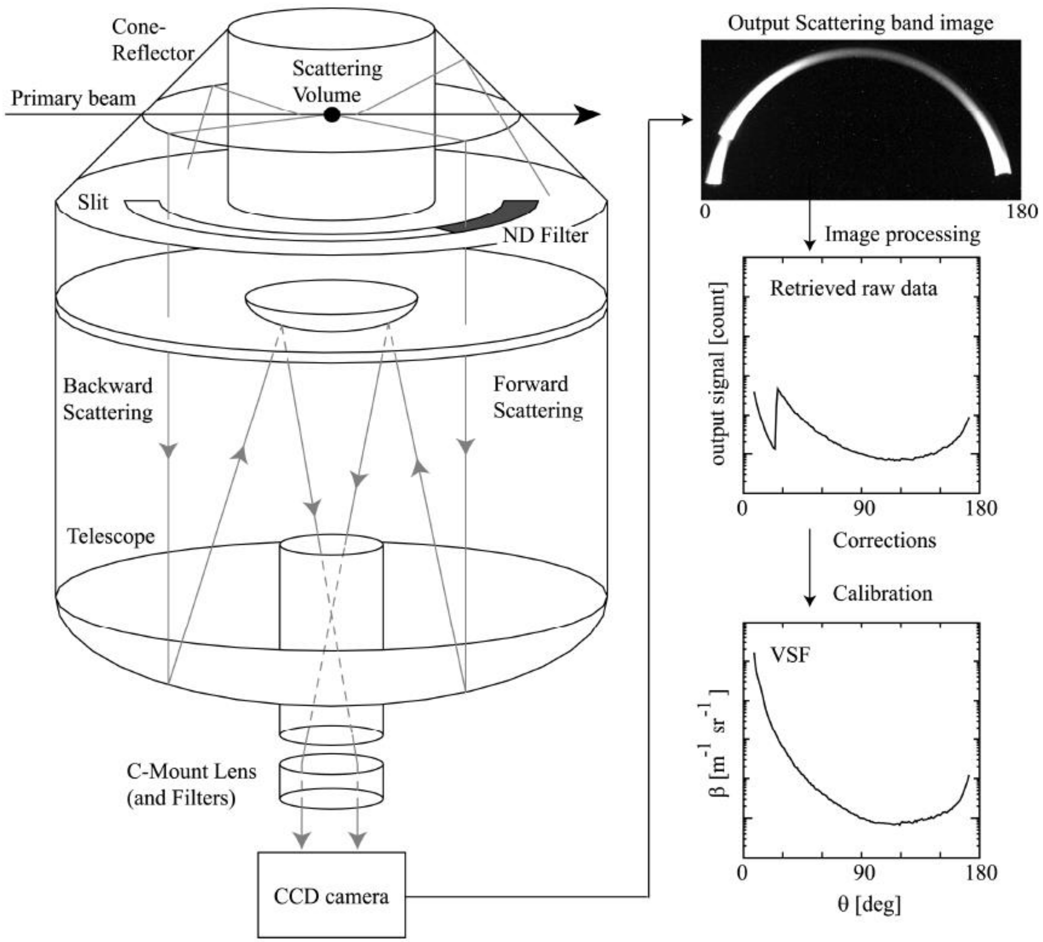

Tan et al. (2013)

Measuring the VSF: MVSM

(Marine Hydrophysical Institute, Academy of Sciences of the Ukraine)

See Zhang and Gray et al. pubs

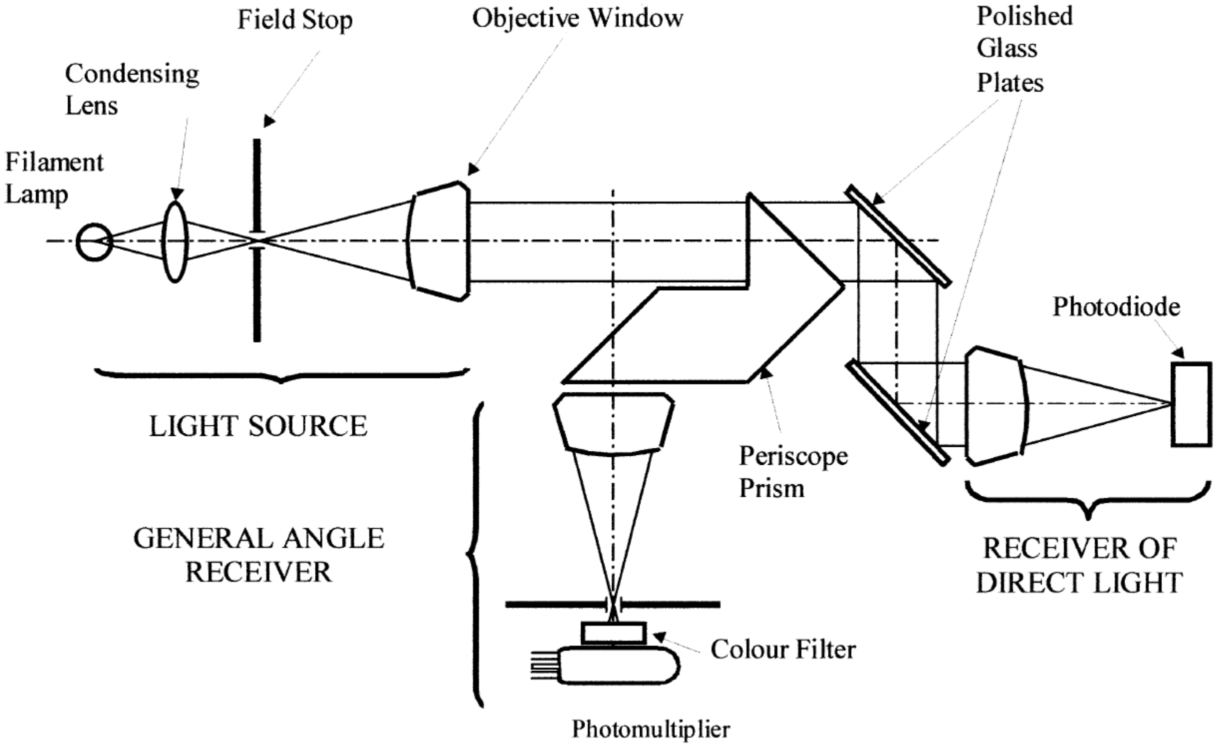

Lee and Lewis (2003)

POLVSM (LOV)

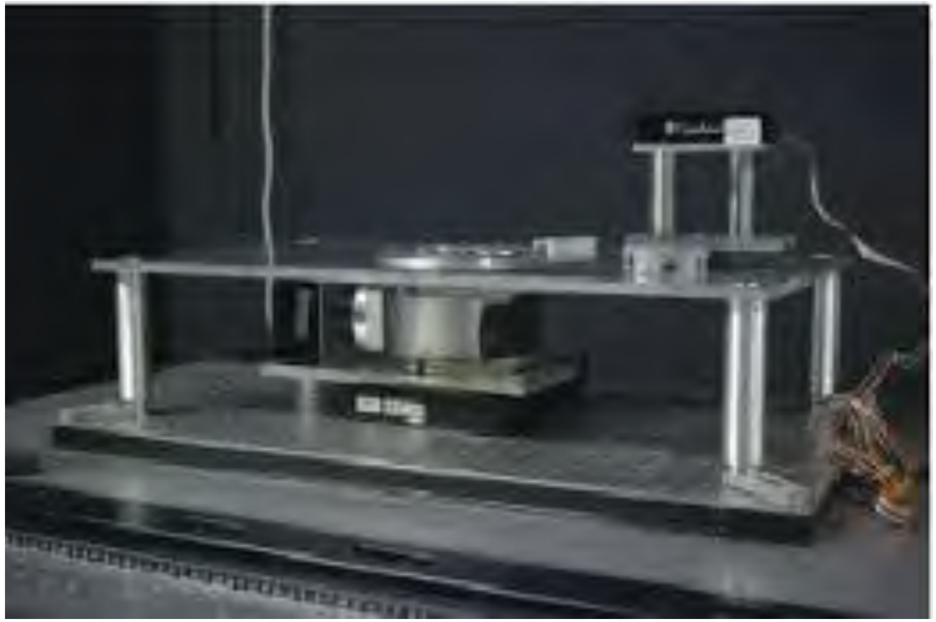

Chami et al. (2014)
Harmel et al. (2015)

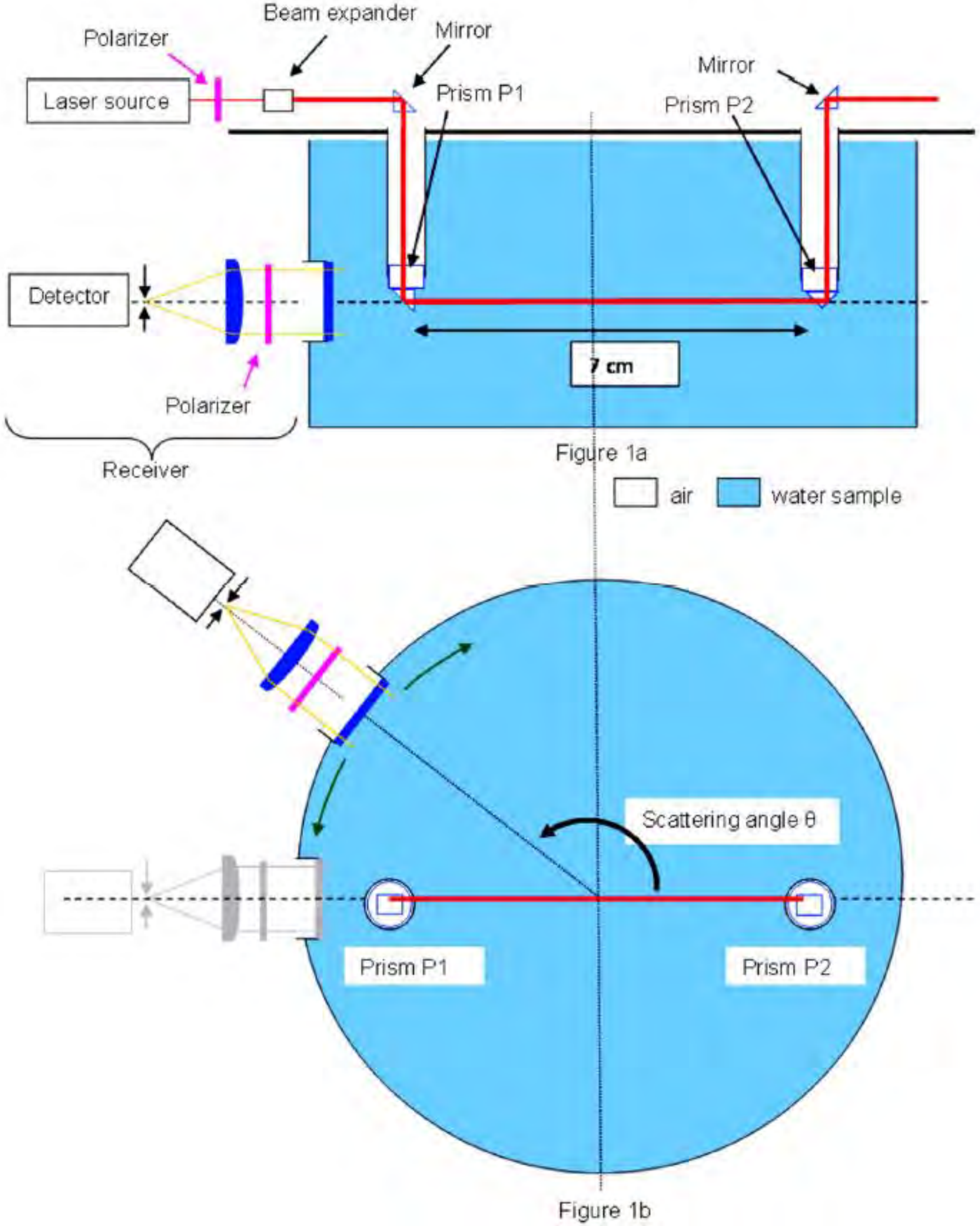

BI-200 Goniometer (Brookhaven)

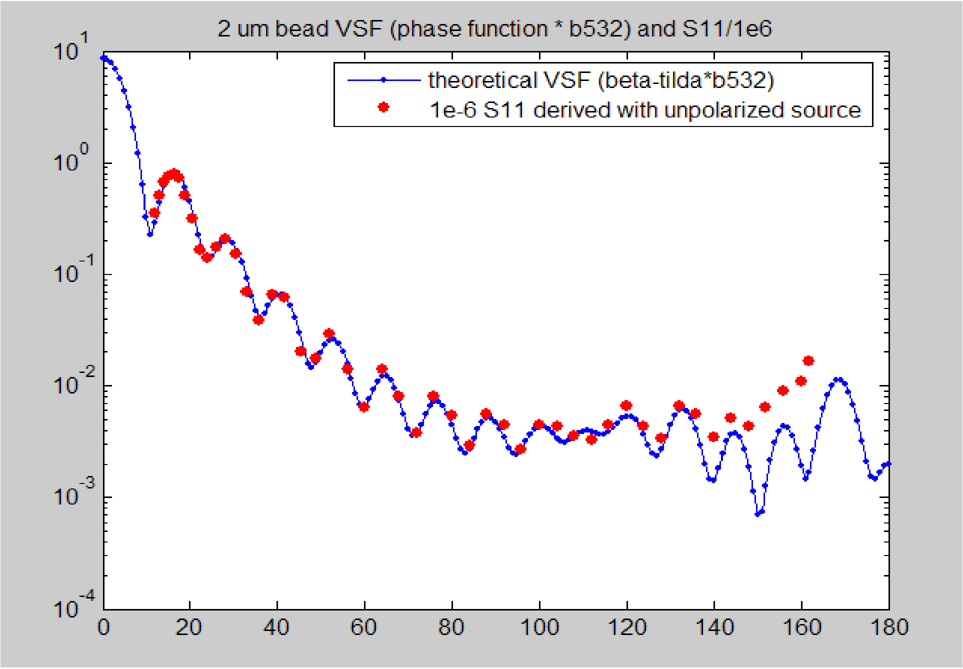

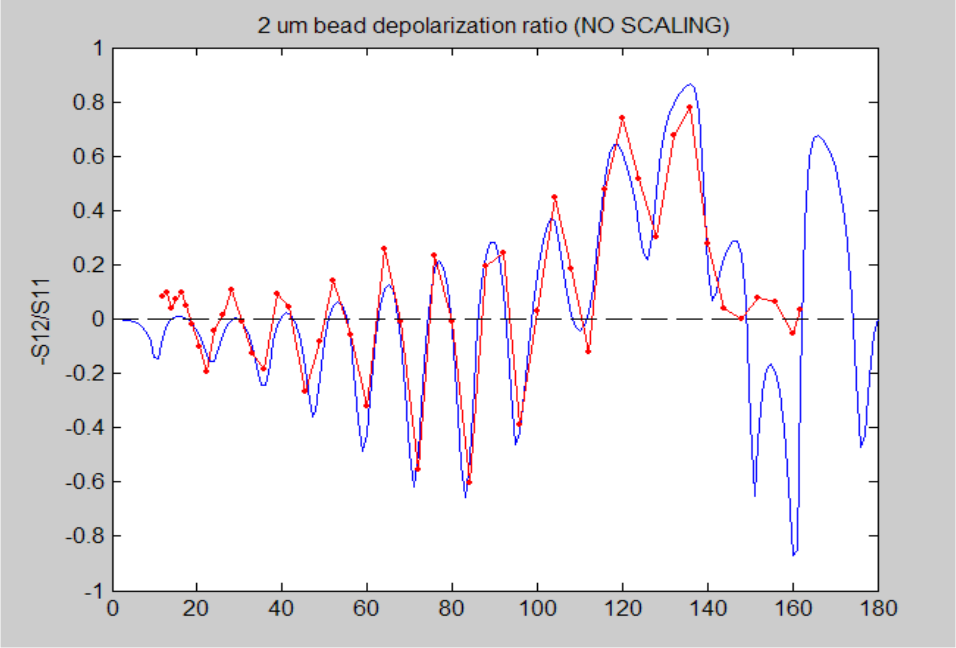

WET Labs (SeaBird) ECOs

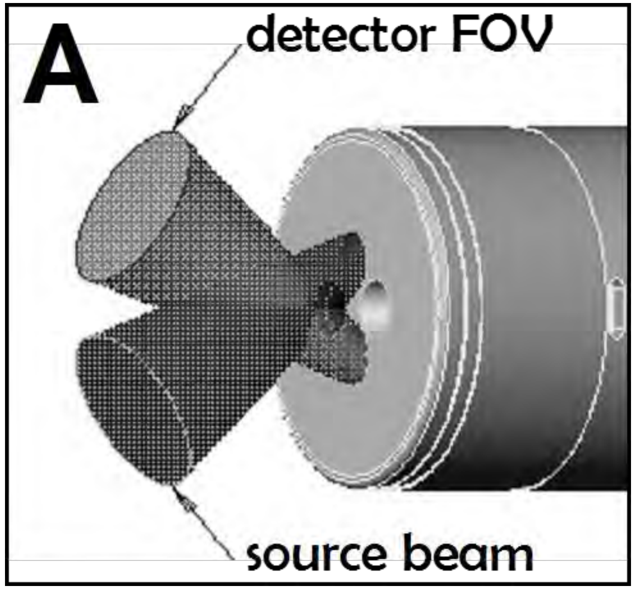

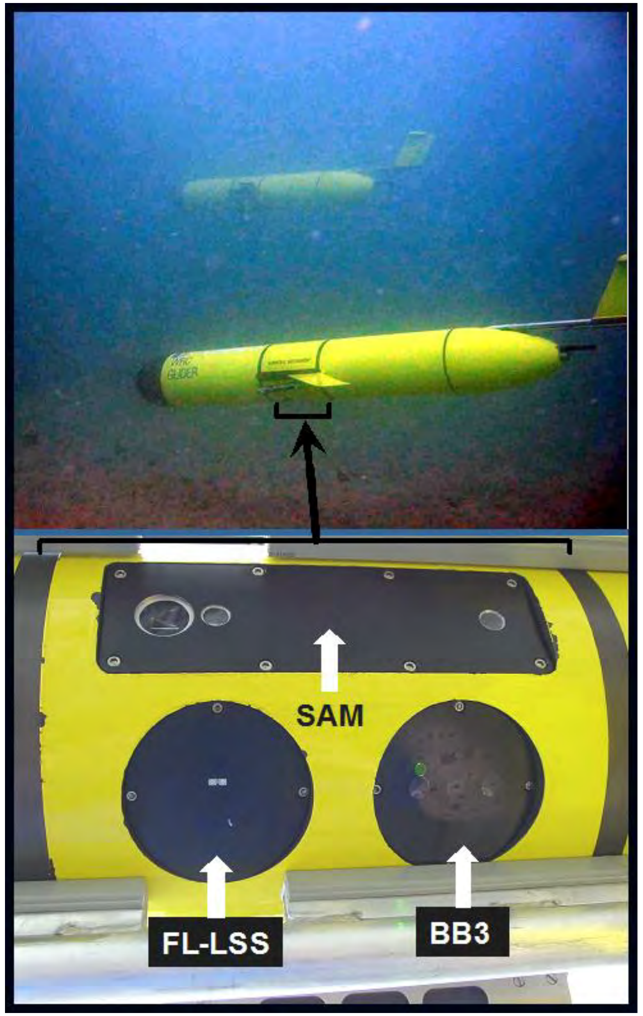

IMO-SC6

In-situ Marine Optics

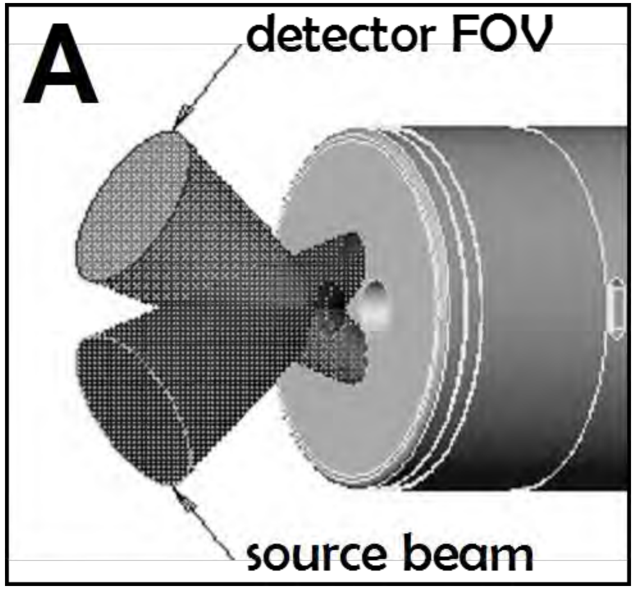

6 wavelengths, centroid angle ~120 deg

Huge dynamic range – best choice for very turbid waters

VSF measurement and calibration

<u>$\beta(\theta)$ *measurements are always resolved over a range of angles*</u>

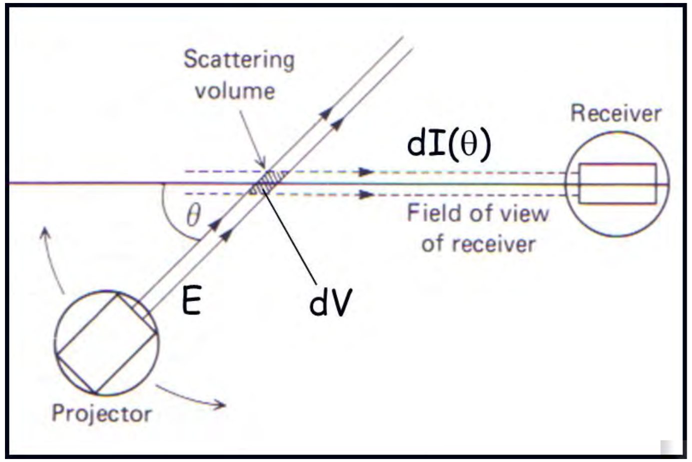

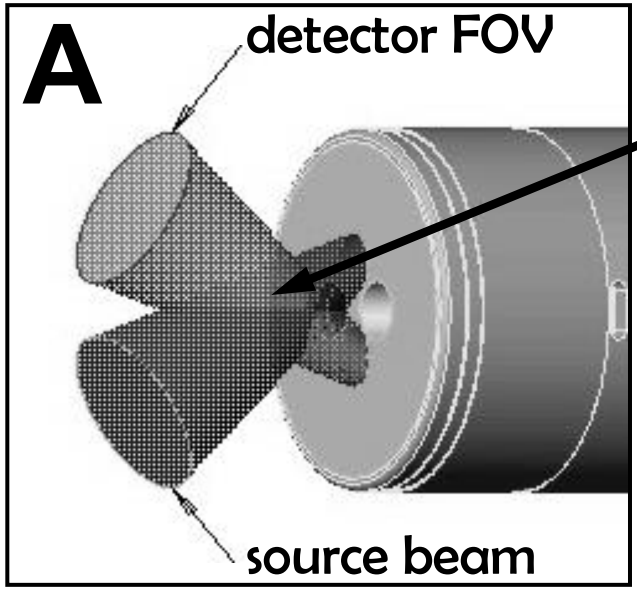

Overlapping volume defines W(θ)

W(θ) weighting function

$\bar{\theta}$ centroid angle

$$\bar{\beta}(\bar{\theta}, \Delta\theta) = \int_0^{\pi} \beta(\theta) W(\theta)\, d\theta$$

See Sullivan et al. (2013) for detailed calibration methodology

Determining W(θ)

Experimentally (Maffione and Dana 1997) – the plaque method
Analytically (Sullivan et al. 2013) – the "virtual plaque" method

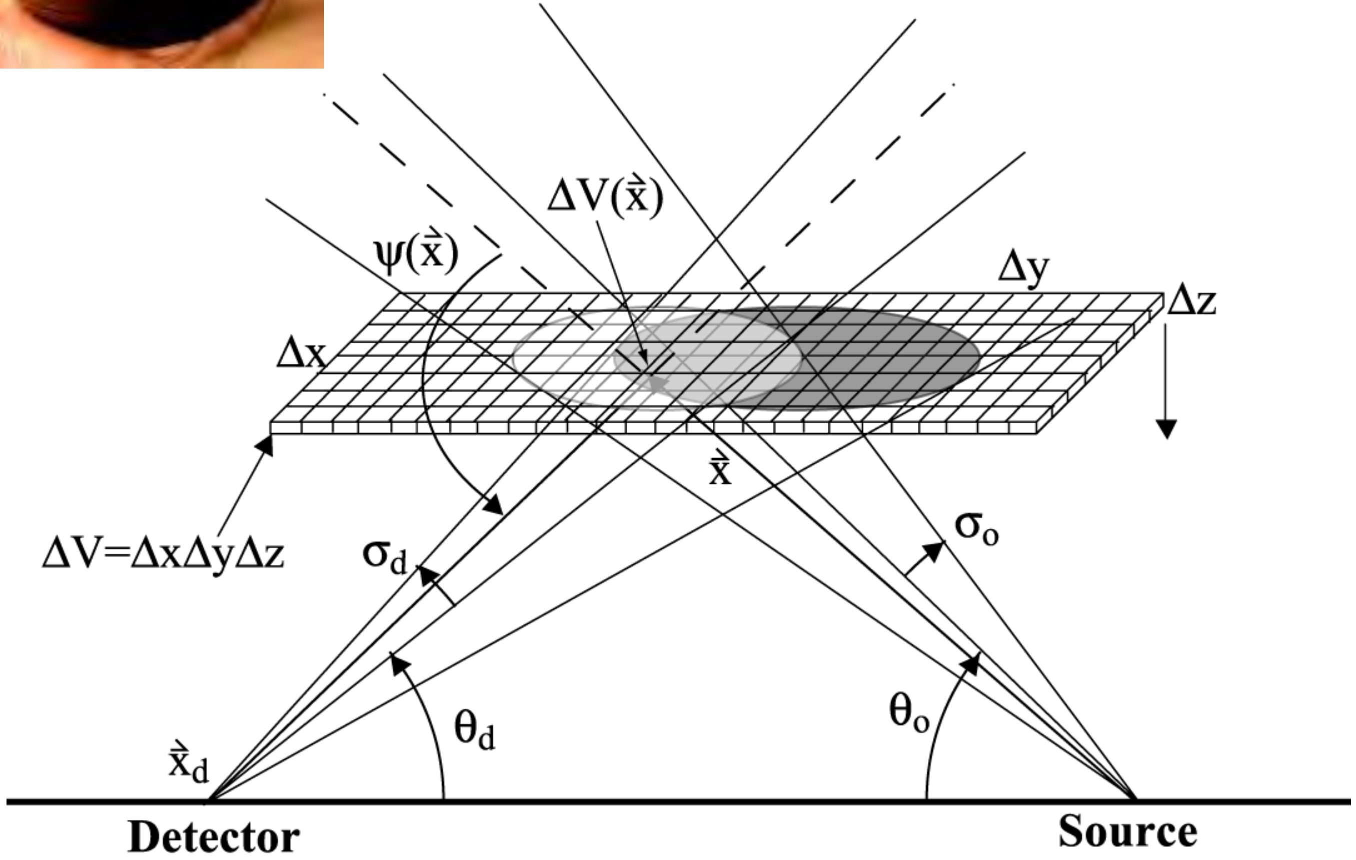

VIRTUAL METHOD

VIRTUAL METHOD

- Step virtual plaque through sample volume
- Determine area where source and detector beam images overlap for each z step
- Calculate power returned to detector at each dV in the overlapping area (note there is no consideration of VSF in doing this)
- Assign θ to each dV
- Compile results (i.e., fill θ bins) to derive weighting function

ECO weighting function history

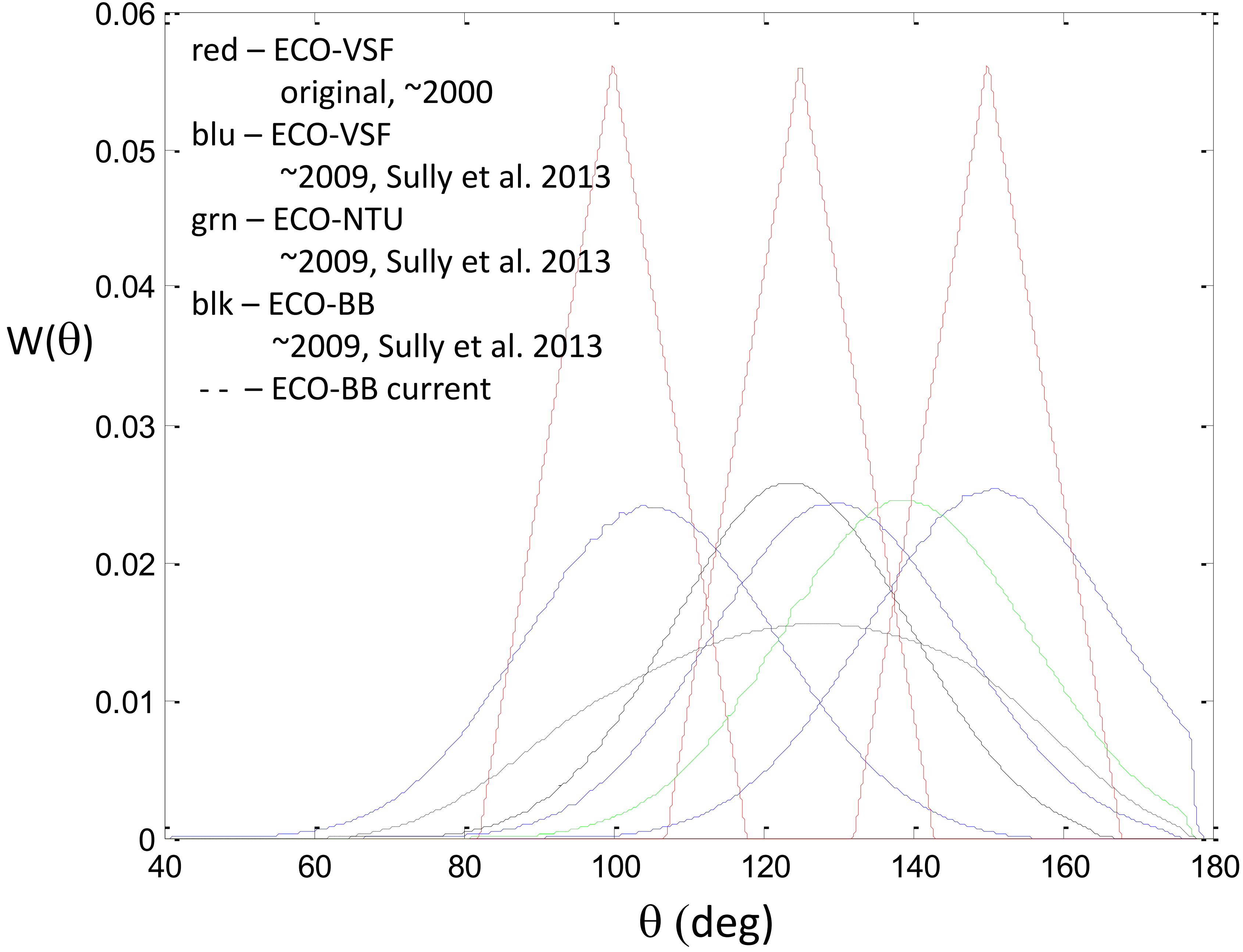

Obtaining backscattering coefficients with β at limited θ

<u>With a single $\beta(\theta)$ in the backward hemisphere</u>

$$b_{bp} = \chi(\theta)2\pi\beta_p(\theta)$$

Past discussion over which θ and which χ are best:

- Oishi (1990): **120°**
- Maffione and Dana (1997): **140 °**
- Boss and Pegau (2001): **117 °**
- Sullivan and Twardowski (2009): **118 °**

- But all β measurements are made over an <u>angular range</u>
- Implicit assumption necessary about VSF shapes in the backward
- For most accurate current protocols, see Sullivan et al. (2013)

What is “Turbidity” ? “NTUs”?

- Typically a measurement of scattering ~90° but many sensors use angles > 90°
- Spectral characteristics vary (“white light,” 880 nm, etc.)
- Angular weighting ($\Delta\theta$) varies
- Calibrated to formazin particles (phase function looks nothing like that of the real ocean)

<u>So what does this mean?</u>

- Every turbidity measurement, and NTU, is different!
- Turbidity is generally not a rigorous optical property
- Turbidity is not “water clarity” (*c* is best for estimating this).
- Signal may be correlated with backscattering.

Measuring total scattering (*b*)

Typically derived from *a* and *c*: WET Labs ac-9 and ac-s

ac-s

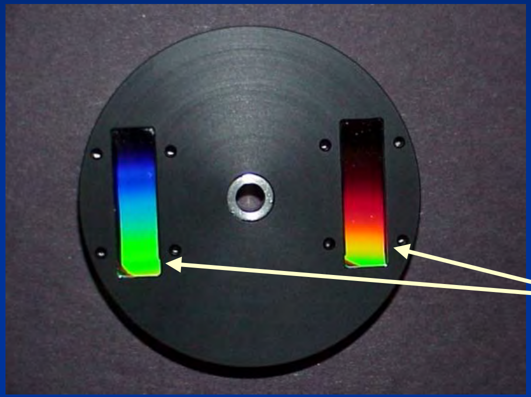

- acs is hyperspectral
- ac-9 has 9 individual interference filters

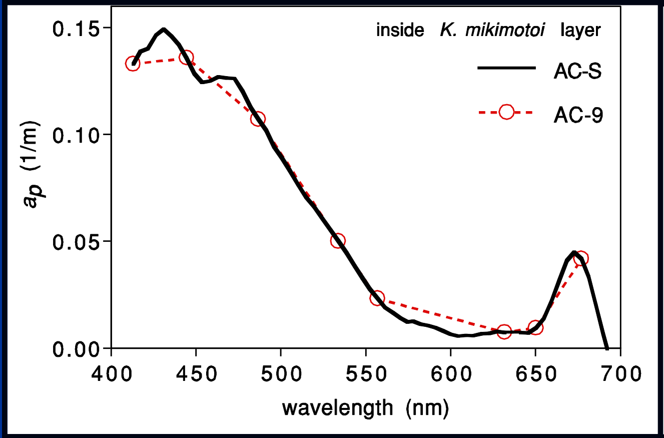

Sullivan and Donaghay (2004)
Irish fjord

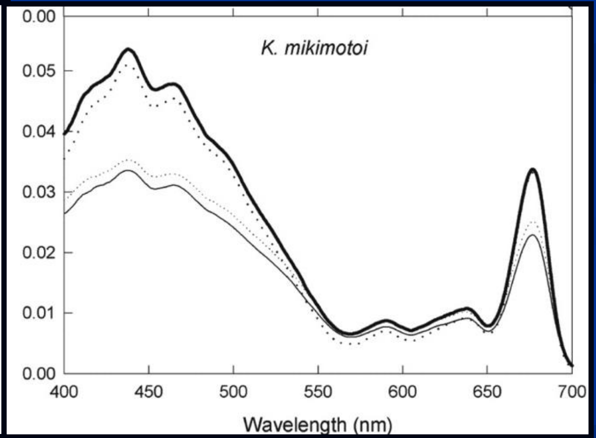

Stahr and Cullen (2003)
In culture

Anatomy of a beam attenuation meter (transmissometer)

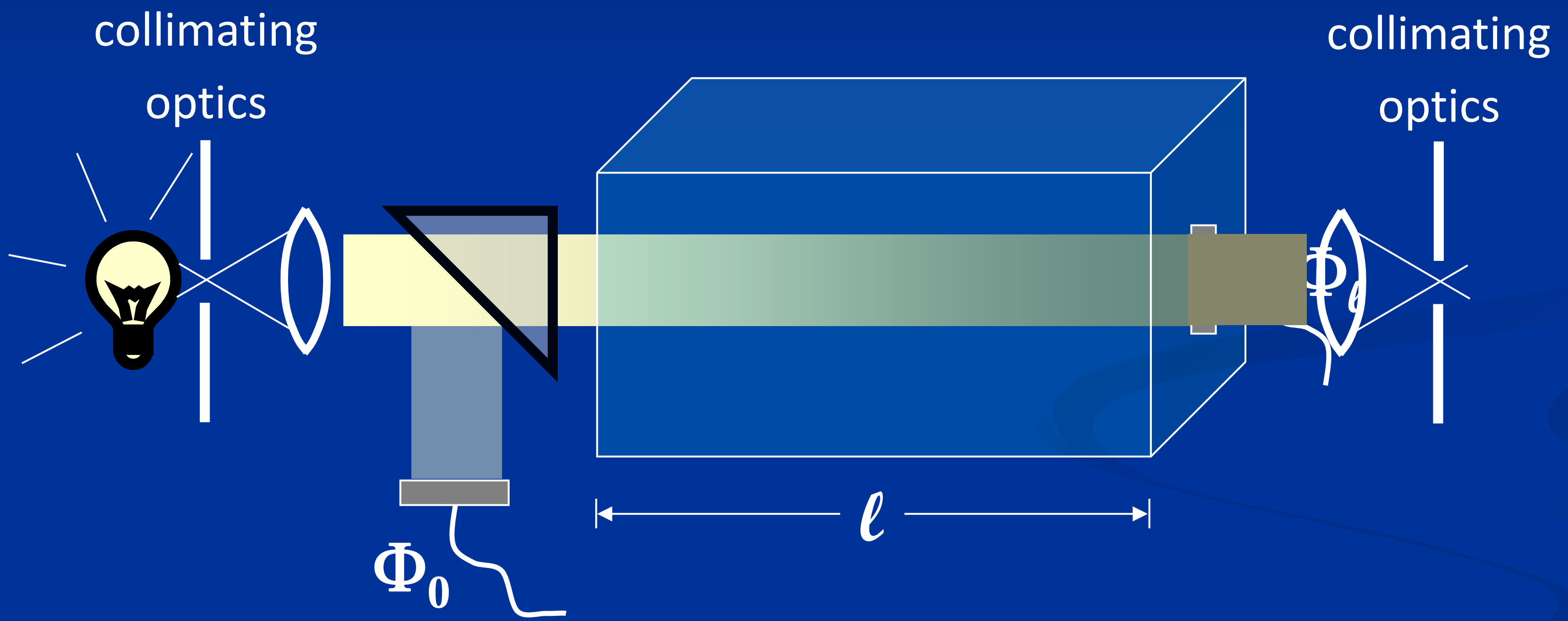

Problem: some scattered light also reaching detector

The theoretically ideal attenuation meter has an acceptance angle of ~0° but at 0° no light is received – need to compromise

***Optimal accuracy reached when ℓ ~ 1/c*

Reflective tube method for absorption

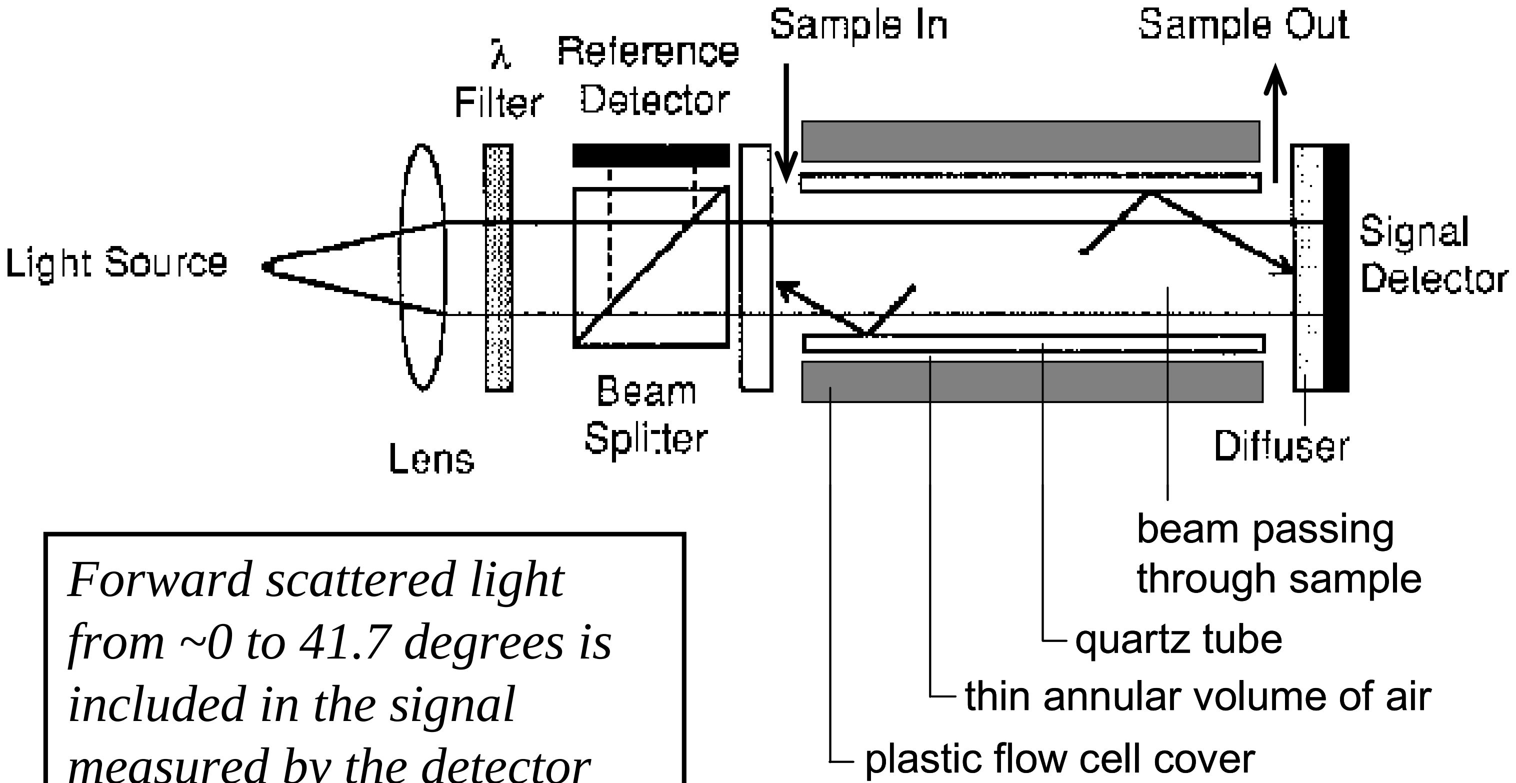

Forward scattered light from ~0 to 41.7 degrees is included in the signal measured by the detector

Light scattered at angles > 41.7 deg is not measured by detector and requires correction….

from Zaneveld et al. (1992)

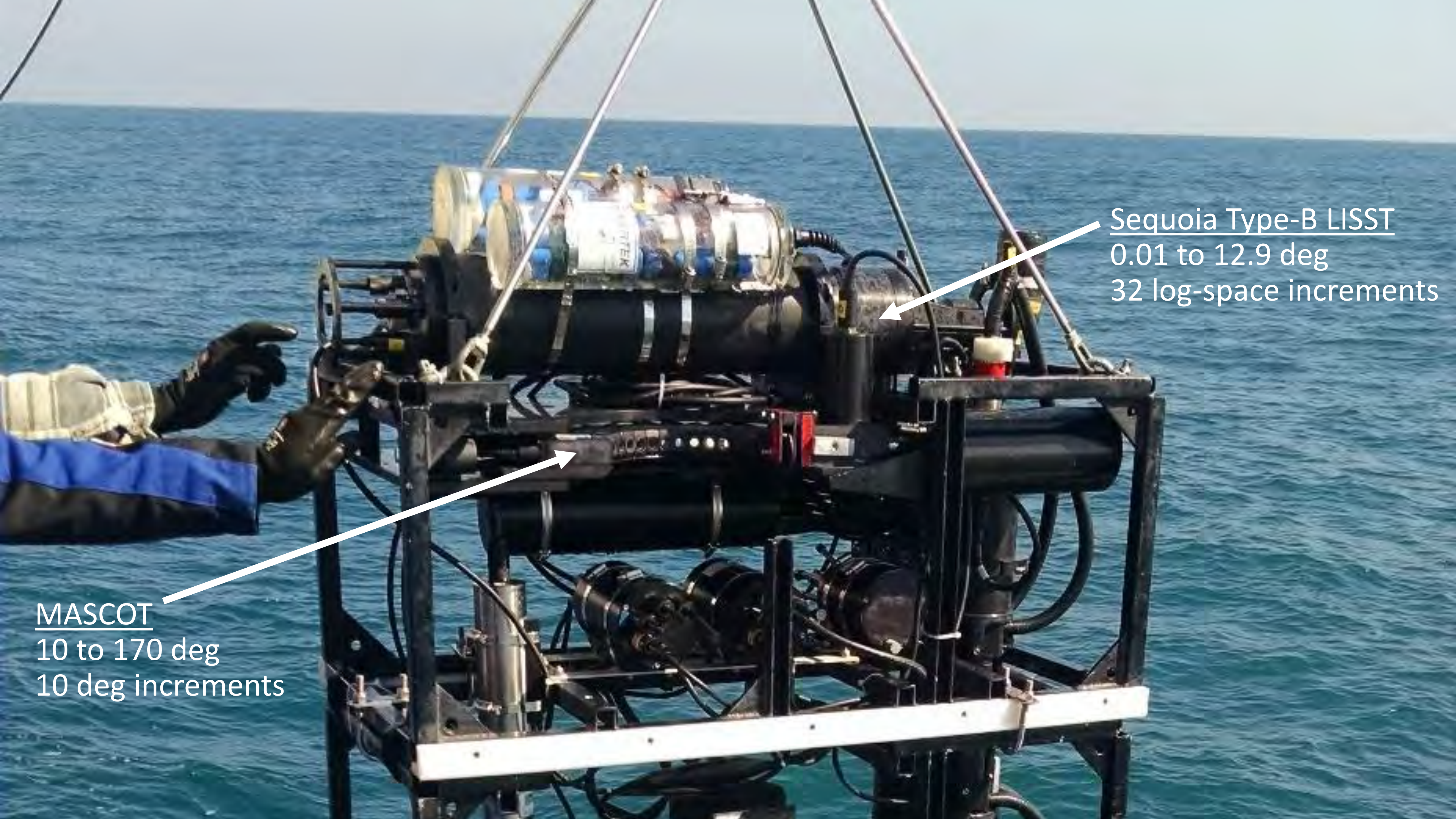
Sequoia Type-B LISST
0.01 to 12.9 deg
32 log-space increments
MASCOT
10 to 170 deg
10 deg increments

VSF profile data – from Santa Barbara Channel 2008

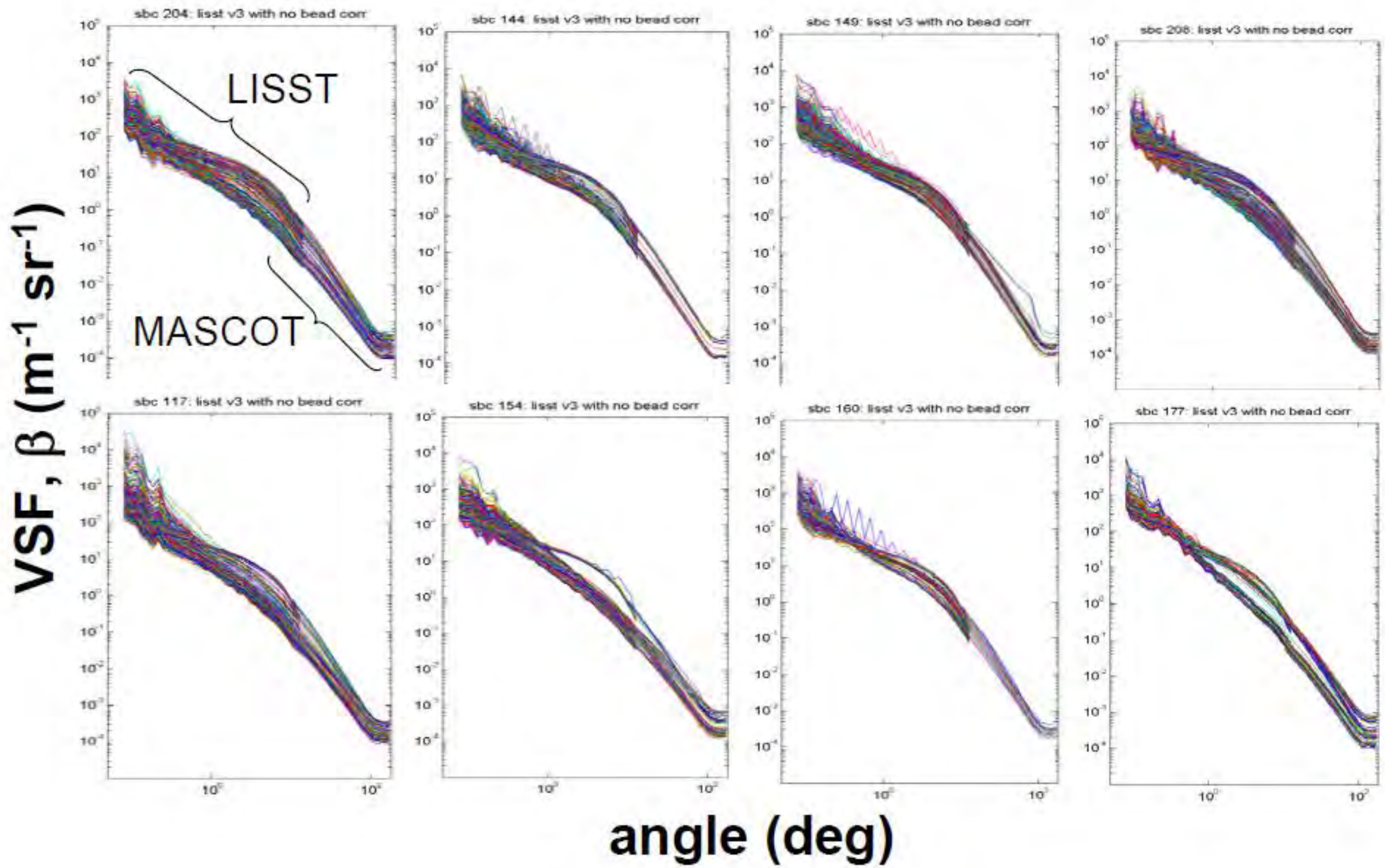

Integrating the VSF: testing closure between sensors

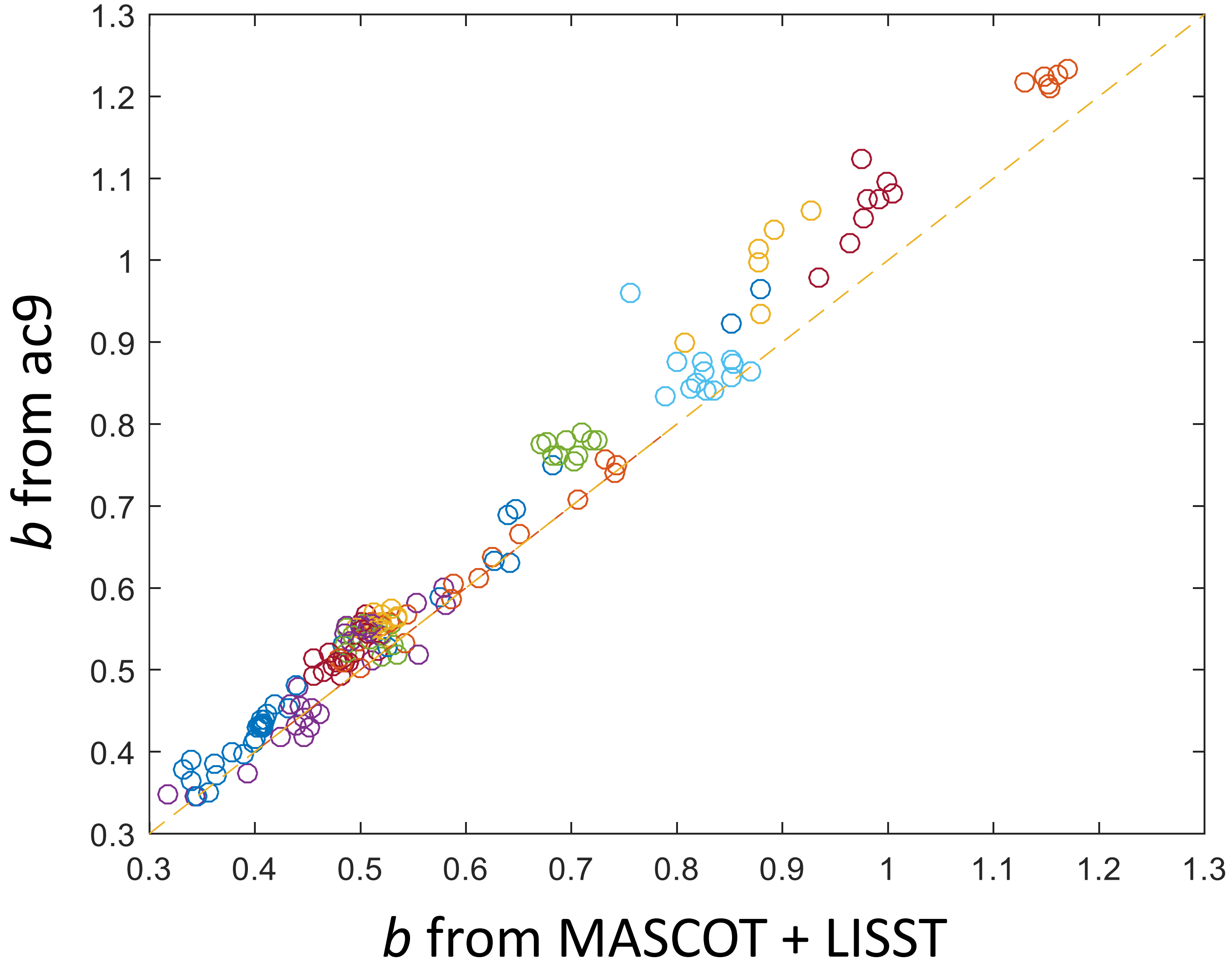

$$\boxed{\boldsymbol{b = c - a}}$$

$$b_{ac9} = 2\pi \int_{0.93}^{180} \sin(\theta)\,\beta(\theta)d\theta$$

Cumulative scattering contribution

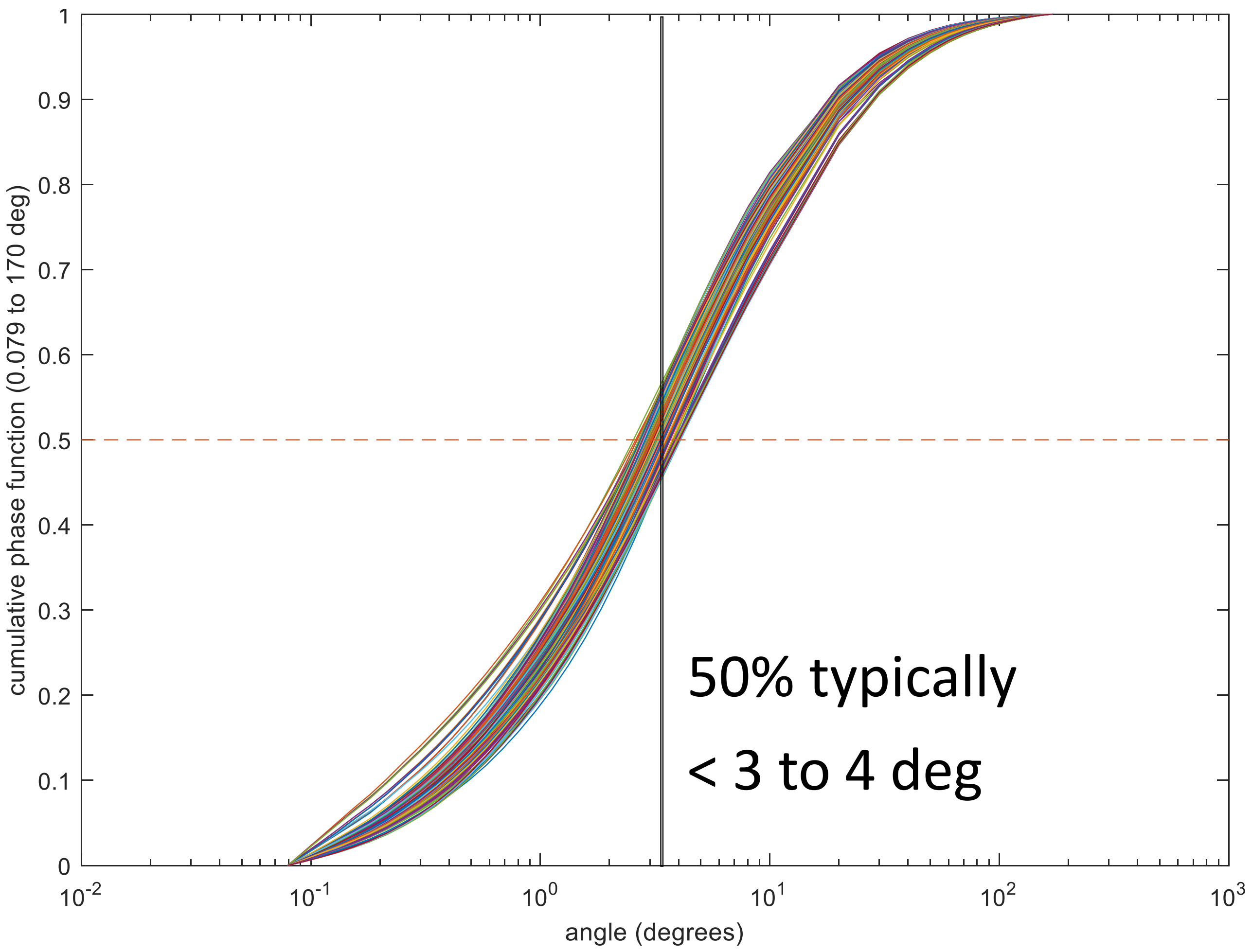

$$\frac{b_x = 2\pi \int_i^j \sin(\theta)\beta(\theta)d\theta}{b}$$

Analytical models of the VSF

Analytical modeling: fitted Kattawar-Haltrin 2-term, 1-parameter Henyey-Greenstein

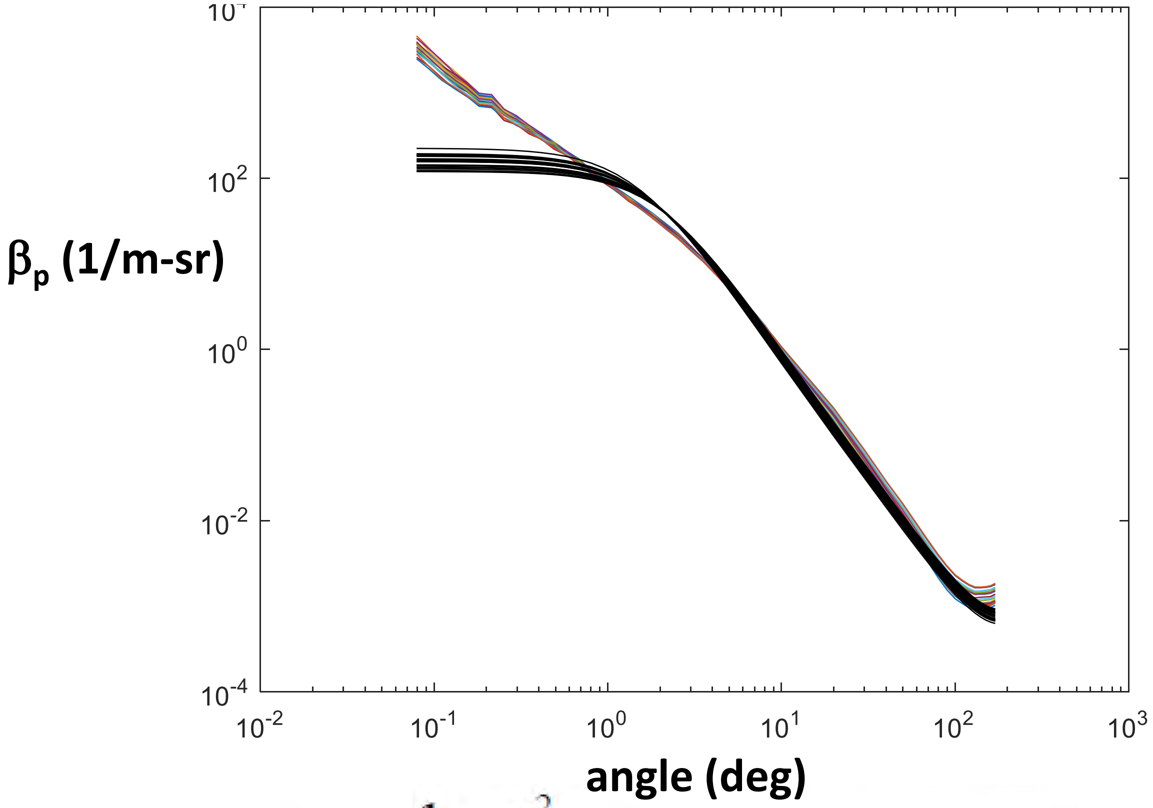

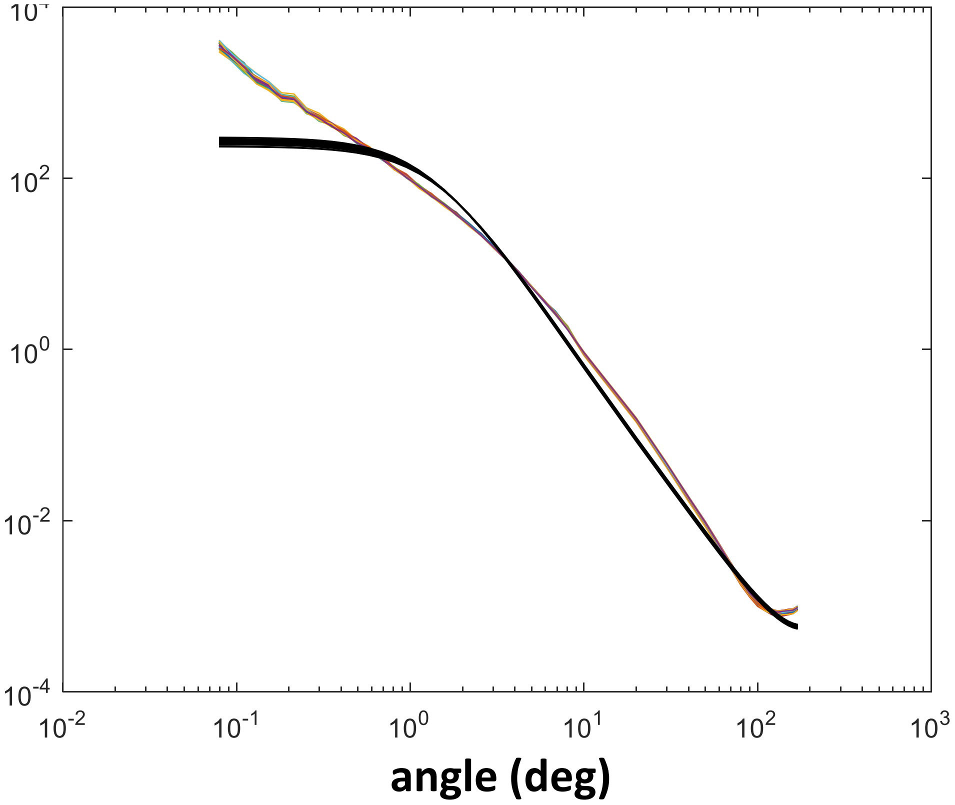

$$p_{HG}(\mu, g) = \frac{1-g^2}{\left(1-2g\mu+g^2\right)^{3/2}}, \quad \mu = \cos\vartheta,$$

$$p_{TTHG}(\mu, \alpha, g, h) = \alpha\, p_{HG}(\mu, g) + (1-\alpha)\, p_{HG}(\mu, -h)$$

$$0 \le \alpha, g, h \le 1.$$

h(g) and α(g)

Analytical modeling: fitted Kopelevich

Fit 2 basis vectors recommended by Kopelevich (1983)

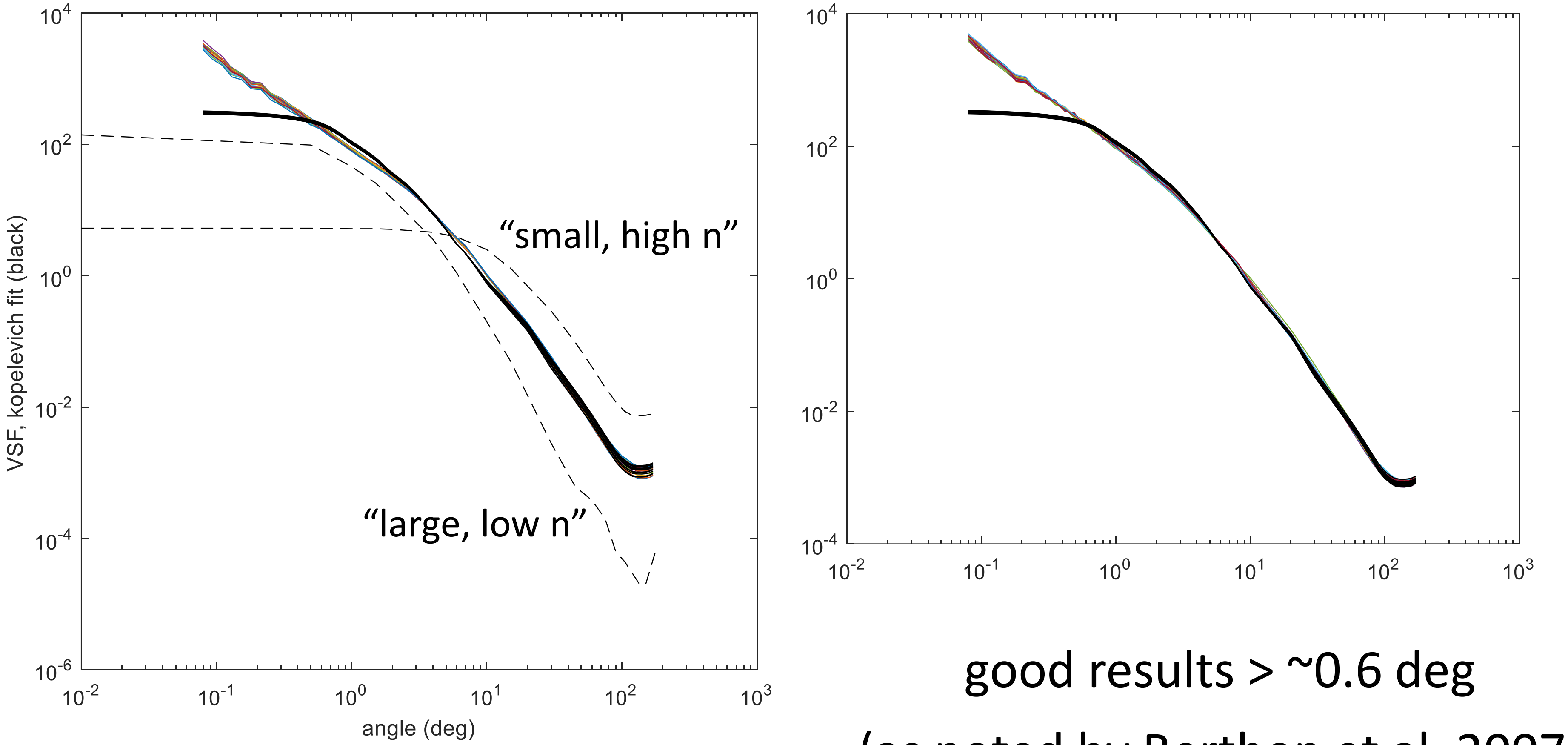

good results > ~0.6 deg

(as noted by Berthon et al. 2007)

Analytical modeling: fitted Fournier-Forand (1994, 1999)

see Jonasz and Fournier (2007, with erratum)

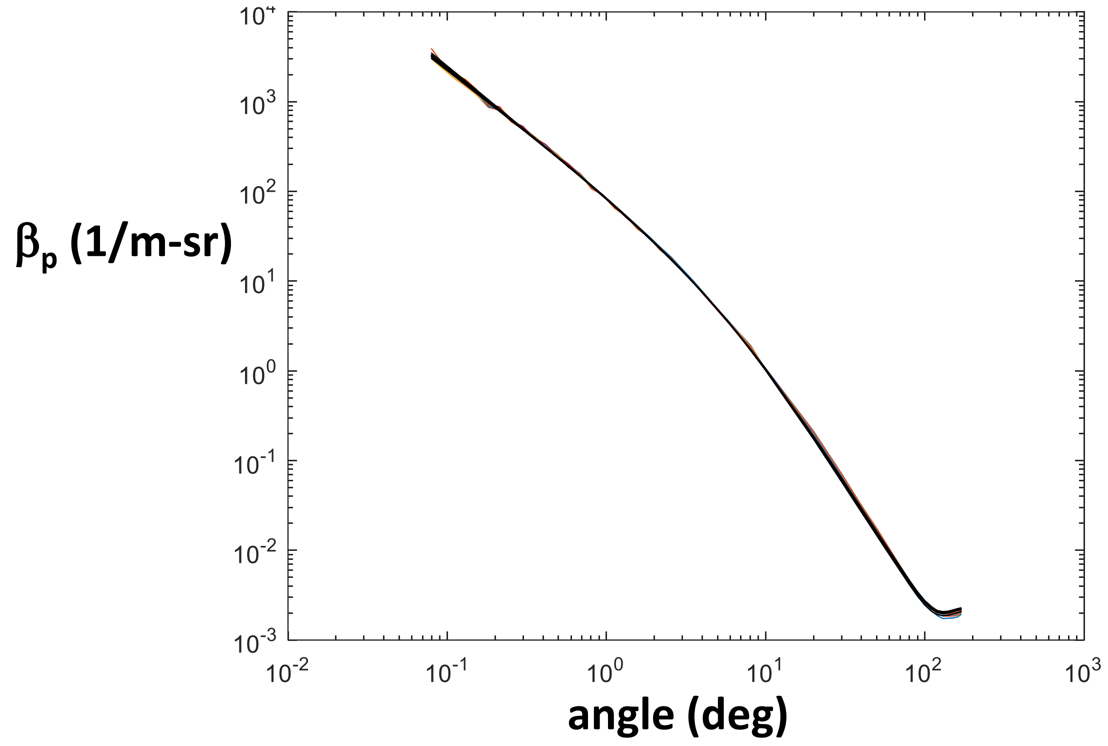

$$\tilde{\beta}(\theta) = \frac{1}{4\pi}\frac{1}{(1-\delta)^2\delta^v}\left(\left[v(1-\delta)-(1-\delta^v)\right]+\frac{4}{u^2}\left[\delta(1-\delta^v)-v(1-\delta)\right]\right)$$

$$v = \frac{3-\mu}{2} \quad , \quad \delta = \frac{u^2}{3(n-1)^2} \quad , \quad u = 2\sin(\theta/2)$$

<u>INPUTS</u>:

μ = power law slope for particle size distribution

n = relative refractive index of particles

Excellent fits for entire measured range (0.079 to 180 deg)

Backward phase function (i.e., backward VSF shape)

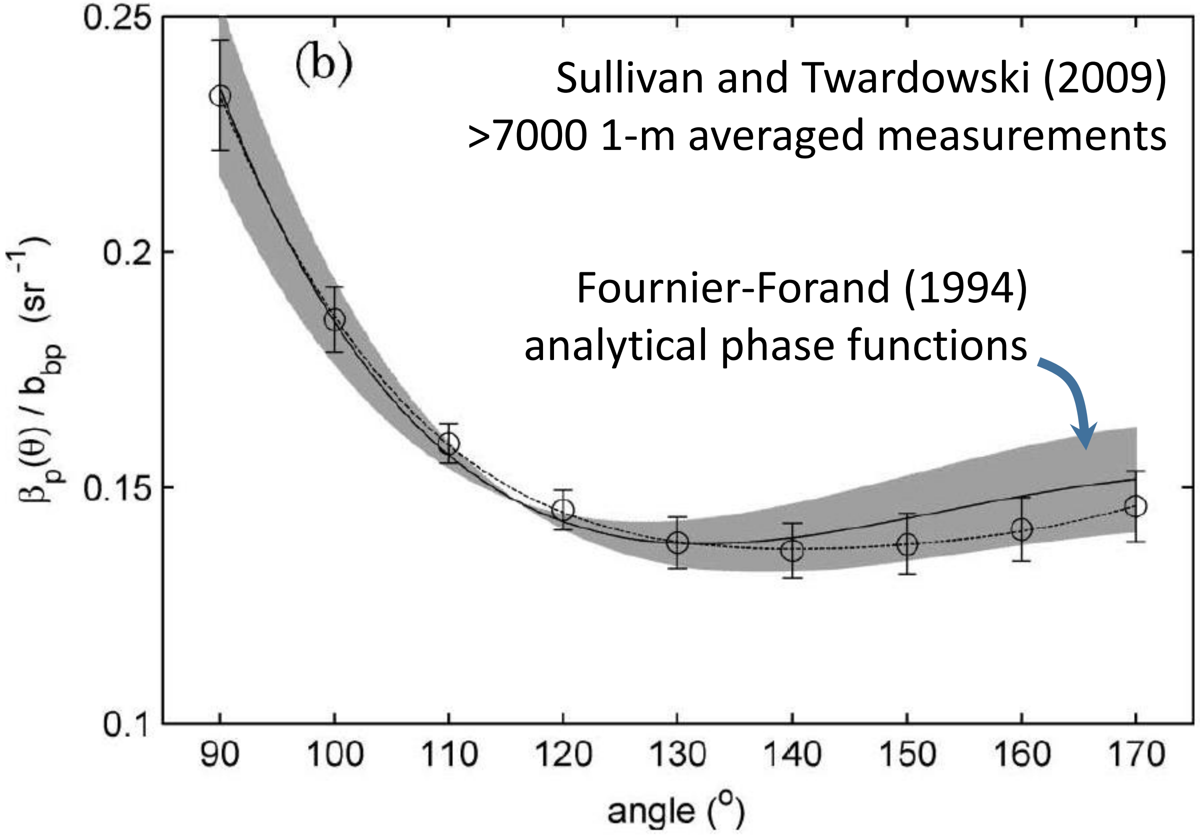

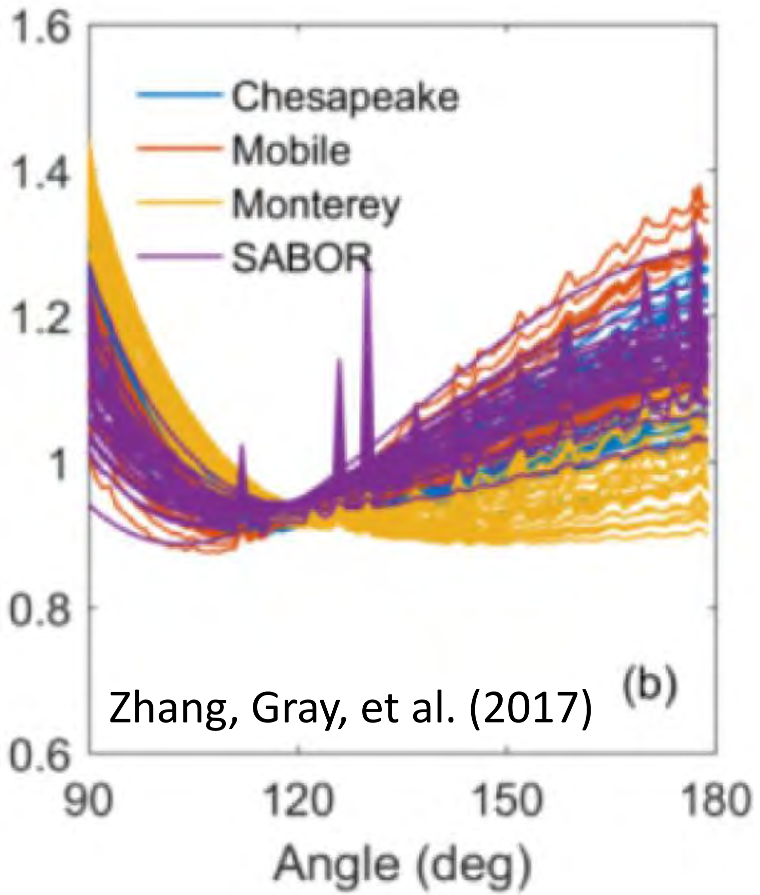

<u>Remarkably consistent shape…</u>
Important implications for ocean color remote sensing

However, some inconsistency in current literature…

Constant backward VSF shape appears realistic…

Radiative transfer simulations
assuming constant VSF shape

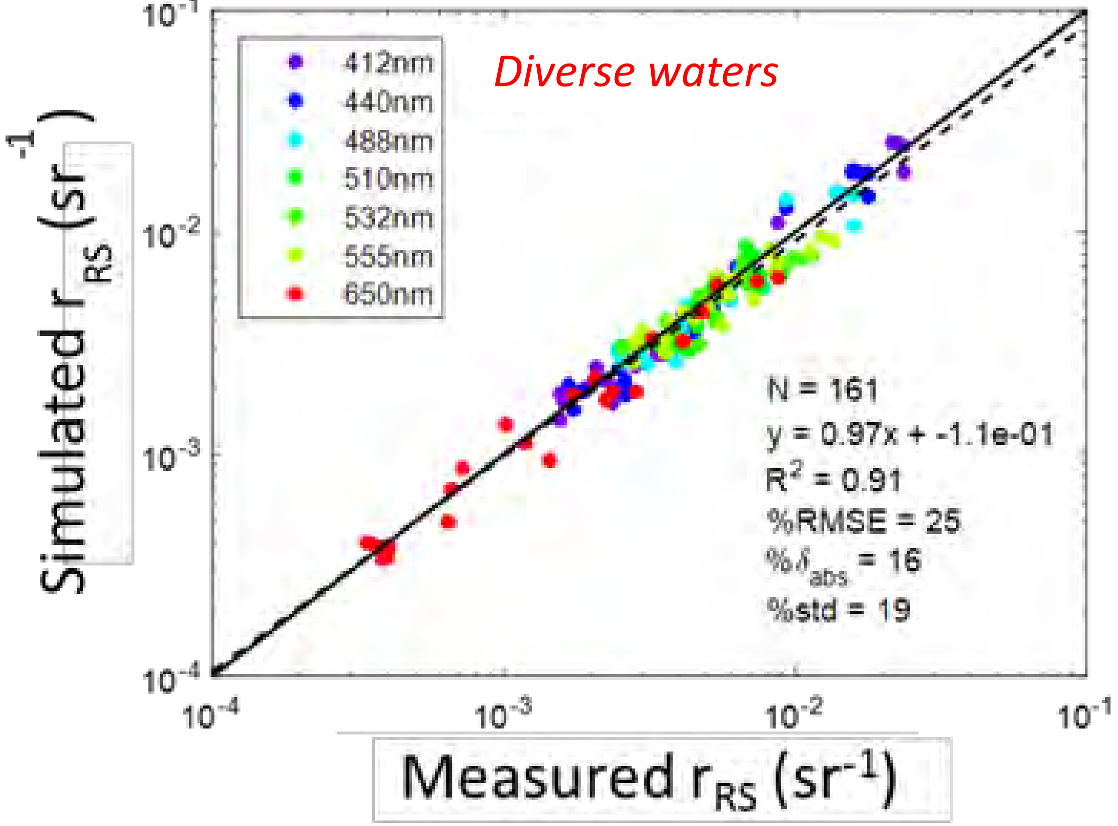

Bidirectional Reflectance Distribution Function
assuming constant VSF shape

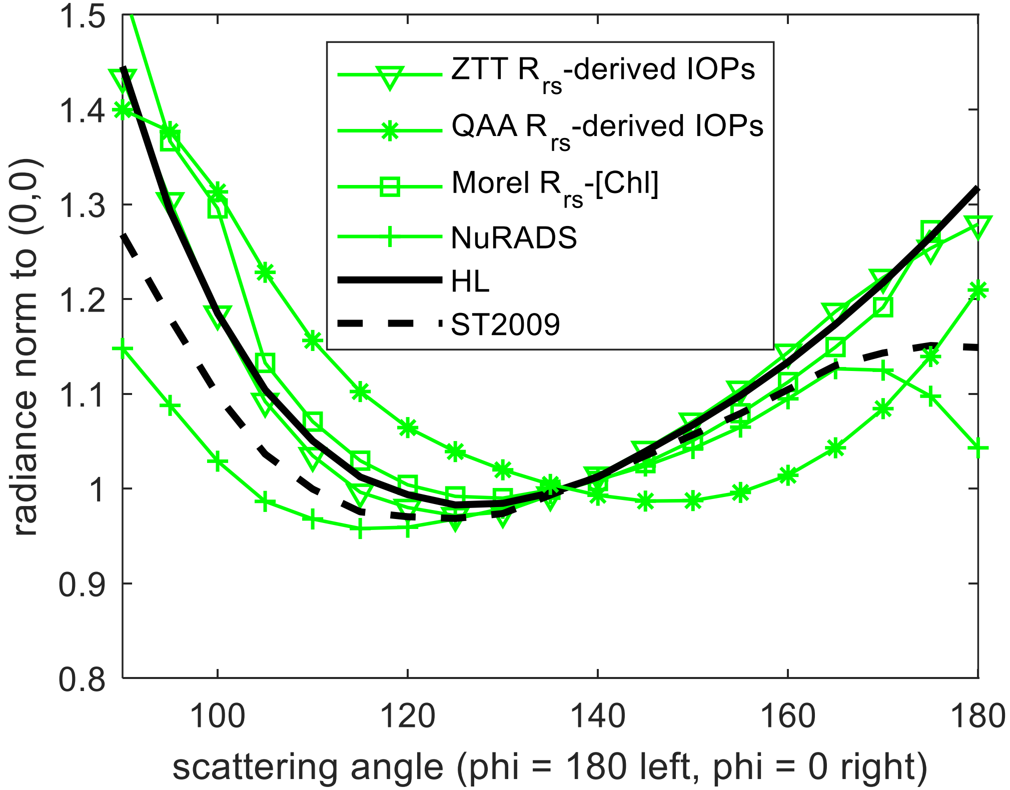

Results are equivalent or better to simulations using measured VSFs

Twardowski and Tonizzo (2018)

Tonizzo and Twardowski (in prep)

Primary scattering components in water

- Pure seawater (molecular)
- Turbulence (i.e., refractive index discontinuities)
- Particles
- Bubbles

Scattering by pure seawater

Zhang and Hu (2009); Zhang et al. (2009); Zhang et al. (2019)

Review: Zhang (2012)

- Uses Einstein-Smoluchowsky theory for refractive index fluctuations with updated constants
- The depolarization ratio used is 0.039, also after Farinato and Rowell (1974)
    - Experimentally verified in Zhang et al. (2019)
- Agrees well with experimental work of Morel (1968)

For backscattering by seawater, divide b_w by 2.

Scattering by clearest natural waters

South Pacific gyre – 2004

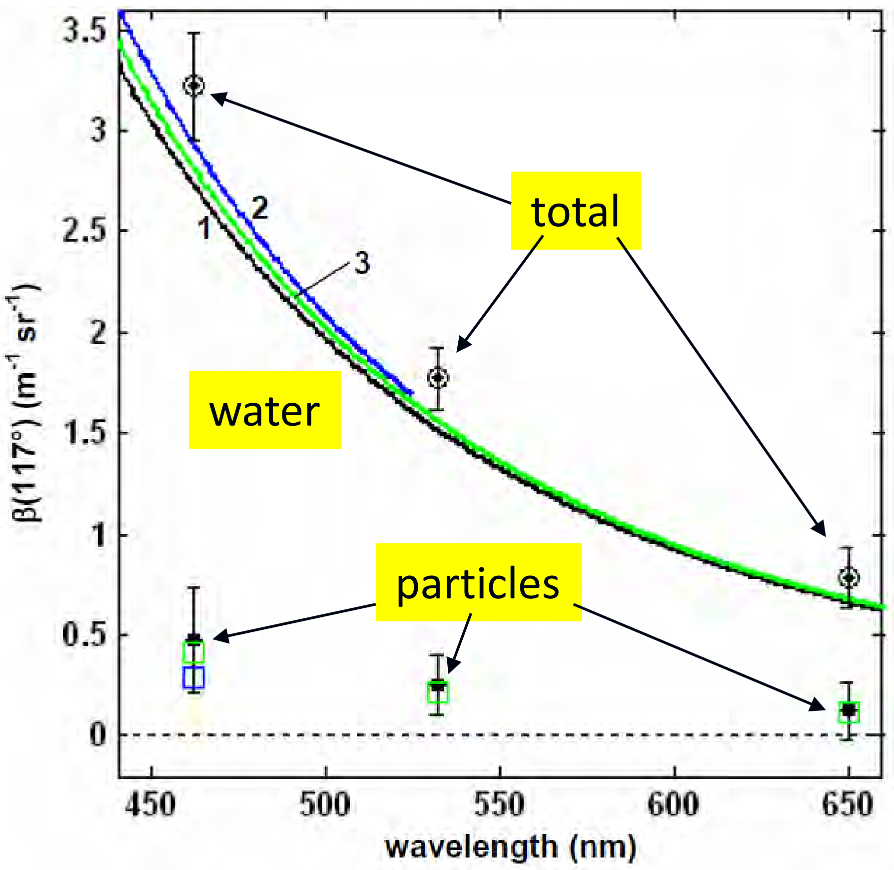

Backscattering by seawater can be 90+% of total b_b in the very clear ocean.

Accuracy is very important if we are interested in b_{bp}

$\lambda^{-4.28}$

Twardowski et al. 2007

Turbulence (refractive index discontinuities)

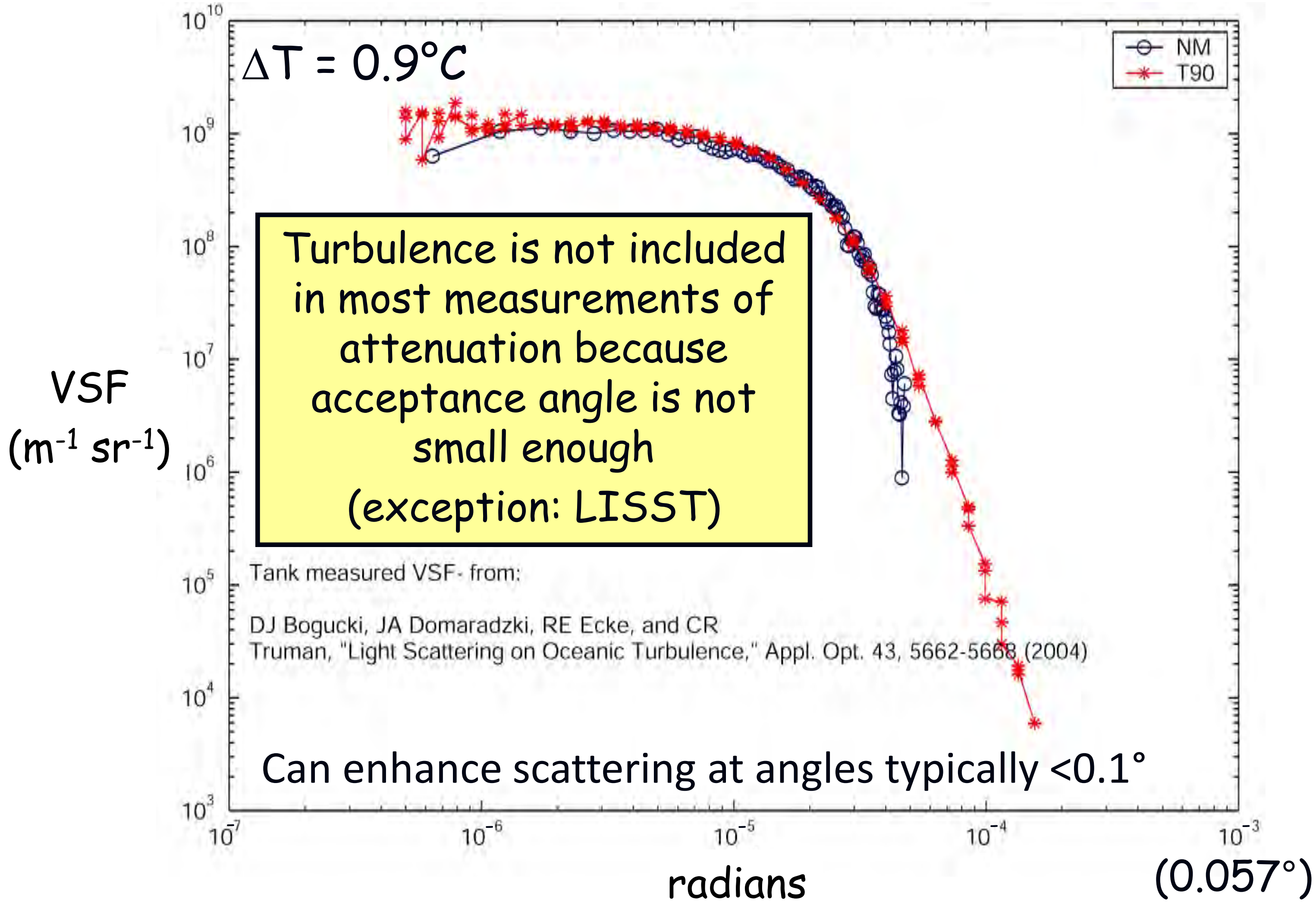

Turbulence measurement with LISST-100X

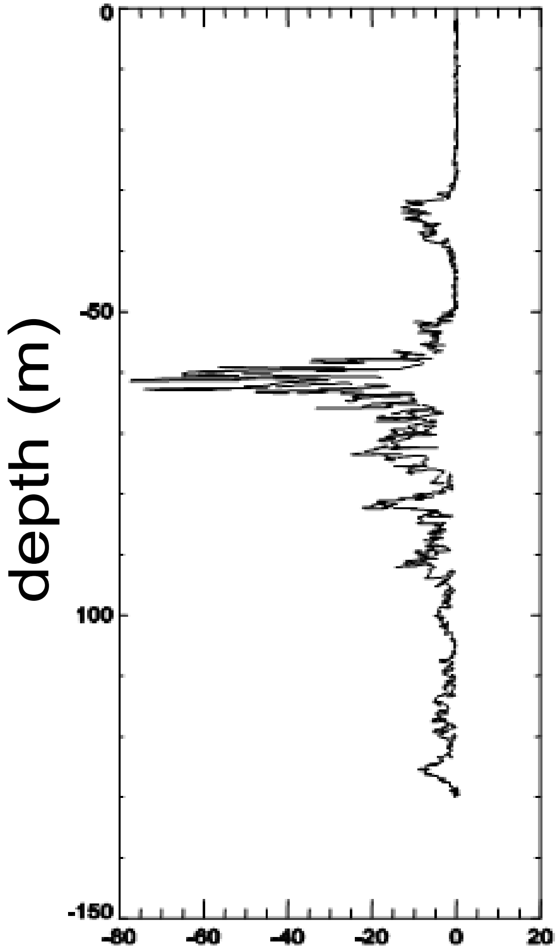

dn/dt
from T&S

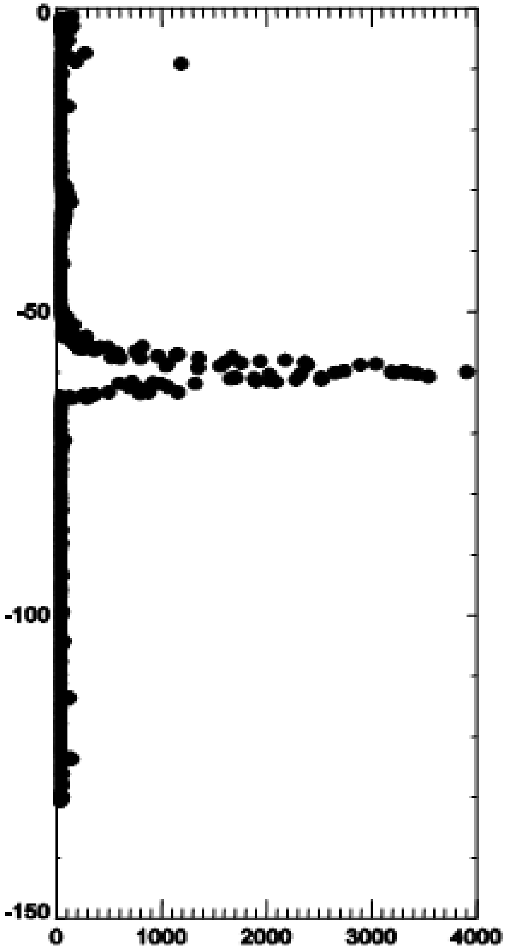

turbulence indicator
from LISST VSF

Hawaii
09/2009

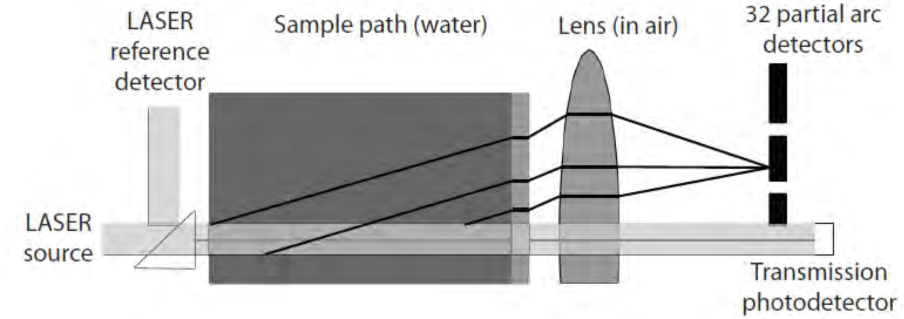

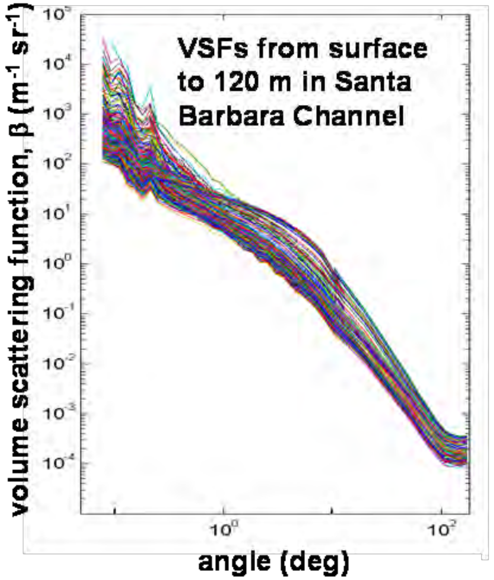

Slivkoff and Twardowski, unpub

Particle scattering

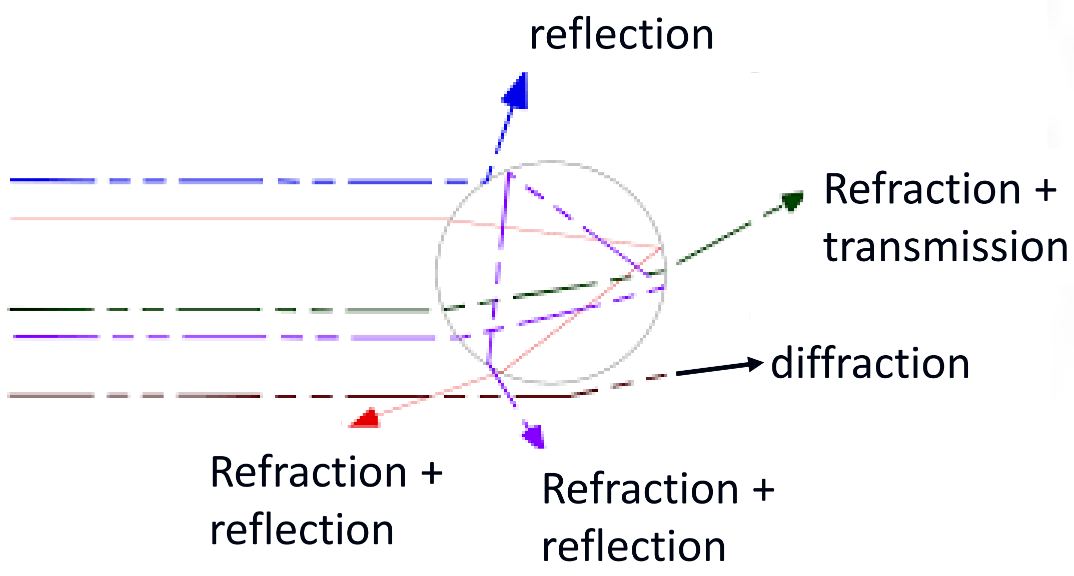

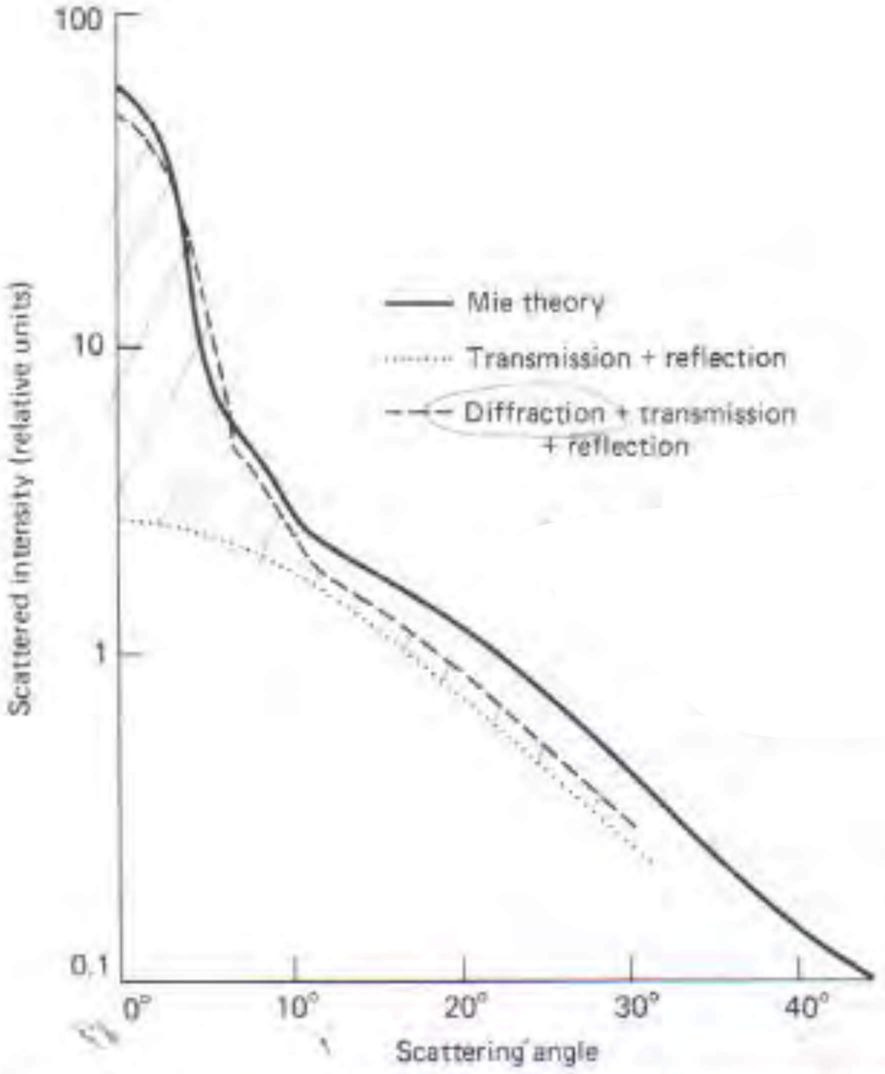

Fig. 4.1. Angular distribution of scattered intensity from transparent spheres calculated from Mie theory (Ashley & Cobb, 1958) or on the basis of transmission and reflection, or diffraction, transmission and reflection (Hodkinson & Greenleaves, 1963). The particles have a refractive index (relative to the surrounding medium) of 1.20, and have diameters 5–12 times the wavelength of the light. After Hodkinson & Greenleaves (1963).

Kirk 1994

"…our present-day interpretation and detailed understanding of major sources of backscattering and its variability in the ocean are uncertain and controversial."

Stramski, D., E. Boss, D. Bogucki, and K. J. Voss, 2004. The role of seawater constituents in light backscattering in the ocean. Progress in Oceanography, 61(1), 27-55.

The Enigma of Phytoplankton Backscattering…

Modeling phytoplankton as homogeneous spheres results in backscattering levels too low (only a few percent contribution) to be consistent with their influence on remote sensing reflectance (R_{RS}).

Stramski and Kiefer 1991; Stramski et al. 2001

Testing the "Complex Particle" Hypothesis

Thalassiosira weissflogii

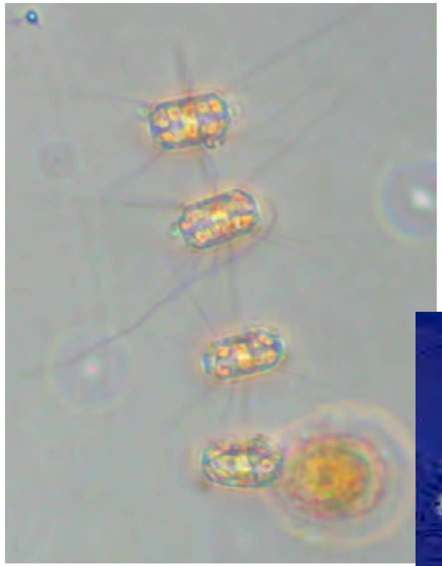

~25 μm diameter

Gyrodinium instriatum

photomicrographs by K. Matsuoka and Y. Fukuyo

~50 mm diameter

~10 μm cell diameter
Up to 1 mm colonies

Chaetoceros socialis

Phytoplankton scattering: measurements and modeling

b_{bp}/b_p

	Measured	Mie theory	Coated Mie theory
Thalassiosira cells	**0.013**	0.006	0.013
Gyrodinium cells	**0.006**	0.003	0.007
C. socialis cells	**0.004**	0.0006	0.0237
C. socialis [1]cell Q_{bb} [2]colony Q_b	**0.004**	0.004	

Twardowski, Sullivan, McFarland (unpubl)

Imaging Particle Backscattering

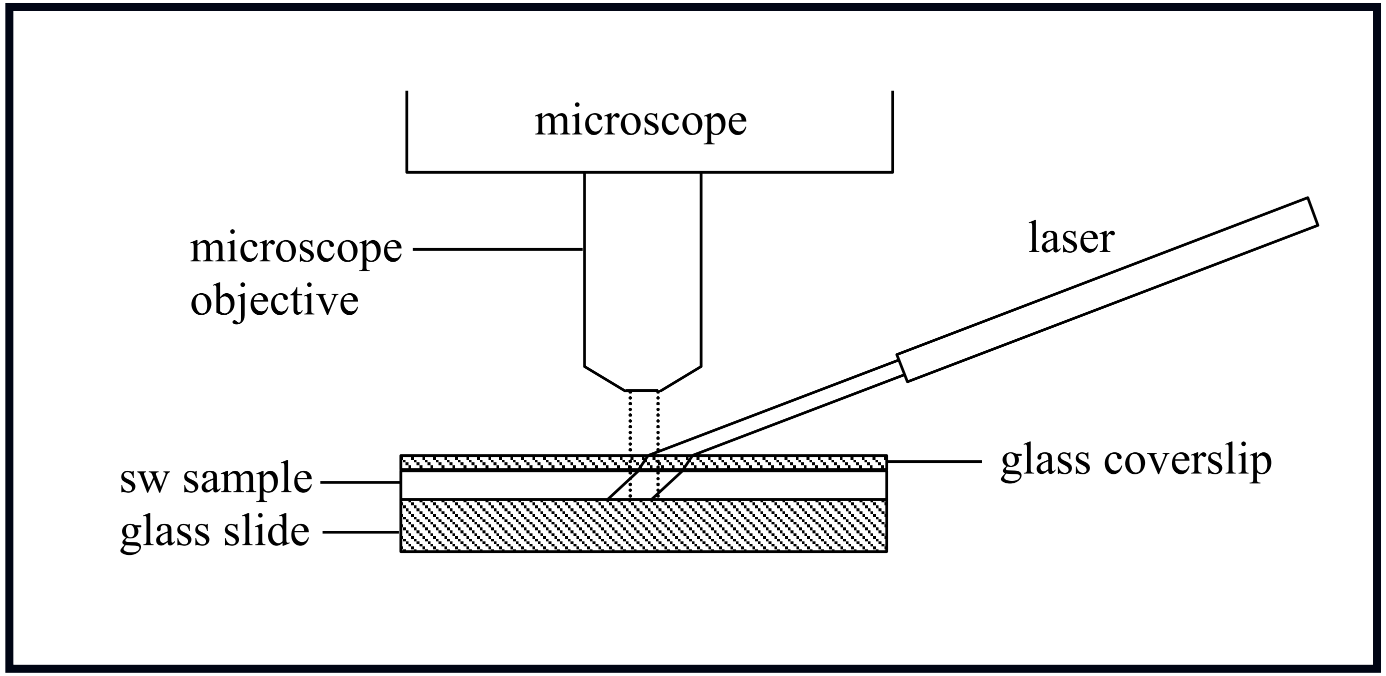

Backscattering imaged at ~140°

Twardowski, Sullivan, McFarland (unpubl)

Imaging Particle Backscattering

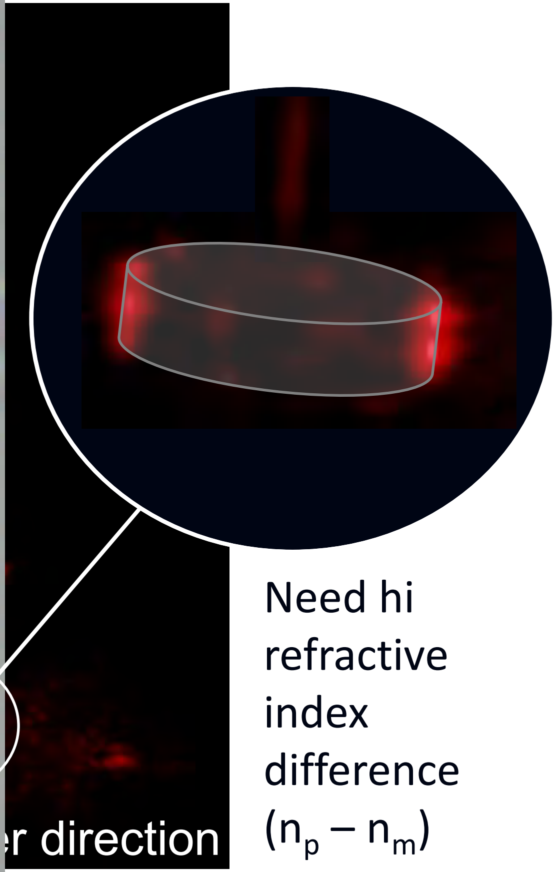

image

Need hi refractive index difference ($n_p - n_m$)

Twardowski, Sullivan, McFarland (unpubl)

Backscattering ratio and chlorophyll

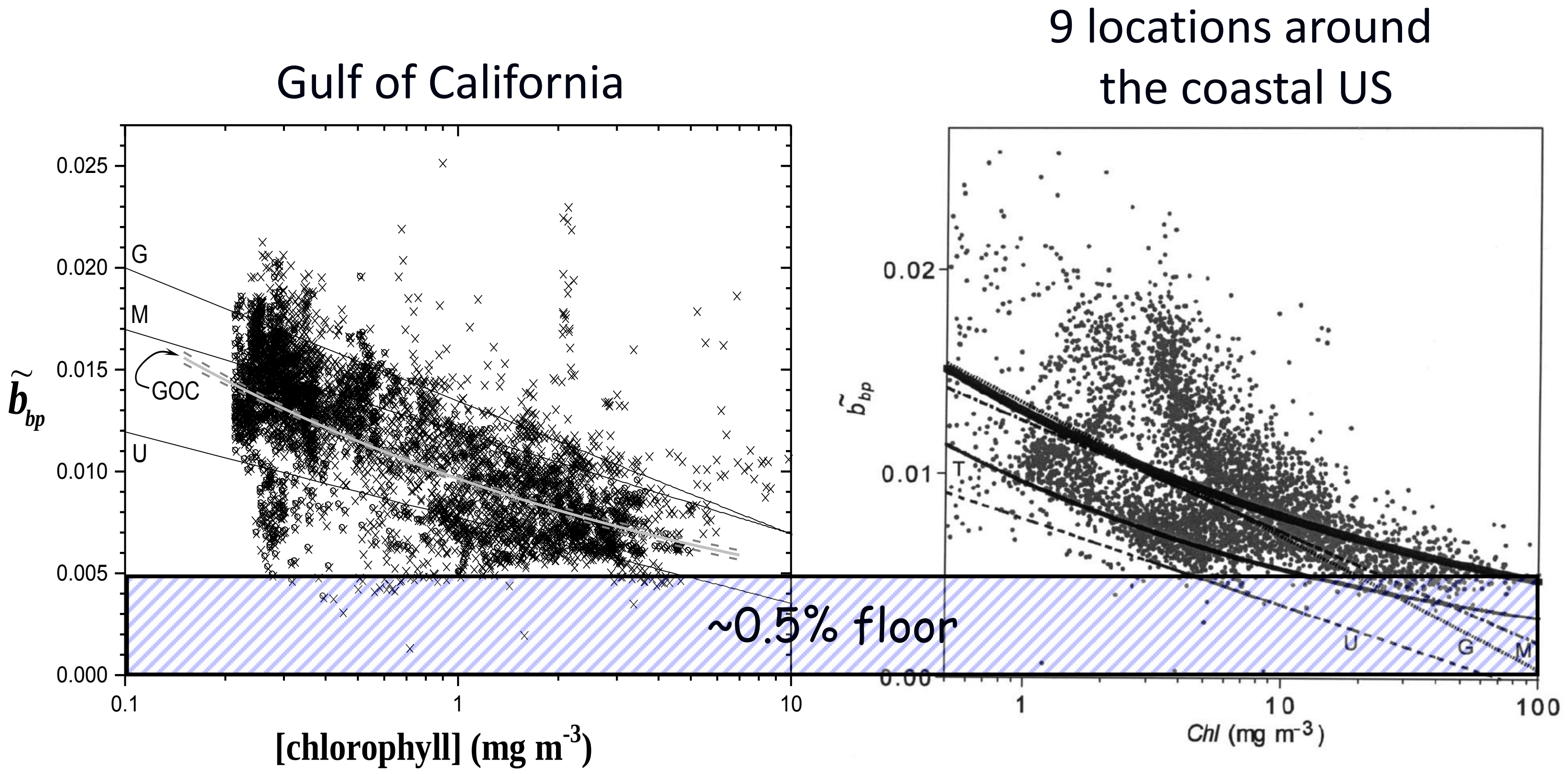

Twardowski et al. 2001

Sullivan et al. 2005

Even in phytoplankton dominated waters, bbp/bp does not fall below ~0.5%

Phytoplankton likely do make a significant direct contribution to b_{bp}

Coated sphere model is a good first approximation

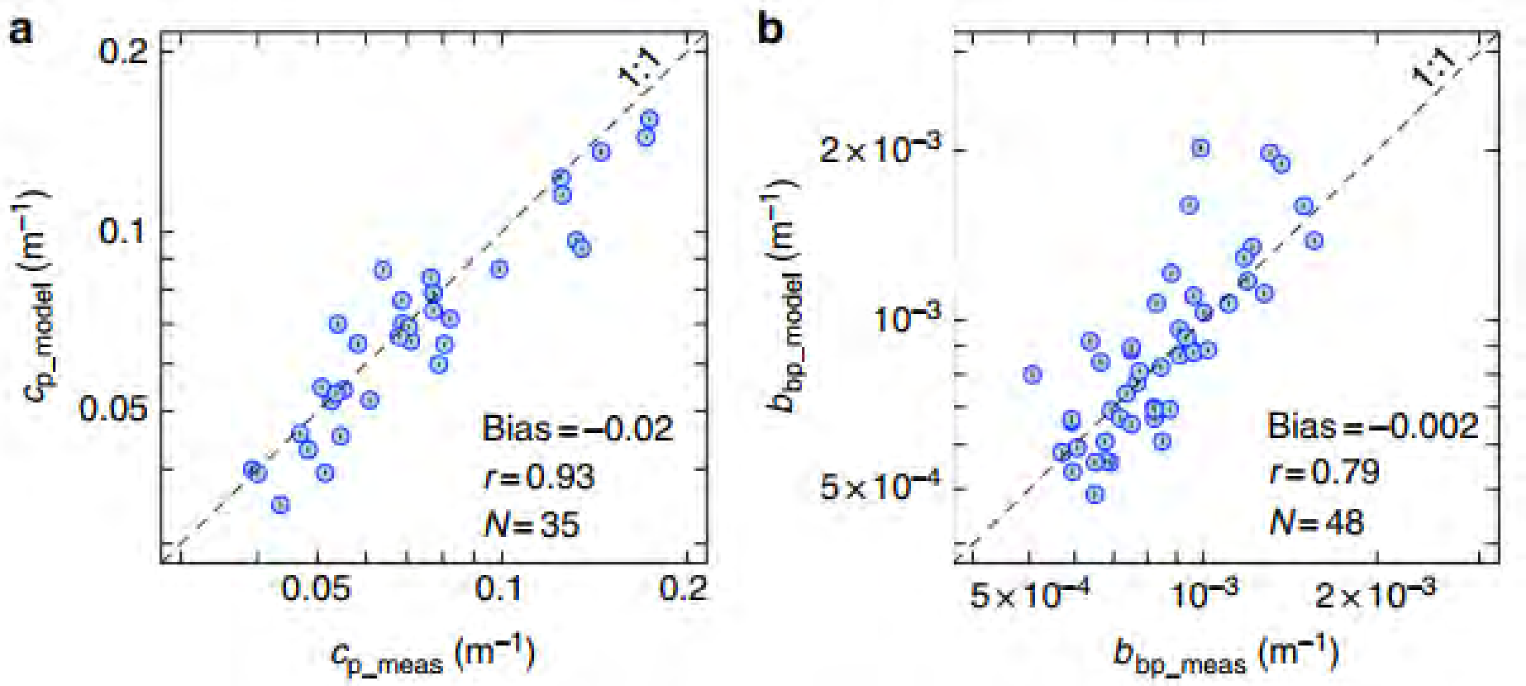

Organelli et al. (2018)

- *Coated sphere model could reproduce both particulate attenuation and backscattering*
- *Homogeneous sphere model could not*

Additional considerations with particle scattering….

Spectral backscattering ratio by particles

For size distribution described by power law, with relatively low absorption, theory predicts <u>spectrally independent b_{bp}/b_p</u>....
(e.g. Morel 1973; Twardowski et al. 2001)

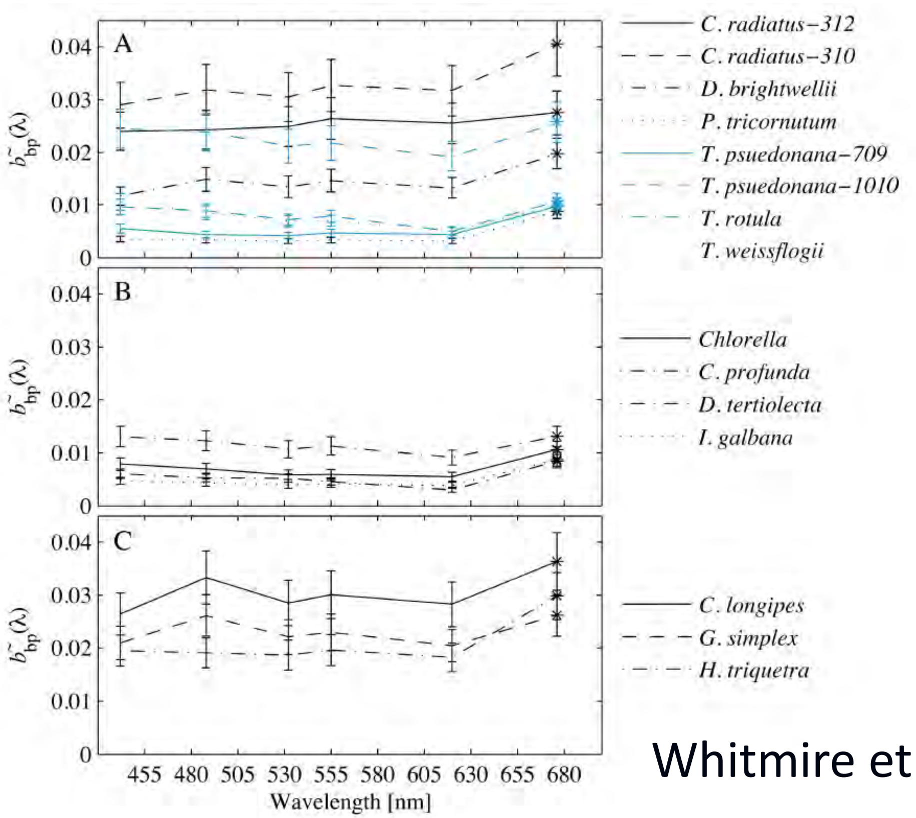

Whitmire et al. 2009

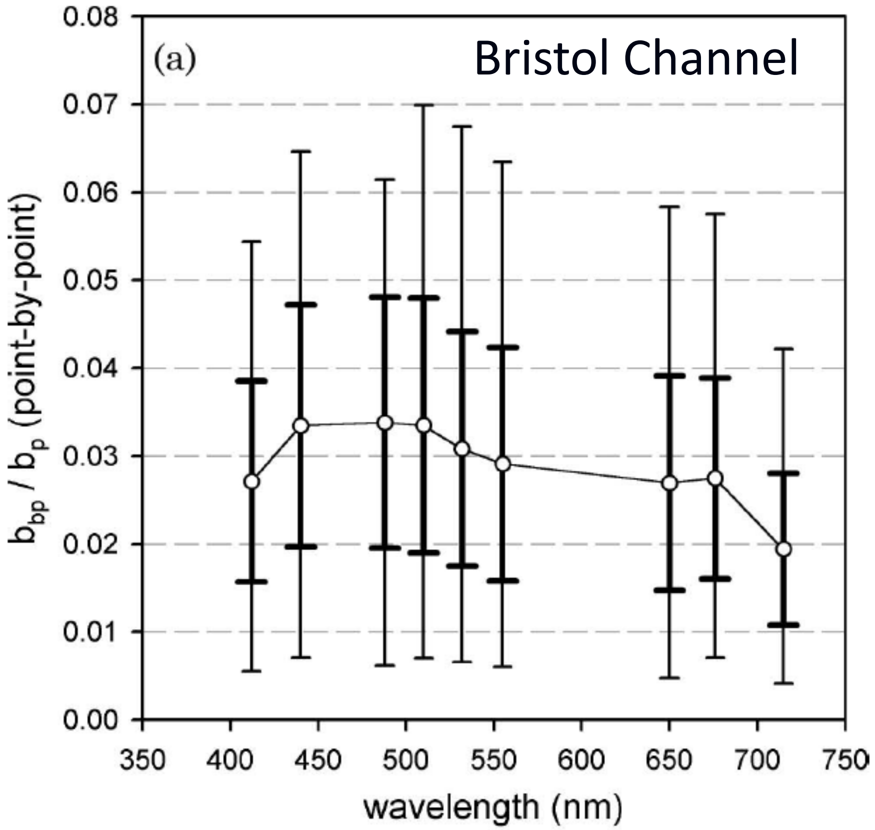

McKee et al. 2009

Anomalous dispersion

Spectral and angular scattering intensity of a particle is principally dependent on:

- size relative to λ
- complex refractive index relative to the medium $(n - in')$

Anomalous dispersion describes how particle absorption alters the refractive index spectrum,

i.e., if you change a_p, you will change b_p, b_{bp}

Synechocystis

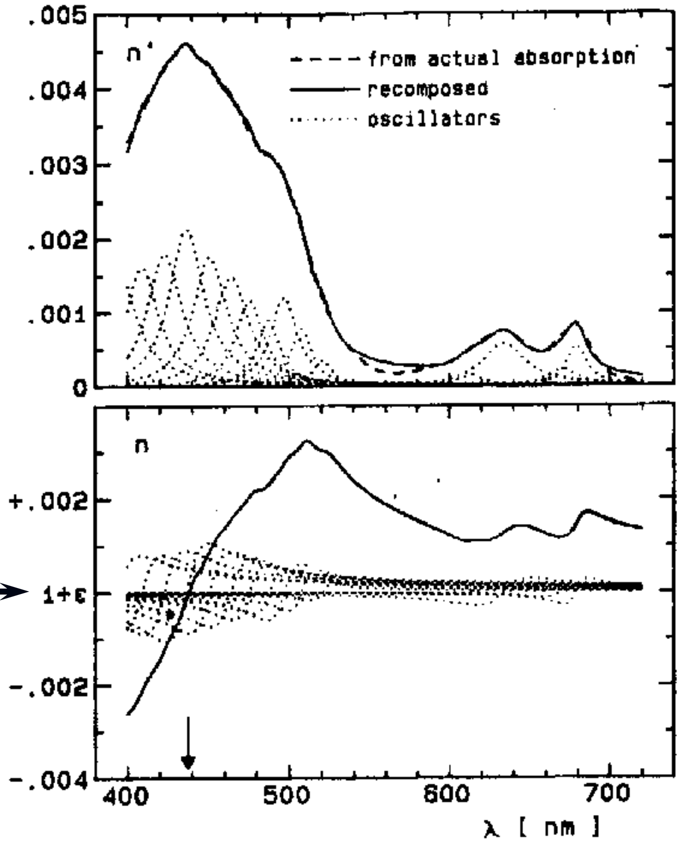

Stramski et al. 1988

backscattering around absorption peak

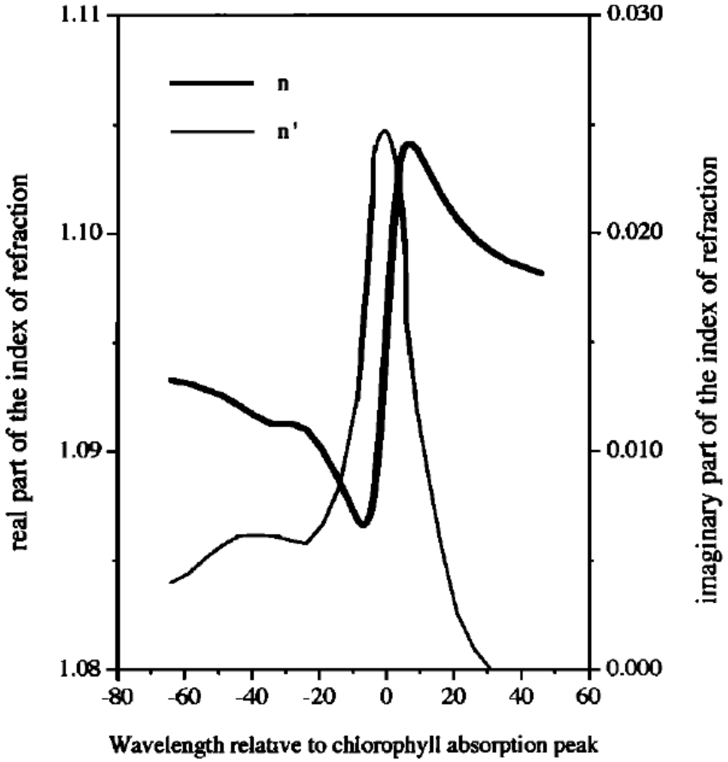

Zaneveld and Kitchen 1995

Near β(180), coherent scattering – the "glory"

Phases interact in a constructive way to enhance scattering near 180 deg

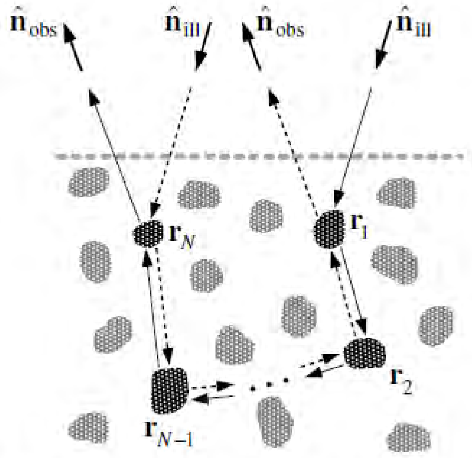

Figure 3.3. Schematic explanation of coherent backscattering.

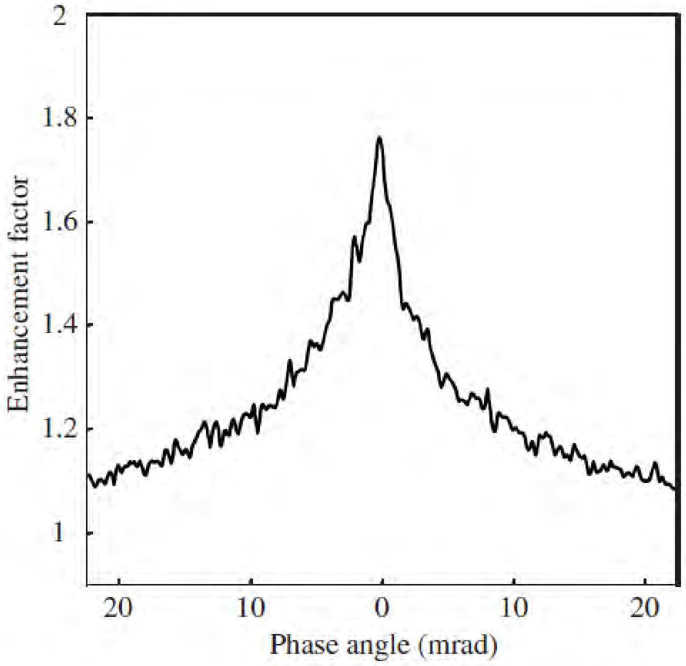

Figure 3.5. Angular profile of the coherent backscattering peak produced by a 1500-μm-thick slab of 9.6 vol% of 0.215-μm-diameter polystyrene spheres suspended in water. The slab was illuminated by a linearly polarized laser beam (λ_1 = 633 nm) incident normally to the slab surface. The scattering plane (i.e., the plane through the vectors $\hat{\mathbf{n}}_{ill}$ and $\hat{\mathbf{n}}_{obs}$, Fig. 3.3) was fixed in such a way that the electric vector of the incident beam vibrated in this plane. The detector measured the component of the backscattered intensity polarized parallel to the scattering plane. The curve shows the profile of the backscattered intensity normalized by the intensity of the incoherent background as a function of the phase angle. The latter is defined as the angle between the vectors $\hat{\mathbf{n}}_{obs}$ and $-\hat{\mathbf{n}}_{ill}$. (After van Albada *et al.* 1987.)

Mishchenko et al. 2002

Polarized Scattering

In 1864, Maxwell wrote "A dynamical theory of the electromagnetic field", where he first proposed that light was in fact undulations in the same medium that is the cause of electric and magnetic phenomena.

Maxwell derived a wave form of the electric and magnetic equations, revealing the wave-like nature of electric and magnetic fields, and their symmetry. His work in producing a unified model of electromagnetism is considered to be one of the greatest advances in physics.

And then there was light…

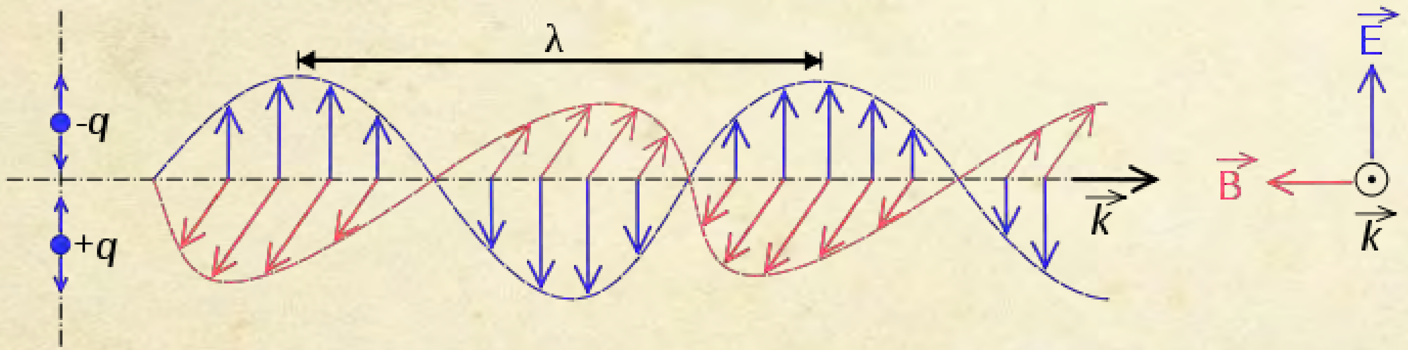

Polarization of light is defined by E only

4-component Stokes vector and polarization parameters

I is the radiance intensity (this is what the human eye sees)

$\oplus$ Q is the amount of radiation that is polarized in the 0/90^0 orientation

$\otimes$ U is the amount of radiation polarized in the +/-45^0 orientation

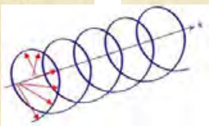

V is the amount of radiation that is right or left circularly polarized

DOP= Degree of polarization= $\sqrt{Q^2+U^2+V^2}/I$

DOLP = Degree of linear polarization = $\sqrt{Q^2+U^2}/I$

DOCP = Degree of circular polarization = $|V|/I$

Orientation of plane of polarization = $\chi = \tan^{-1}(U/Q)/2$

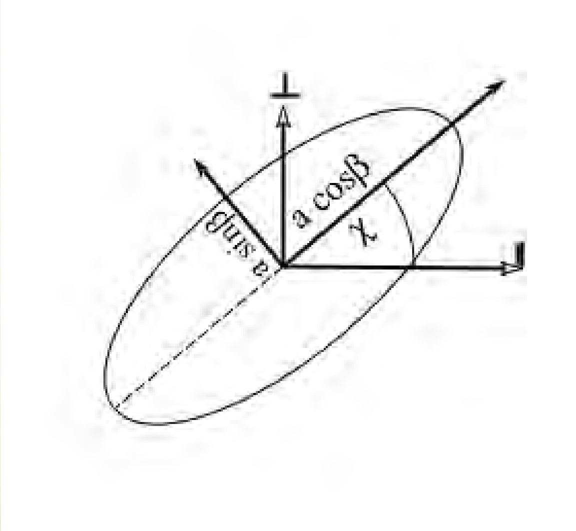

The four components of the Stokes vector are all real numbers and satisfy the relation:

$$I^2 = Q^2 + U^2 + V^2$$

Polarized scattering – Mueller matrix

VSF **V, H linear polarization** **particle orientation**

Stokes vector describing intensity and polarization of incident beam

$$\begin{pmatrix} I_s \\ Q_s \\ U_s \\ V_s \end{pmatrix} = \frac{1}{k^2 r^2} \begin{pmatrix} S_{11} & S_{12} & \cancel{S_{13}} & \cancel{S_{14}} \\ S_{21} & S_{22} & \cancel{S_{23}} & \cancel{S_{24}} \\ \cancel{S_{31}} & \cancel{S_{32}} & S_{33} & \cancel{S_{34}} \\ \cancel{S_{41}} & \cancel{S_{42}} & \cancel{S_{43}} & S_{44} \end{pmatrix} \begin{pmatrix} I_i \\ Q_i \\ U_i \\ V_i \end{pmatrix}$$

total intensity

$\oplus$

$\otimes$

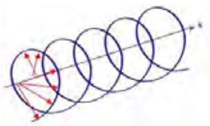

SCATTERED BEAM

particle nonsphericity

INCIDENT BEAM

(θ, λ)

Mueller matrix
(for a “scattering event”)

For randomly oriented particles with symmetry

Every element has wavelength and angular dependencies

Mueller matrix: Voss and Fry (1984)

All normalized to S11 Modeled for very small particles (Rayleigh)

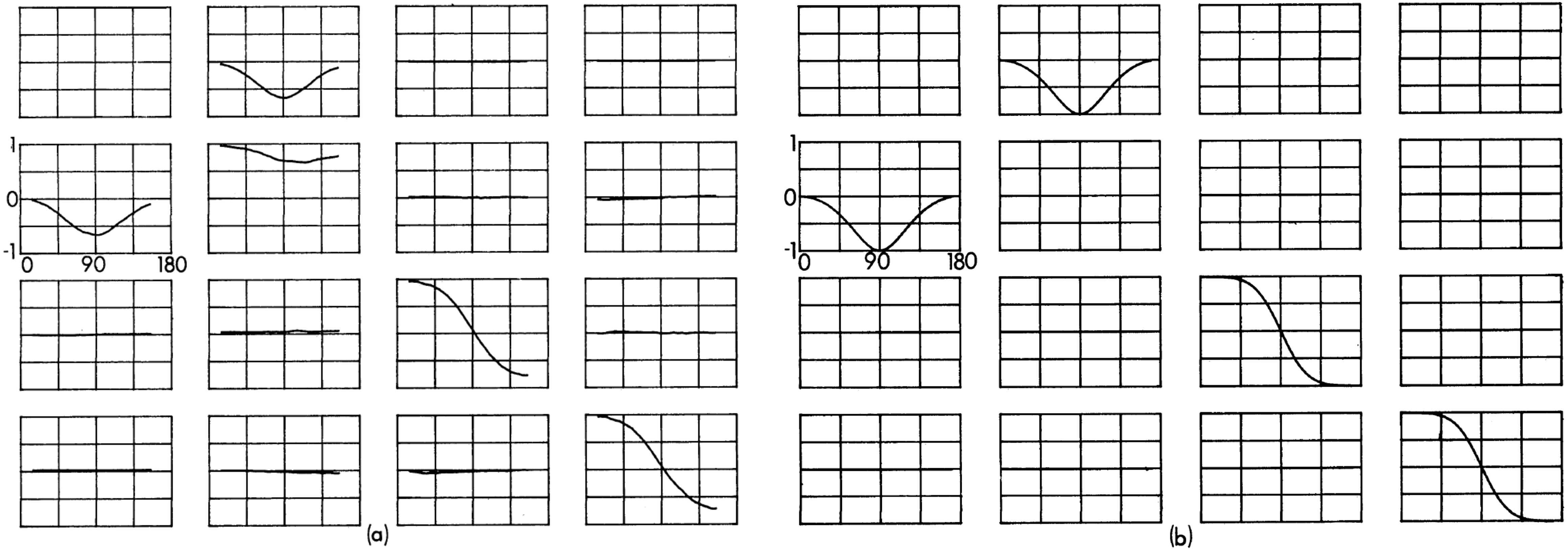

Averaged from Atlantic and Pacific Oceans

> 60 samples

Polarization: Measuring the Mueller matrix

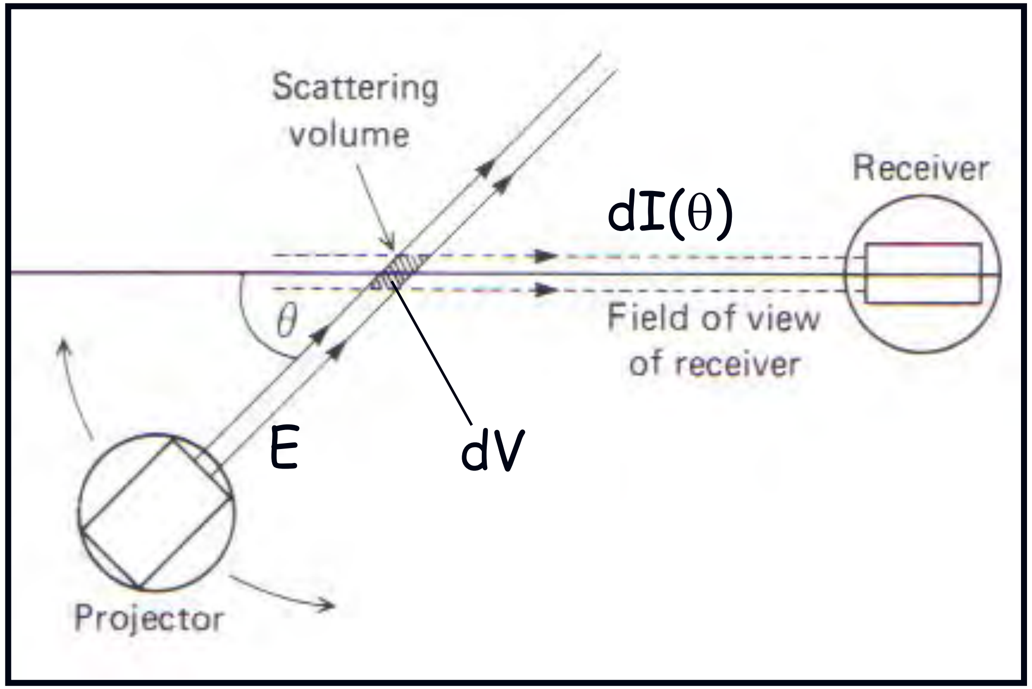

Bohren and Huffman 1983

Table 13.1 Combinations of Scattering Matrix Elements That Result from Measurements with a Polarizer P_s Forward of the Scattering Medium and an Analyzer A_s aft[a]

U	U	S_{11}	$P_\perp$	U	$\frac{1}{2}(S_{11} - S_{12})$
U	$A_\parallel$	$\frac{1}{2}(S_{11} + S_{21})$	$P_\perp$	$A_\parallel$	$\frac{1}{4}(S_{11} - S_{12} + S_{21} - S_{22})$
U	$A_\perp$	$\frac{1}{2}(S_{11} - S_{21})$	$P_\perp$	$A_\perp$	$\frac{1}{4}(S_{11} - S_{12} - S_{21} + S_{22})$
U	A_+	$\frac{1}{2}(S_{11} + S_{31})$	$P_\perp$	A_+	$\frac{1}{4}(S_{11} - S_{12} + S_{31} - S_{32})$
U	A_-	$\frac{1}{2}(S_{11} - S_{31})$	$P_\perp$	A_-	$\frac{1}{4}(S_{11} - S_{12} - S_{31} + S_{32})$
U	A_R	$\frac{1}{2}(S_{11} - S_{41})$	$P_\perp$	A_R	$\frac{1}{4}(S_{11} - S_{12} - S_{41} + S_{42})$
U	A_L	$\frac{1}{2}(S_{11} + S_{41})$	$P_\perp$	A_L	$\frac{1}{4}(S_{11} - S_{12} + S_{41} - S_{42})$
$P_\parallel$	U	$\frac{1}{2}(S_{11} + S_{12})$	P_+	U	$\frac{1}{2}(S_{11} + S_{13})$
$P_\parallel$	$A_\parallel$	$\frac{1}{4}(S_{11} + S_{12} + S_{21} + S_{22})$	P_+	$A_\parallel$	$\frac{1}{4}(S_{11} + S_{13} + S_{21} + S_{23})$
$P_\parallel$	$A_\perp$	$\frac{1}{4}(S_{11} + S_{12} - S_{21} - S_{22})$	P_+	$A_\perp$	$\frac{1}{4}(S_{11} + S_{13} - S_{21} - S_{23})$
$P_\parallel$	A_+	$\frac{1}{4}(S_{11} + S_{12} + S_{31} + S_{32})$	P_+	A_+	$\frac{1}{4}(S_{11} + S_{13} + S_{31} + S_{33})$
$P_\parallel$	A_-	$\frac{1}{4}(S_{11} + S_{12} - S_{31} - S_{32})$	P_+	A_-	$\frac{1}{4}(S_{11} + S_{13} - S_{31} - S_{33})$
$P_\parallel$	A_R	$\frac{1}{4}(S_{11} + S_{12} - S_{41} - S_{42})$	P_+	A_R	$\frac{1}{4}(S_{11} + S_{13} - S_{41} - S_{43})$
$P_\parallel$	A_L	$\frac{1}{4}(S_{11} + S_{12} + S_{41} + S_{42})$	P_+	A_L	$\frac{1}{4}(S_{11} + S_{13} + S_{41} + S_{43})$
P_-	U	$\frac{1}{2}(S_{11} - S_{13})$	P_L	U	$\frac{1}{2}(S_{11} - S_{14})$
P_-	$A_\parallel$	$\frac{1}{4}(S_{11} - S_{13} + S_{21} - S_{23})$	P_L	$A_\parallel$	$\frac{1}{4}(S_{11} - S_{14} + S_{21} - S_{24})$
P_-	$A_\perp$	$\frac{1}{4}(S_{11} - S_{13} - S_{21} + S_{23})$	P_L	$A_\perp$	$\frac{1}{4}(S_{11} - S_{14} - S_{21} + S_{24})$
P_-	A_+	$\frac{1}{4}(S_{11} - S_{13} + S_{31} - S_{33})$	P_L	A_+	$\frac{1}{4}(S_{11} - S_{14} + S_{31} - S_{34})$
P_-	A_-	$\frac{1}{4}(S_{11} - S_{13} - S_{31} + S_{33})$	P_L	A_-	$\frac{1}{4}(S_{11} - S_{14} - S_{31} + S_{34})$
P_-	A_R	$\frac{1}{4}(S_{11} - S_{13} - S_{41} + S_{43})$	P_L	A_R	$\frac{1}{4}(S_{11} - S_{14} - S_{41} + S_{44})$
P_-	A_L	$\frac{1}{4}(S_{11} - S_{13} + S_{41} - S_{43})$	P_L	A_L	$\frac{1}{4}(S_{11} - S_{14} + S_{41} - S_{44})$
P_R	U	$\frac{1}{2}(S_{11} + S_{14})$			
P_R	$A_\parallel$	$\frac{1}{4}(S_{11} + S_{14} + S_{21} + S_{24})$			
P_R	$A_\perp$	$\frac{1}{4}(S_{11} + S_{14} - S_{21} - S_{24})$			
P_R	A_+	$\frac{1}{4}(S_{11} + S_{14} + S_{31} + S_{34})$			
P_R	A_-	$\frac{1}{4}(S_{11} + S_{14} - S_{31} - S_{34})$			
P_R	A_R	$\frac{1}{4}(S_{11} + S_{14} - S_{41} - S_{44})$			
P_R	A_L	$\frac{1}{4}(S_{11} + S_{14} + S_{41} + S_{44})$			

= S_{11} for sphere goniometer

$\frac{S_{12}}{S_{11}}$ = degree of linear polar

See p. 65 and p. 112

$S_{21} = S_{12}$, $S_{11} = S_{22}$ for sp

[a] U indicates the absence of a polarizer or analyzer.

Voss and Fry (1984): Mueller matrix

MASC-POLMOD

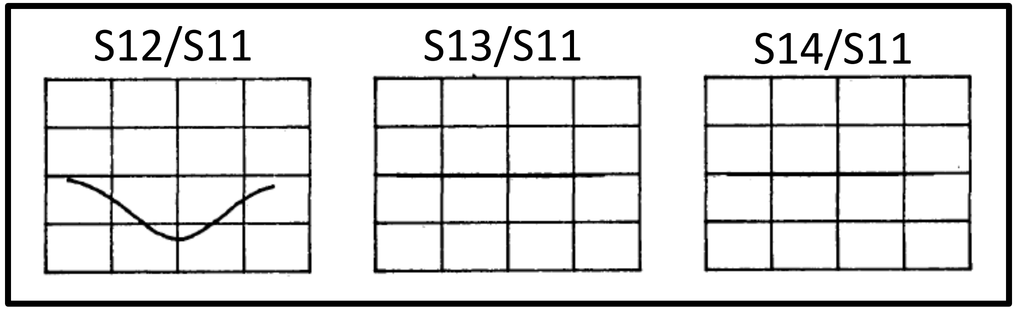

Degree of Linear Polarization

DoLP = -S12 / S11
= -(H-V)/(H+V)

H = ½(S11 + S12)
V = ½(S11 – S12)

4 positions

1 - OPEN

2 - DARK

3 - H ⟷

4 - V ↕

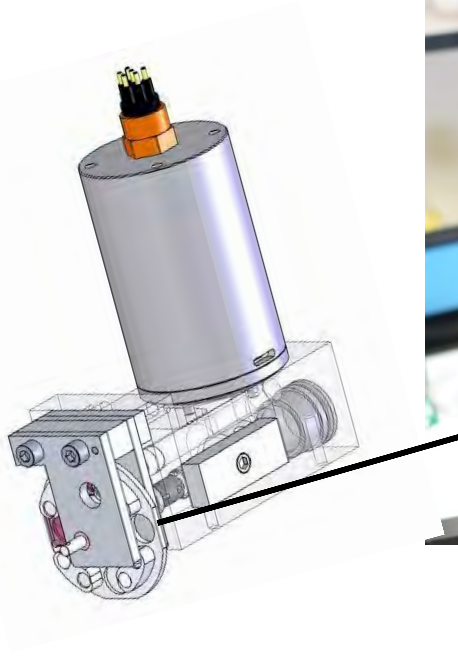

Curaçao, 2012: single vertical profile

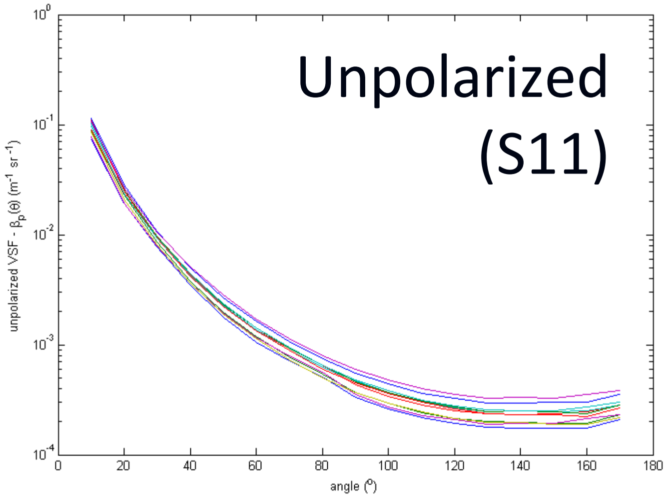

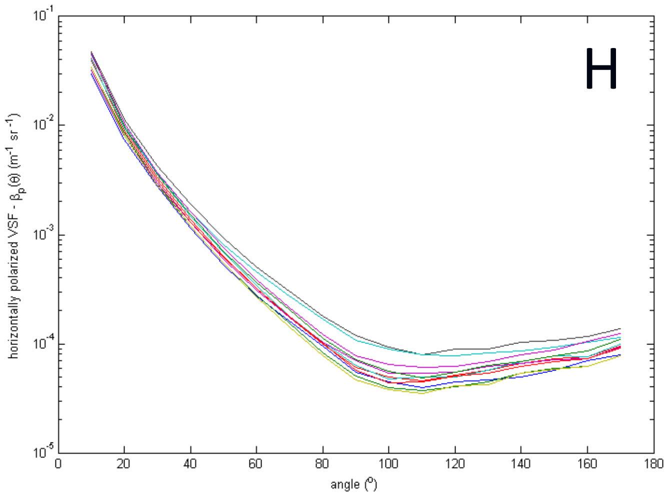

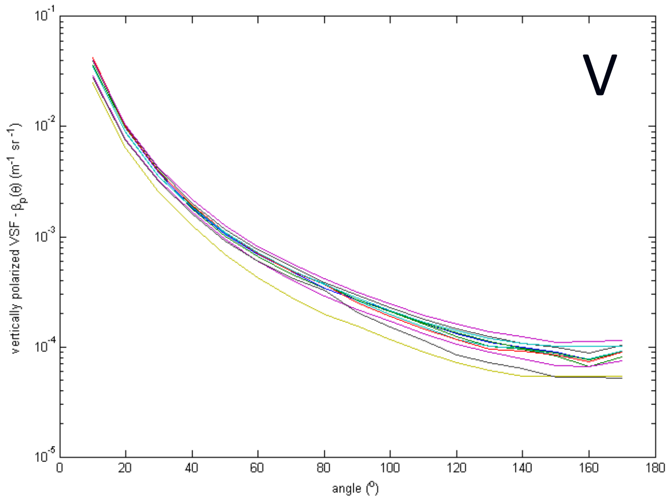

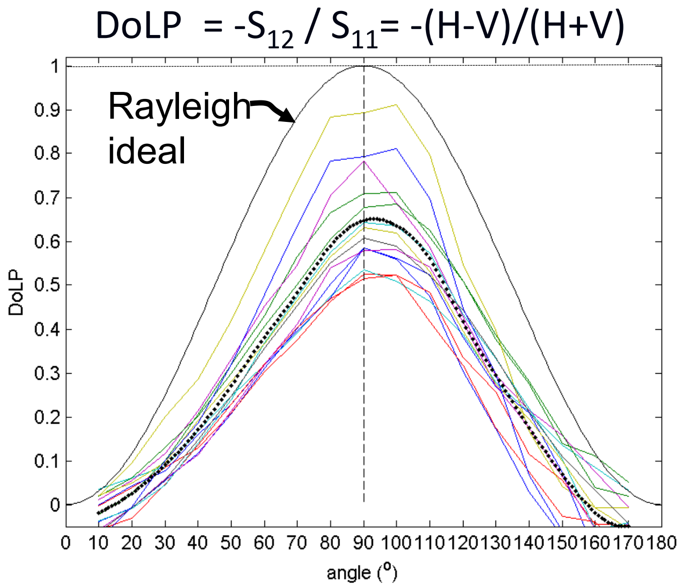

Cruise locations with MASCOT polarization measurements (since 2008)

- Ligurian Sea (S13 and S14 also)
- NY bight
- Santa Barbara Channel
- Gulf of Mexico
- Port Aransas, TX
- Florida Keys (2X)
- Curacao
- East Sound, WA
- Florida, Indian lagoon
- N. Lake Michigan

Polarized scattering measurements

VSF

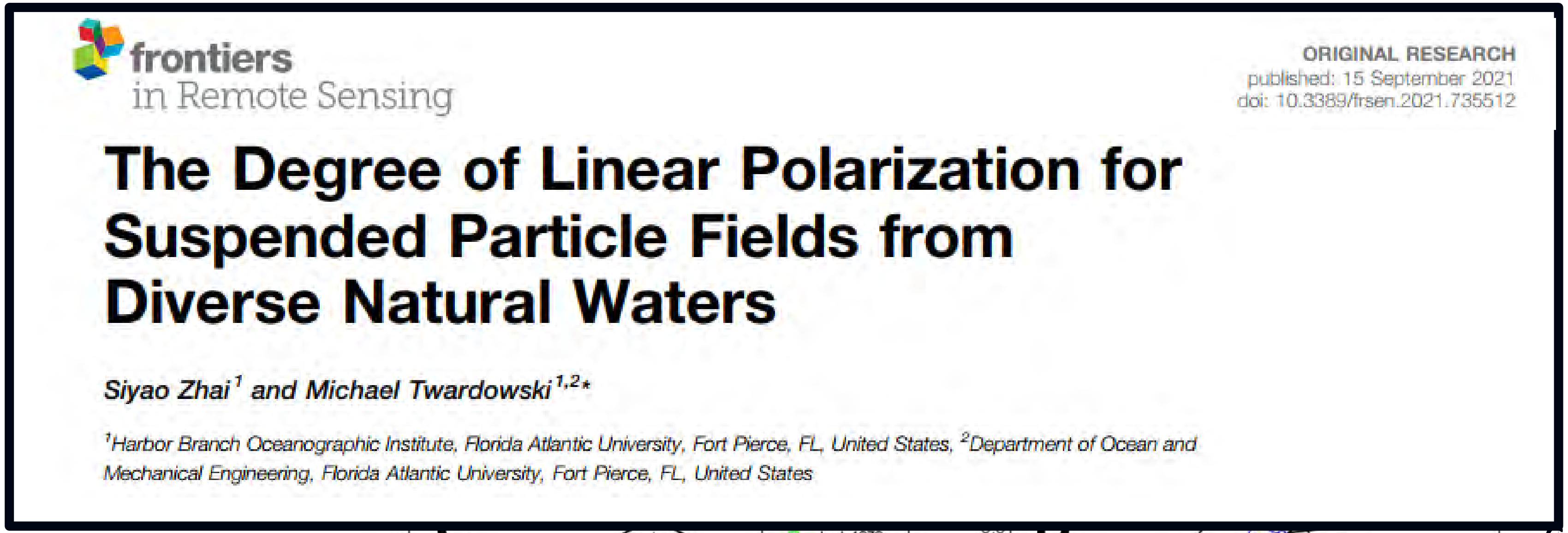
frontiers in Remote Sensing

ORIGINAL RESEARCH
published: 15 September 2021
doi: 10.3389/frsen.2021.735512

The Degree of Linear Polarization for Suspended Particle Fields from Diverse Natural Waters

*Siyao Zhai[1] and Michael Twardowski[1,2]**

[1]Harbor Branch Oceanographic Institute, Florida Atlantic University, Fort Pierce, FL, United States, [2]Department of Ocean and Mechanical Engineering, Florida Atlantic University, Fort Pierce, FL, United States

As of 2020, there were only 3 other measurements of S12/S11 for ocean water in the literature!

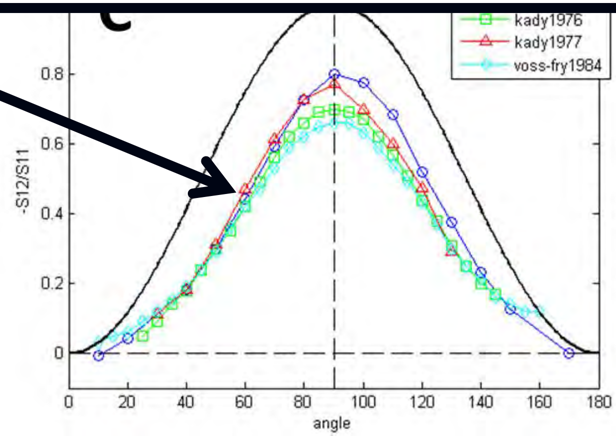

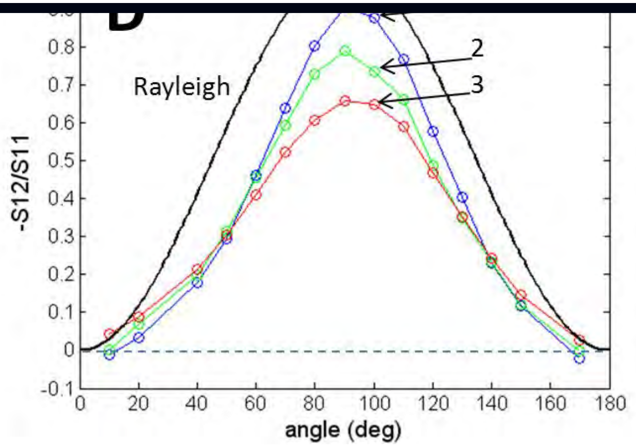

S12/S11: degree of linear polarization (DOLP)

Santa Barbara Channel, September 2008

Polarized scattering

phytoplankton species

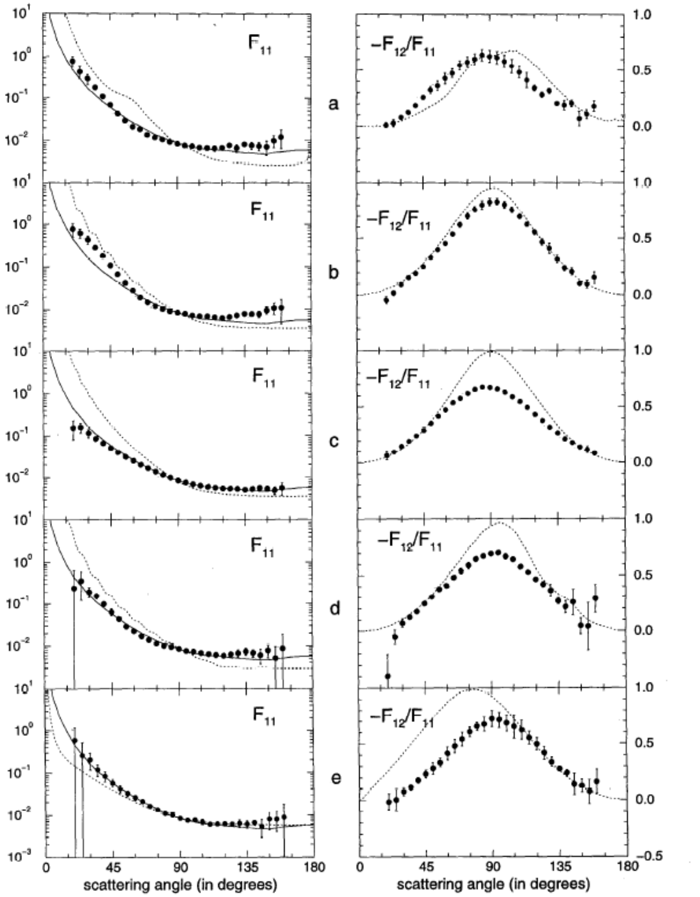

Fig. 6. The measured scattering functions, F_{11}, and ratios $-F_{12}/F_{11}$ are shown in the left and right panels, respectively (filled circles) for (a) *Microcystis acruginosa* without gas vacuoles, (b) *Microcystis aeruginosa* with gas vacuoles, (c) *Microcystis* sp., (d) *Phaeocystis,* and (e) *Volvox aureus.* Also plotted are the scattering function for San Diego Harbor (solid, left panels) and the results of Mie calculations (dashed, left and right panels). The $F_{11}(\theta)$ functions are scaled at 90° to the scattering function of San Diego Harbor. Errors are smaller than symbols if no error bar is indicated.

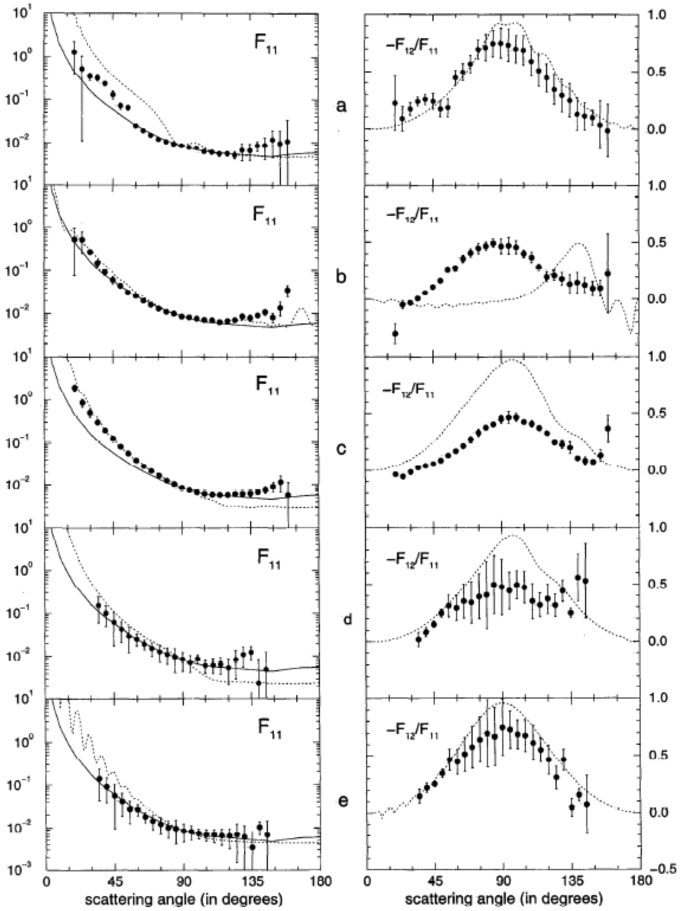

Fig. 8. Same as Fig. 6 for (a) *Astrionella formosa,* (b) *Selenastrum capricornutum,* (c) *Phaeodactylum,* (d) *Emiliania huxleyi* with coccoliths, and (e) *Emiliania huxleyi* without coccoliths.

sediment samples

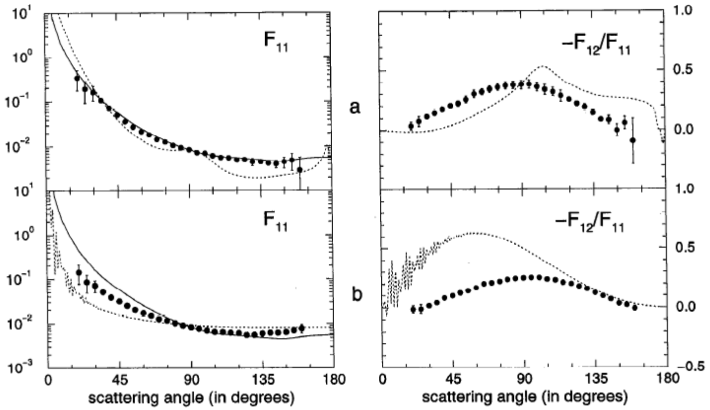

Fig. 9. Same as Fig. 6 for (a) Westerschelde silt with diameters ranging between 3 and 5 μm, and (b) Westerschelde silt with diameters ranging between 5 and 12 μm.

Included reflection corrections

Volten et al. (1998)

Contrast enhancement using polarization

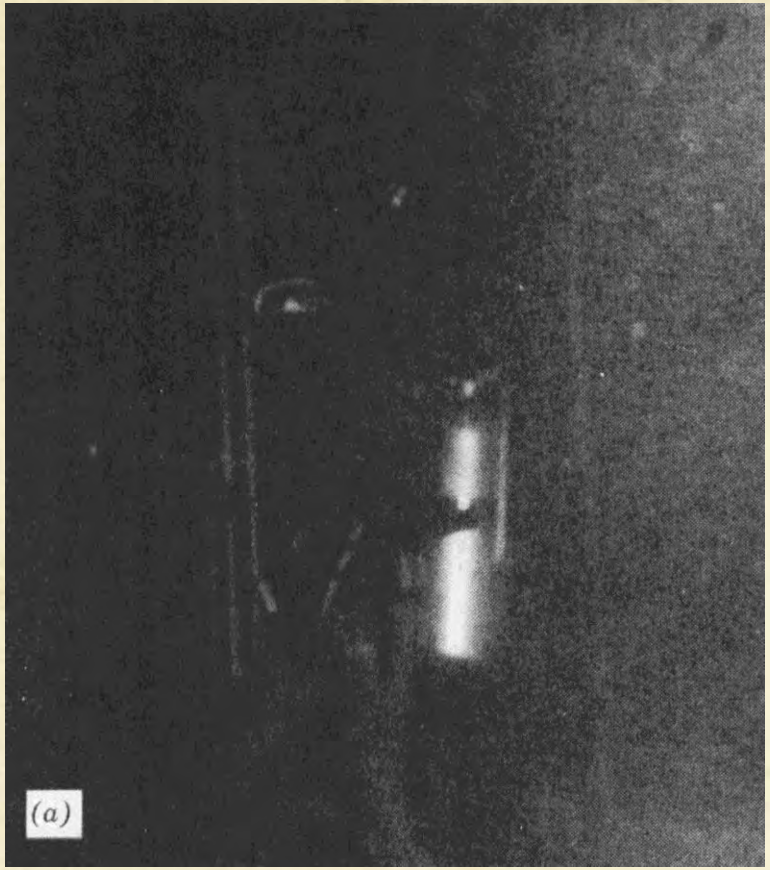

No polarization optics

Circular polarized light for illumination, circular analyzer for viewing

Seeing a target underwater is a function of

- character of incident light
- scattering properties of target
- capabilities of viewer
- contrast relative to background

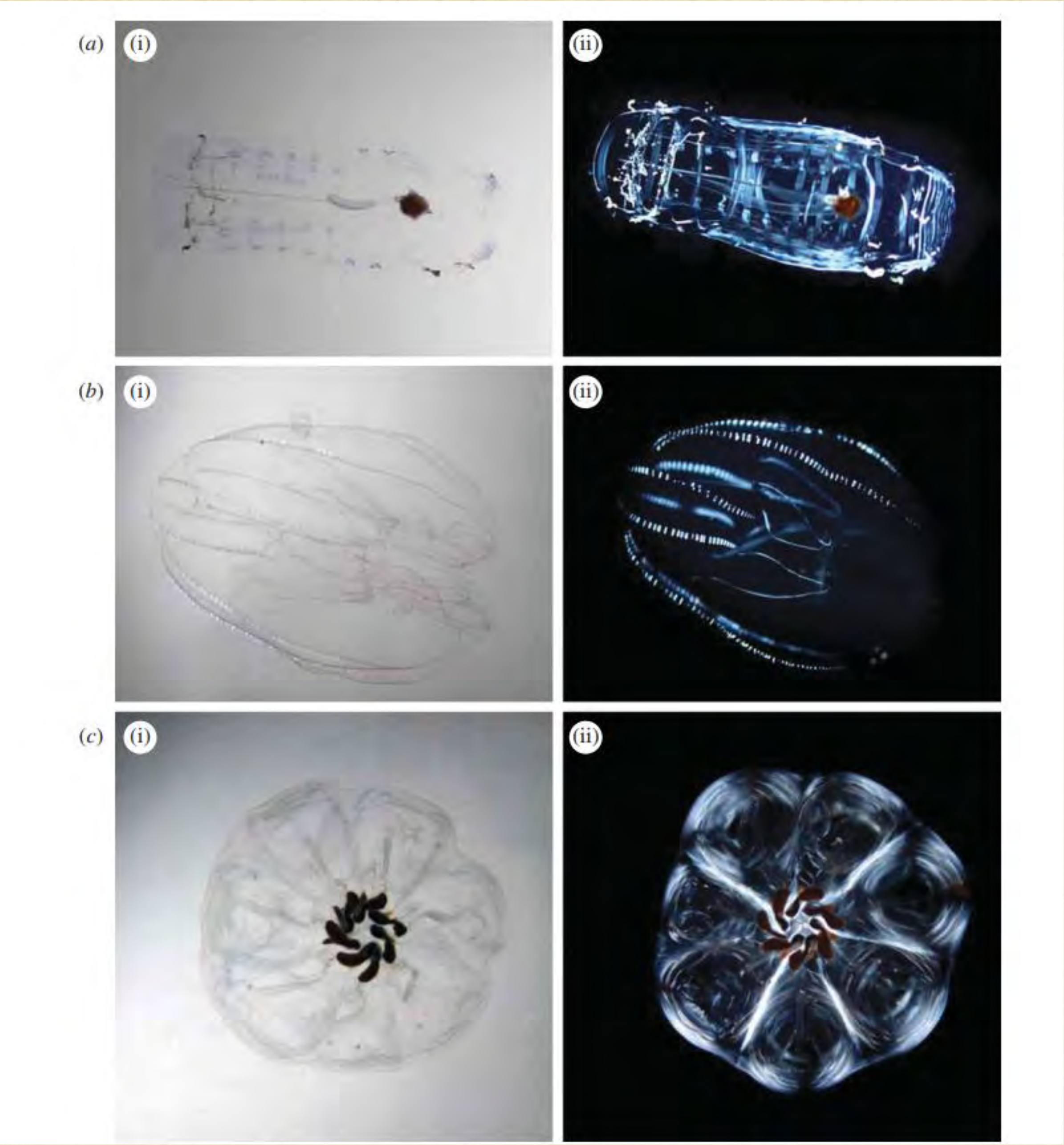

salp

ctenophore

salp

Between parallel polarizers

Between cross polarizers

Johnsen et al. 2011

Interpreting polarized scattering of particles

The angular and spectral characteristics of the Mueller scattering matrix parameters are a function of several properties of the particle population, including:

- Refractive index (n) composition
- Size distribution
- Particle shape
- Particle orientation

Much to be done!

New polarimeters on PACE!

Modeling scattering

Models for computing particle scattering

- Rayleigh
- Lorenz-Mie (also coated sphere, multi-layer sphere versions)
- van de Hulst anomalous diffraction approximation
- Geometric optics (IGOM, RBR)
- Discrete dipole approximation (DDA)

Combination pioneered by Yang, Kattawar for nonspherical particles

- Finite difference, time-domain (FDTD)
- Pseudo-spectral time-domain (PSTD)
- T-matrix (invariant imbedding, multiple sphere, extended boundary condition, many body iterative…)
- Surface roughness models….

Each has restrictions: size ranges, *n*, shape and symmetries

Why model particle scattering?

- Models can help qualitatively interpret scattering measurements in terms of particle characteristics
- Sometimes this can be done explicitly, which is known as an inversion

Degree of Linear Polarization

asymmetric hexahedra

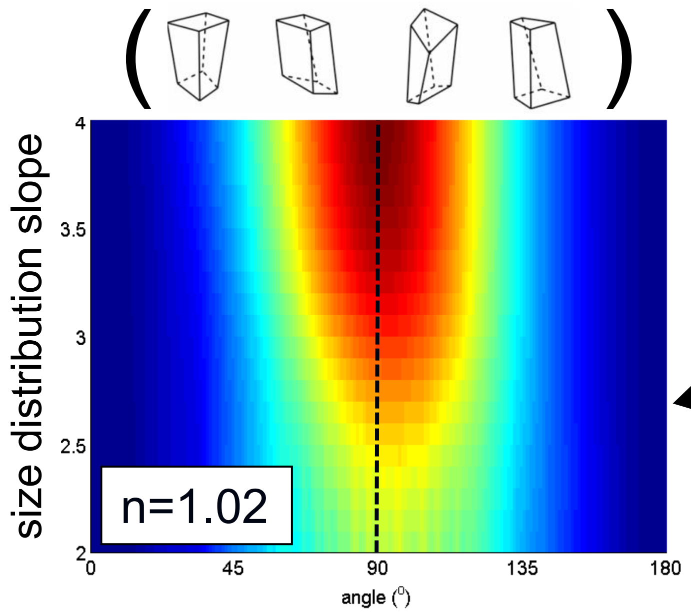

another view

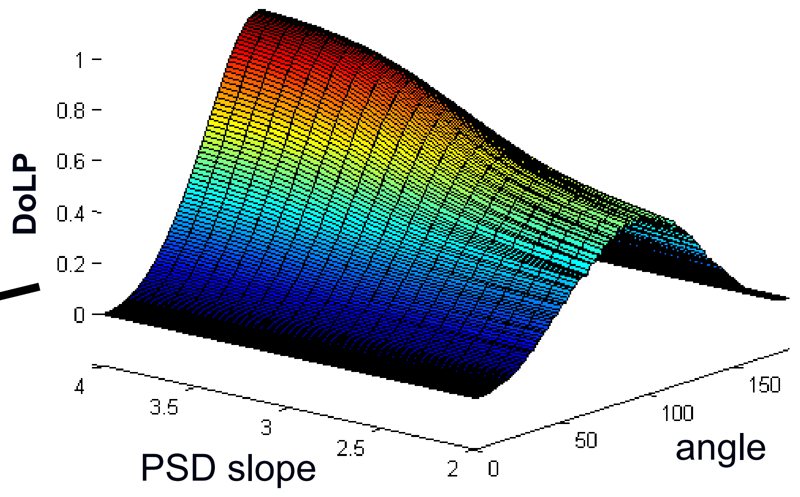

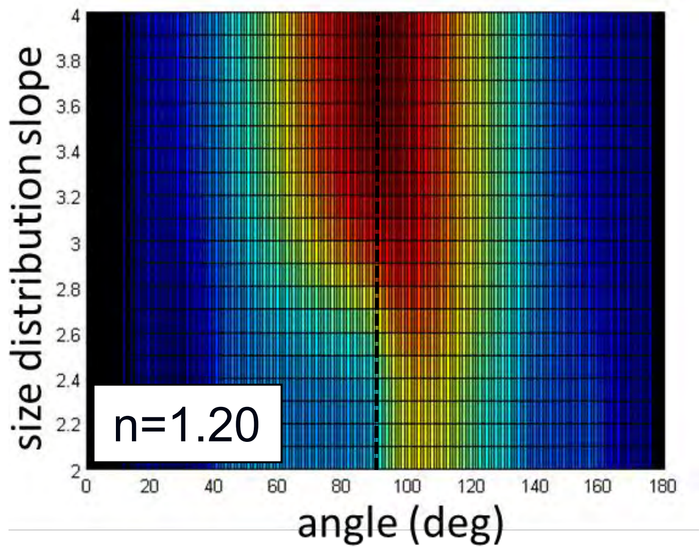

- **Increasing nonsphericity** lowers DoLP and shifts the DoLP peak to larger angles
- **Increasing refractive index** lowers DoLP, particularly for populations with relatively flat size distributions
- **As size distributions become increasingly flat**, the DoLP decreases and the maximum shifts to larger angles

Zhai and Twardowski (2021)

Interpretation and Application for Biogeochemical Properties

Scattering as a proxy for biogeochemical properties

EMPIRICAL

A common example → Beer's Law: IOP = ε[conc]

Some biogeochemical properties that influence scattering properties:

Chlorophyll and other phytoplankton pigments, particle size, particle density, particle composition, particle shape, particle concentration, total particle mass (TSM, SPM), POM/C, DOM/C, biomass, humic substances, hydrocarbons, $CaCO_3$,…

However: pools of particulate and dissolved matter can be highly variable and complex in composition, especially in coastal regions, usually confounding simple relationships.

How is c_p (or b_p or b_{bp}) directly linked to particles?

For population of spherical particles:

$$c_p = \pi \int_{r_{\min}}^{r_{\max}} Q_c(r,n)F(r)r^2 dr$$

- Q_c is attenuation efficiency
- F(r) is size distribution
- *n* is refractive index
- *r* is radius

Q_c, attenuation efficiency

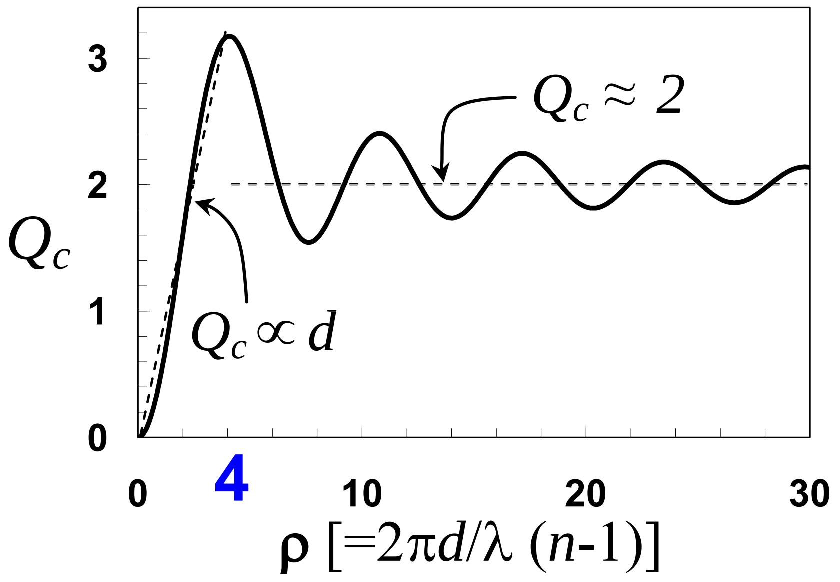

Can be modeled well for spheres with approximation from van de Hulst (1957, 1981)

Widely varying PSDs and particle *n* are the main reason why c_p-TSM, c_p-POC etc relationships vary

$$c_p \propto \begin{cases} \sum_{i=1}^{N} d_i^3, & \rho < 4 \xrightarrow{\propto} \text{total particle volume } (\textbf{TPV}) \\ \sum_{i=1}^{N} d_i^2, & \rho > 4 \xrightarrow{\propto} \text{total surface area } (\textbf{TSA}) \text{ OR total cross-sectional area } (\boldsymbol{\sum}\textbf{G}) \end{cases}$$

<u>See reviews</u>: Morel and Bricaud 1986 and Morel 1991

Example:
c_p and TSM

Reasonable correlations for each regression, but slopes are different for different water masses

EMPIRICAL

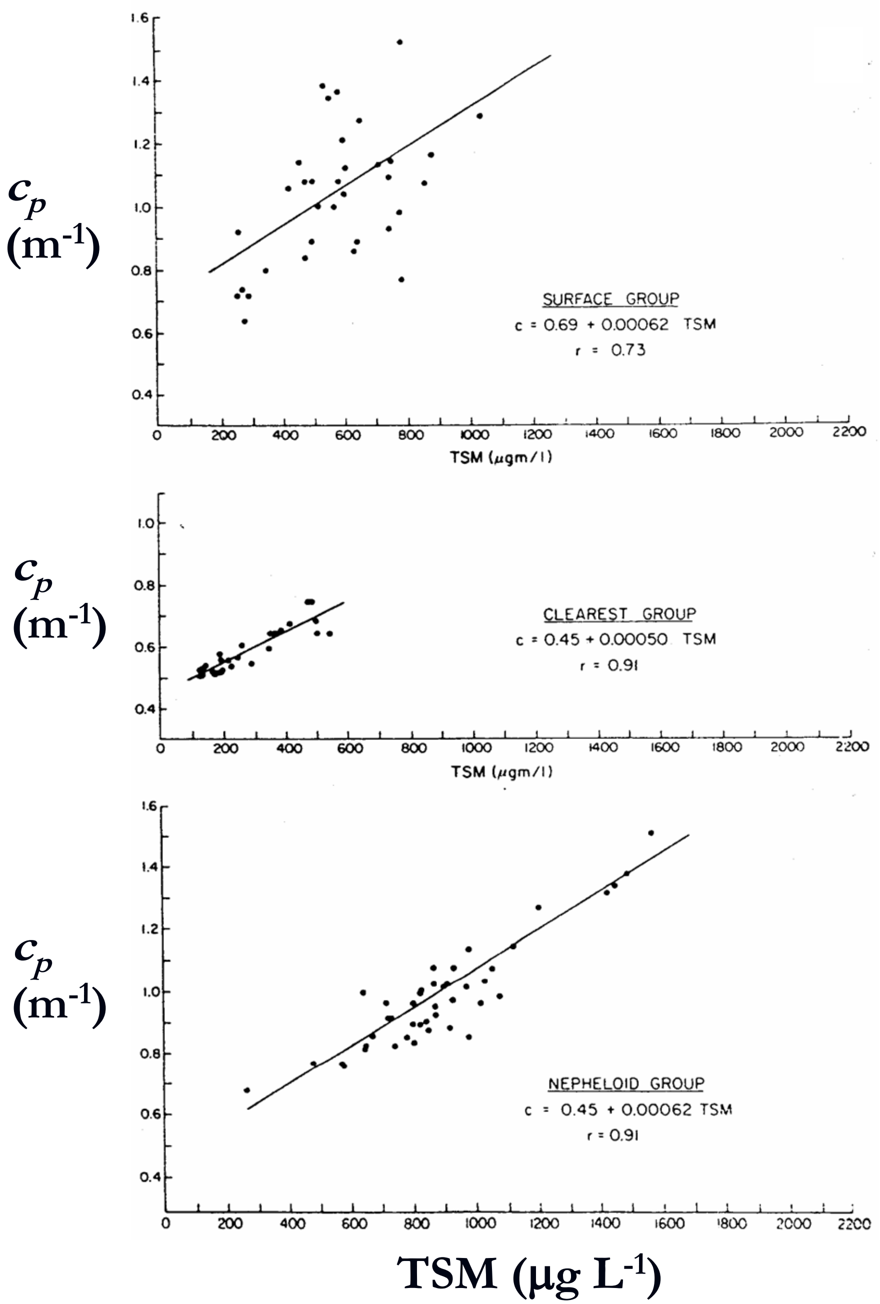

Peterson 1977

Assessment with first modern transmissometer

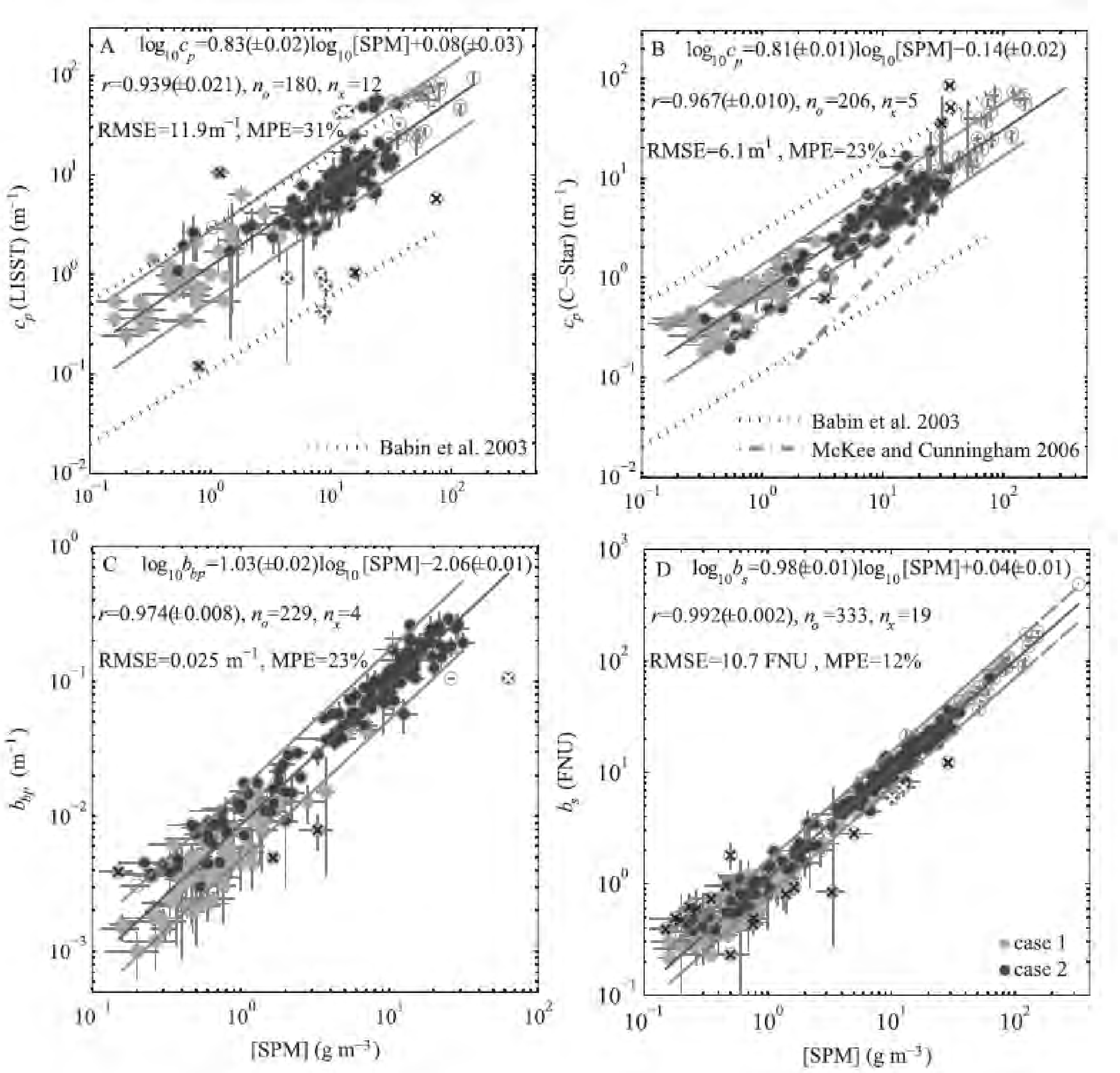

LISST

C-star

EMPIRICAL

ECO bb

NTU

Neukermans et al. (2012)

Published slopes for TSM-c_p and POC-c_p

Table 1. Published biogeochemical-optical data.

reference	**location**	**TSM** (μg-m/L) / c_p^a	**POC** (μg-m/L) / c_p^a
Peterson (1977)	OR coast - nepheloid layer	1600	
	OR coast - clearest waters	2000	
	OR coast - surface	1600	
Mishonov et al. (2000)	Ross Sea		674
	NABE		319
	APFZ		455
Bishop et al. (1999)	N. Pacific		195
Gardner et al. (1992)	N. Atlantic	1020	378
Gardner et al. (2001)	NW Atlantic - pre-hurricane 1996, surface	1000	400
	NW Atlantic - pre-hurricane 1996, subsurface	1100	105
	NW Atlantic - post-hurricane 1996, surface	770	455
	NW Atlantic - post-hurricane 1996, subsurface	2500	135
	NW Atlantic - Spring 1997, surface	770	
	NW Atlantic - Spring 1997, subsurface	1700	
	NW Atlantic - Spring 1997, mid-water		1250
Walsh et al. (1995)	Eq. Pac April, 1992	451	
	Eq. Pac October, 1992	642	
Walsh (1990)	Gulf of Mexico	660	
Mishonov et al. (2003)	BATS		323
	NABE (revised from Mishonov et al. 2000)		303

[a] – wavelength typically 660 nm

TSM/c_p range: ~450-2500

POC/c_p range: ~100-1250

EMPIRICAL

Analytical inversion to solve for bulk particle refractive index

$$\hat{n}_p(\widetilde{b}_{bp},\gamma) = 1 + \widetilde{b}_{bp}^{\,0.5377+0.4867(\gamma)^2}[1.4676 + 2.2950(\gamma)^2 + 2.3113(\gamma)^4].$$

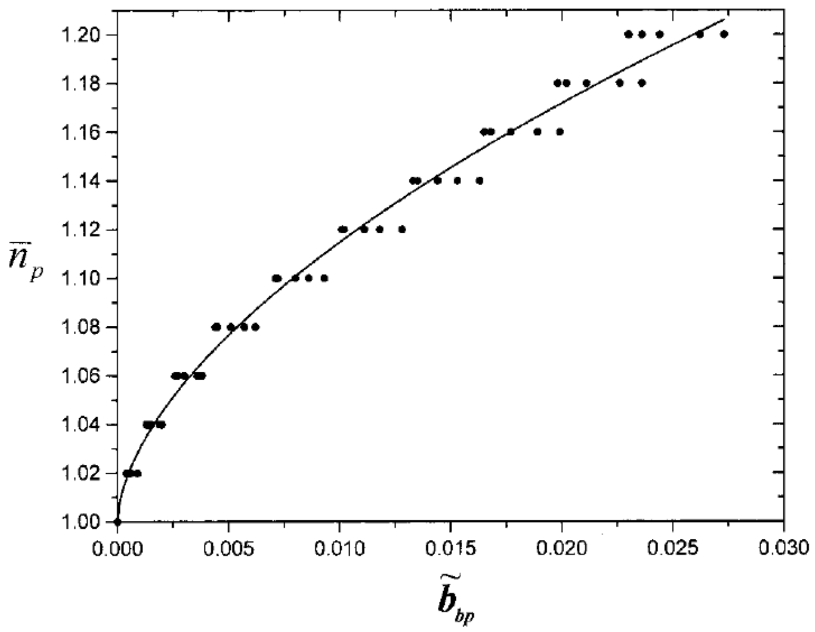

Inputs: b_{bp}/b_p, $c(\lambda)$

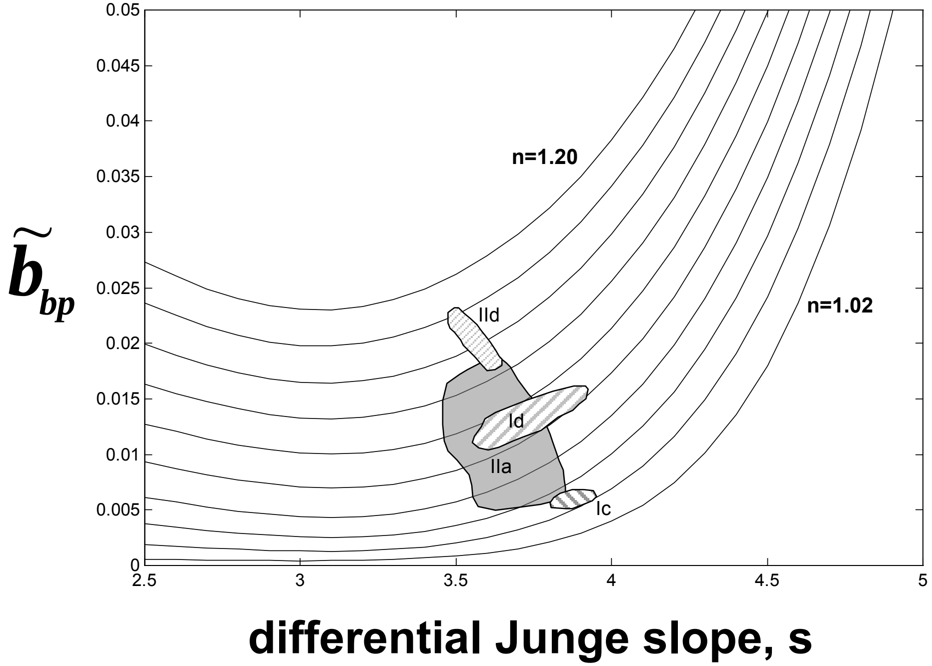

Based on Lorenz-Mie theory

Field data from Gulf of California

Typically gives reasonable values

Twardowski et al. (2001)

VSF inversion

Scripps Pier, 2008

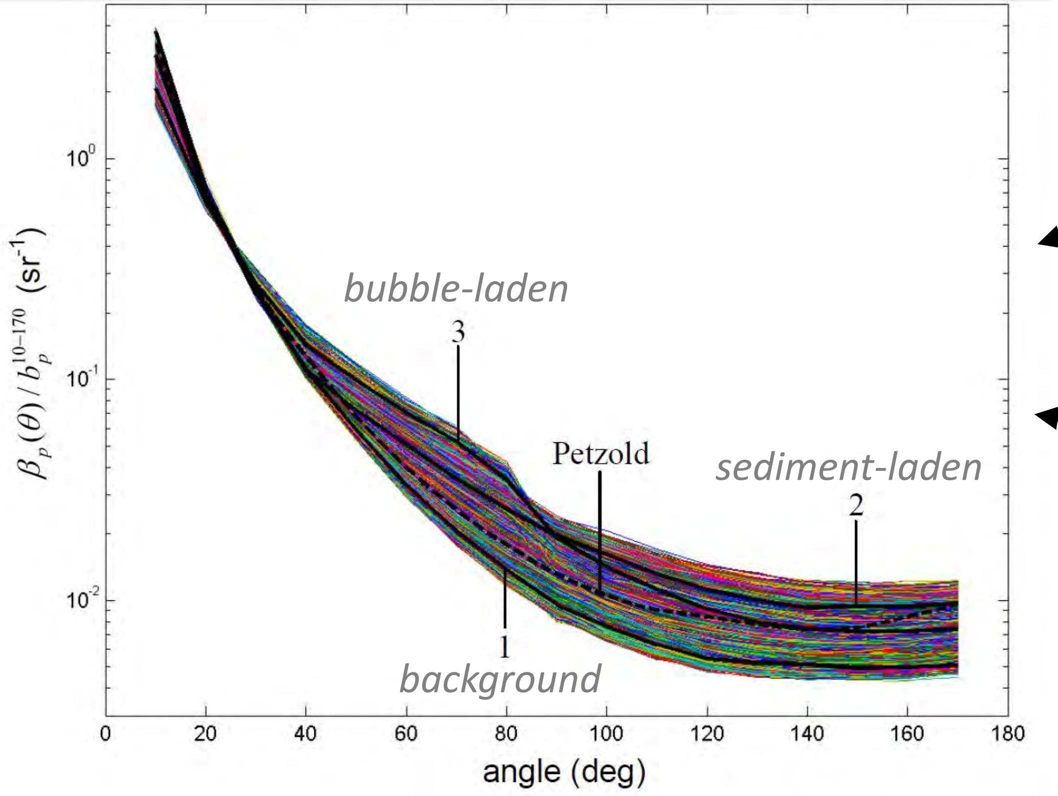

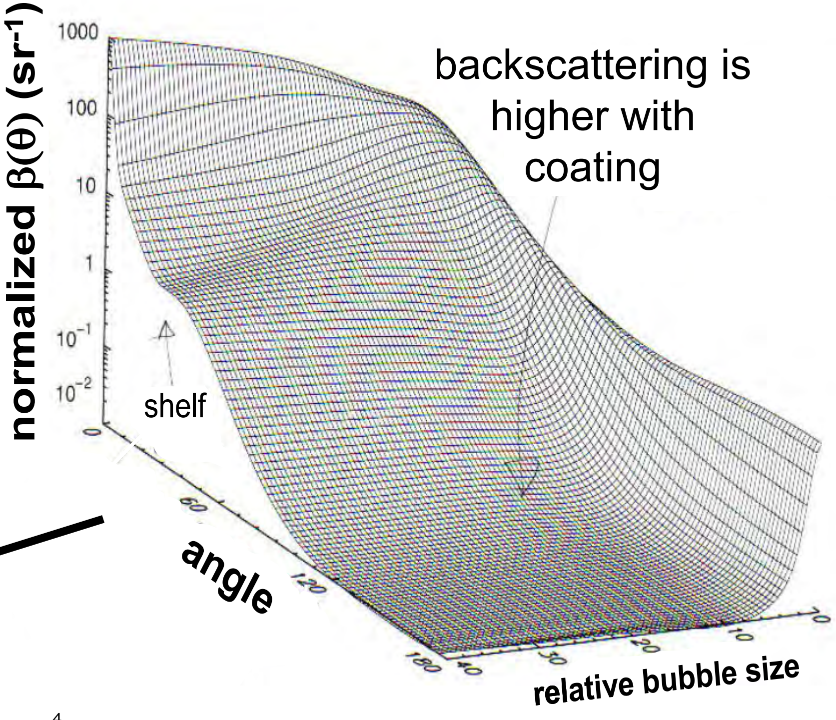

Fit to measured VSFs

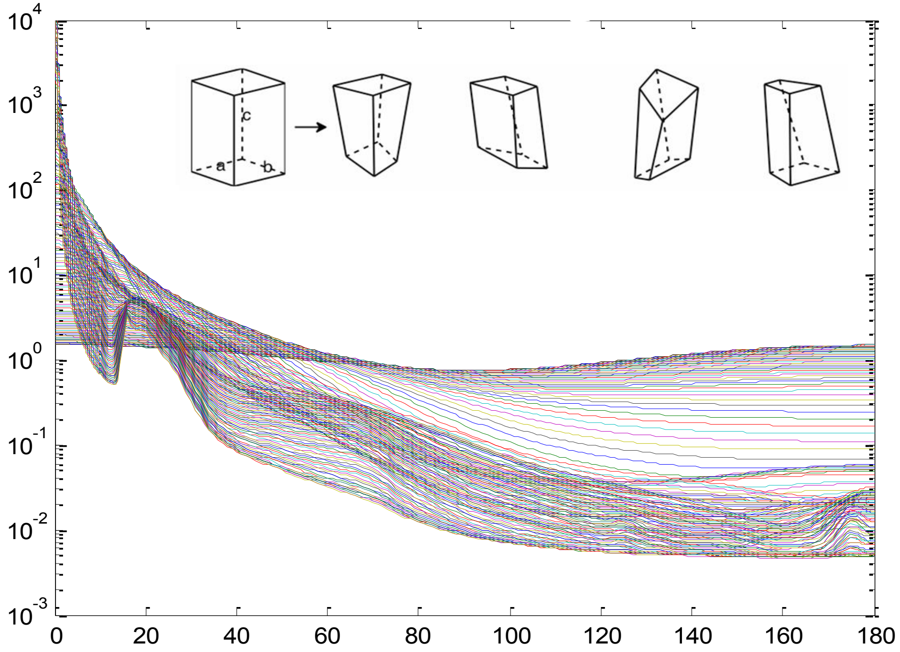

Twardowski et al. (2012)

Scripps Pier

Bubbles resolved with optics and acoustics

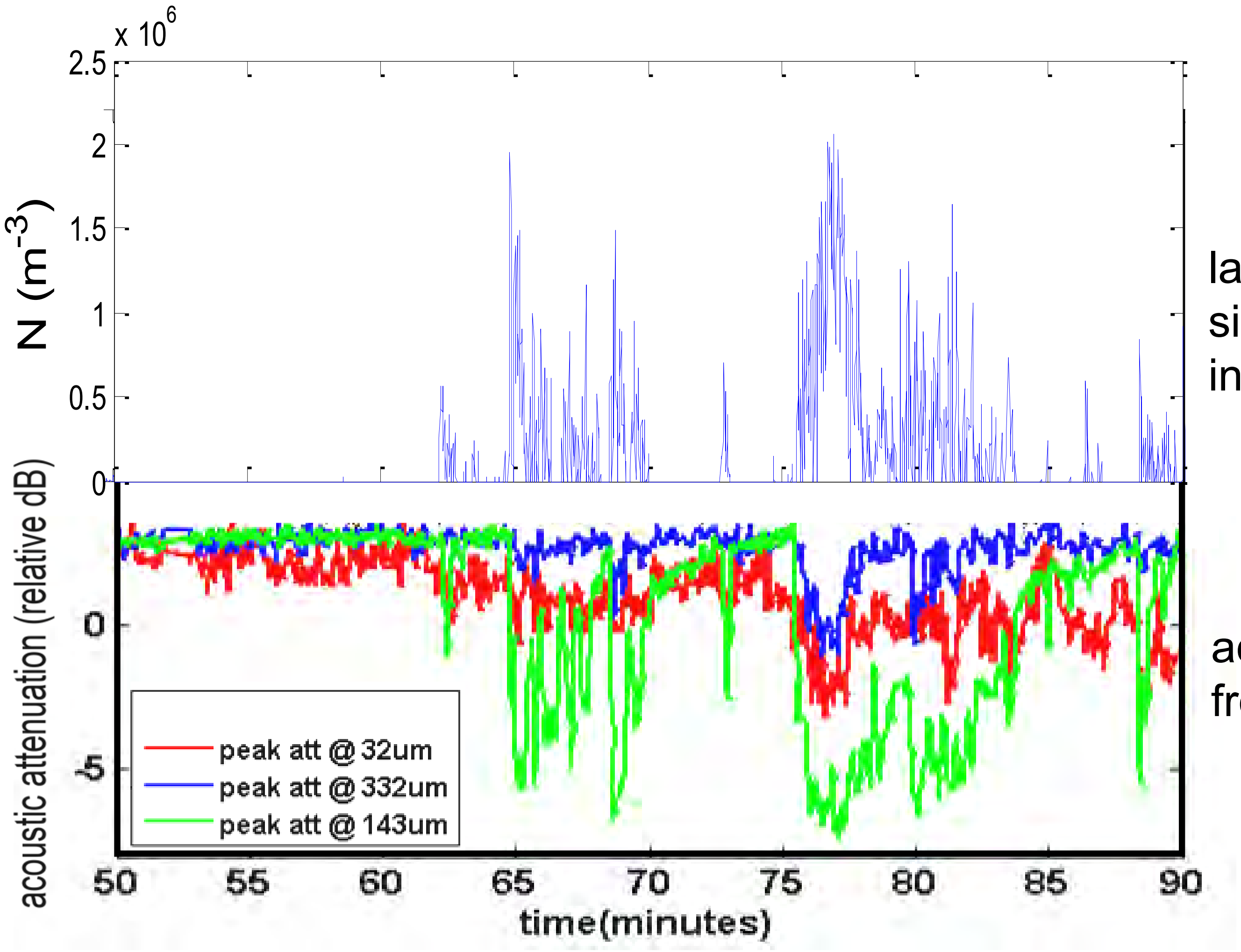

large bubble size class from inversion

acoustic signal from bubbles

Twardowski et al. (2012)

Relevance of VSF to ocean color

2 3

$$R_{rs}(0^-) = \frac{L_u(0^-)}{E_d(0^-)} \simeq \Psi\left(\frac{b_b}{a+b_b}\right)$$

Gordon (1975)
Morel and Prieur (1975)

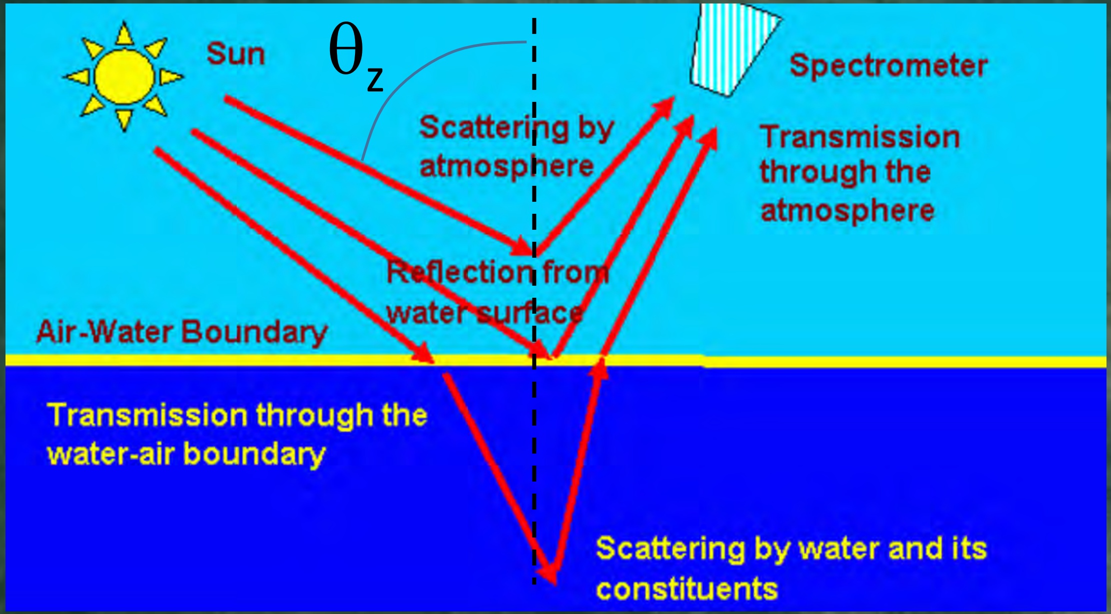

Algorithms…

1

$$L_w(\theta,\phi,\theta_z) \xrightarrow[\textit{BRDF}]{} L_{wN}(\pi, \theta_z = 0)$$

THIS IS CONTROLLED BY THE VSF

SO MUCH TO DO…!

For example…

- Spectral scattering:
  - hyperspectral bb
  - phase function shape
  - anomalous dispersion
- $\beta(180)$
- Scattering by nonspherical, complex particle populations
- Effect of scattering by nonrandomly oriented particles
- Anything to do with polarized scattering
- Remote algorithms from space including both ocean color and polarimetry that explicitly include VSF

BACKUP

Akashiwo Layer in Monterey Bay

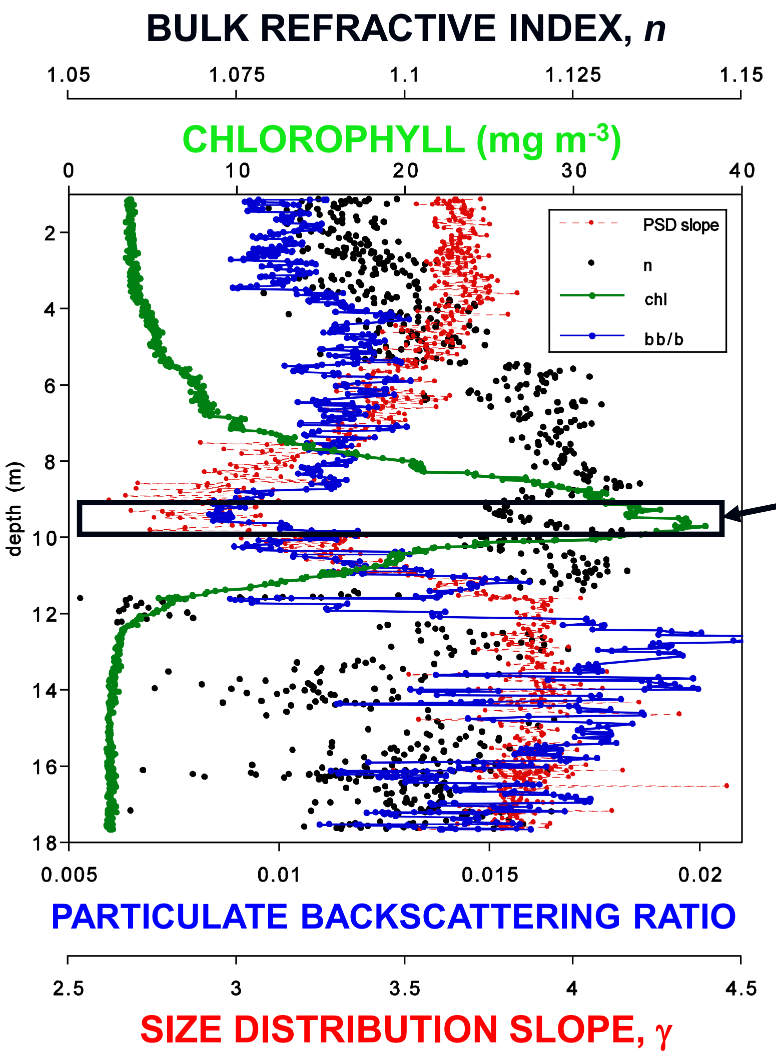

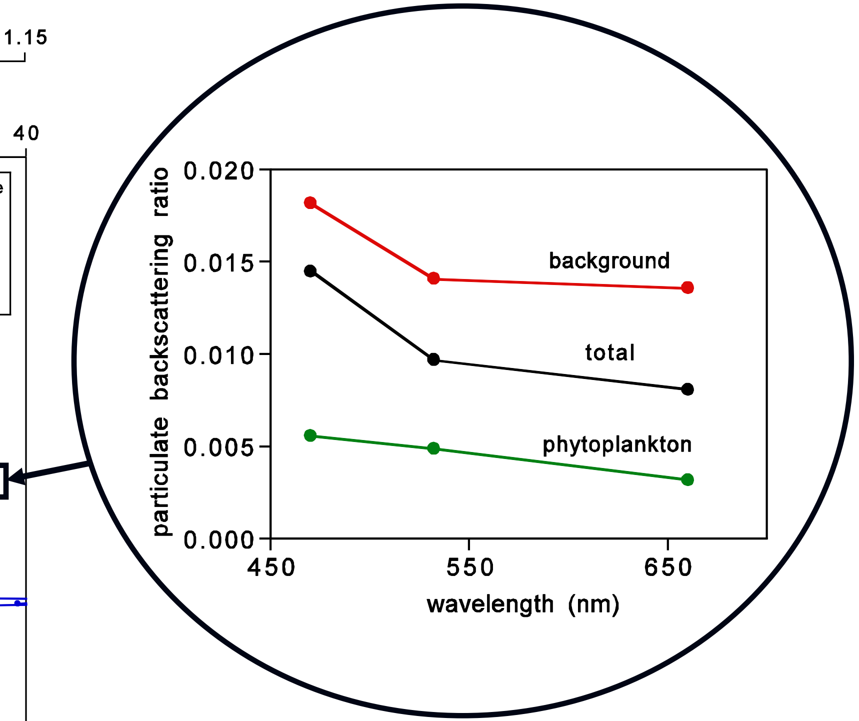

Akashiwo et al.

$b_{bp}(532) / b_p(532) \approx \underline{0.005}$

~<u>20%</u> of $b_{bp}(532)$

Sullivan and Donaghay (unpubl)

Phytoplankton b_b/b

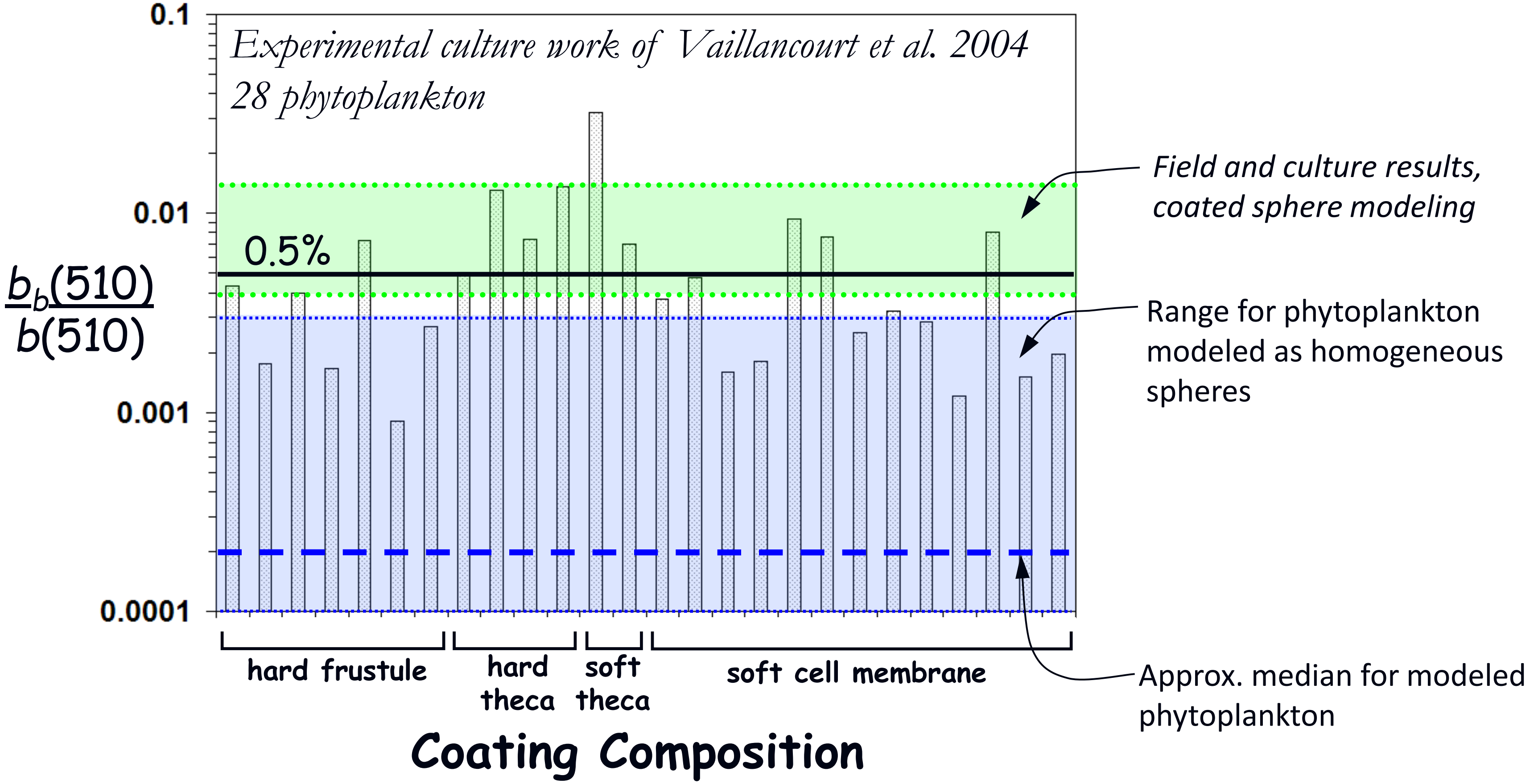

Phytoplankton likely do make a significant direct contribution to b_{bp}

Component decomposition of linear Polarization

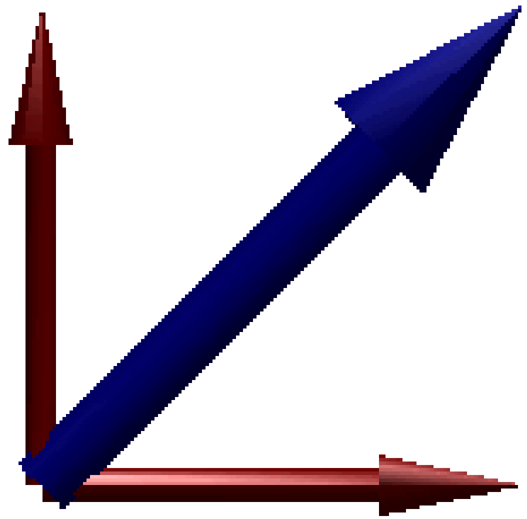

Component decomposition of circular Polarization

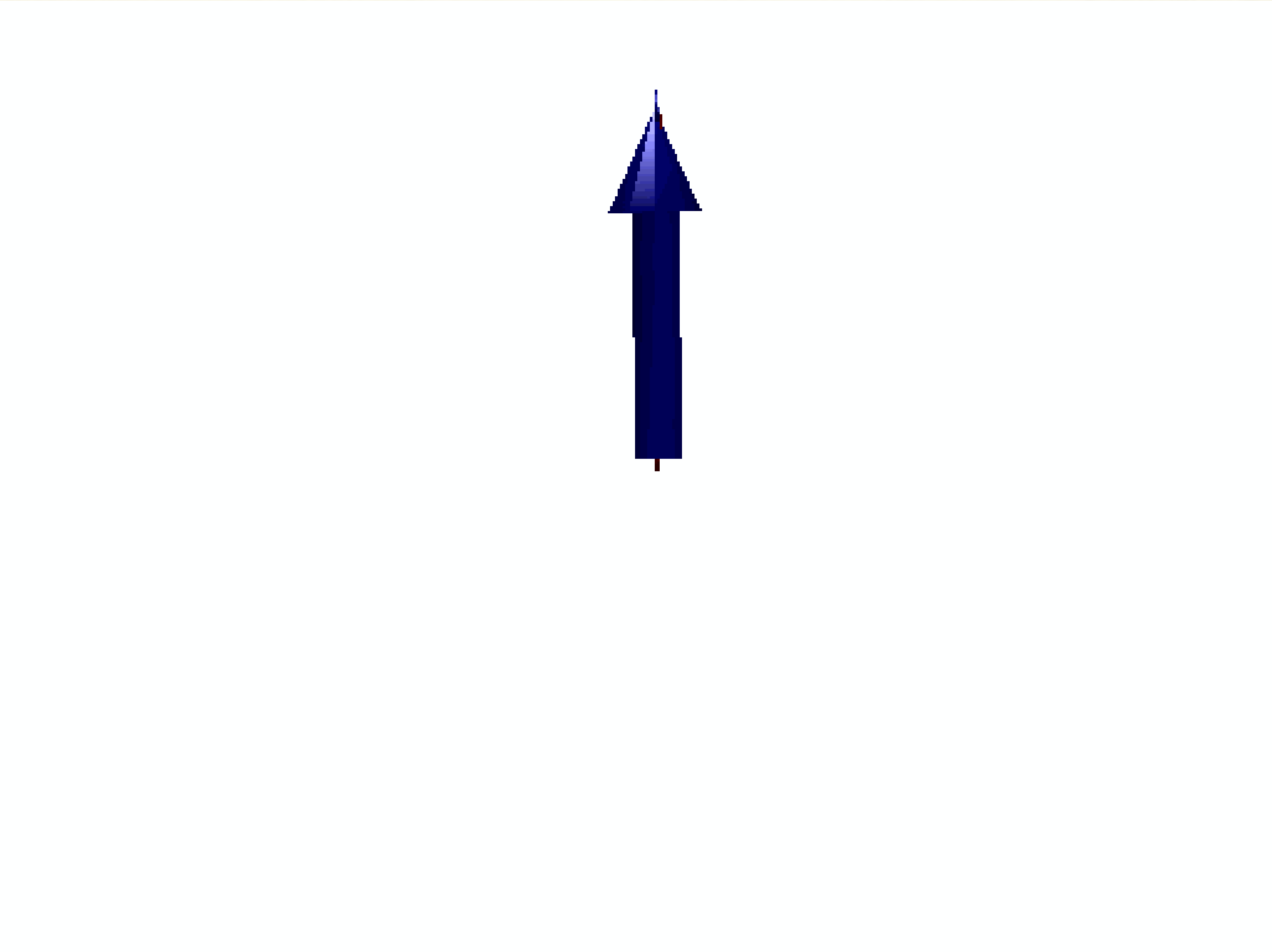

Accuracy

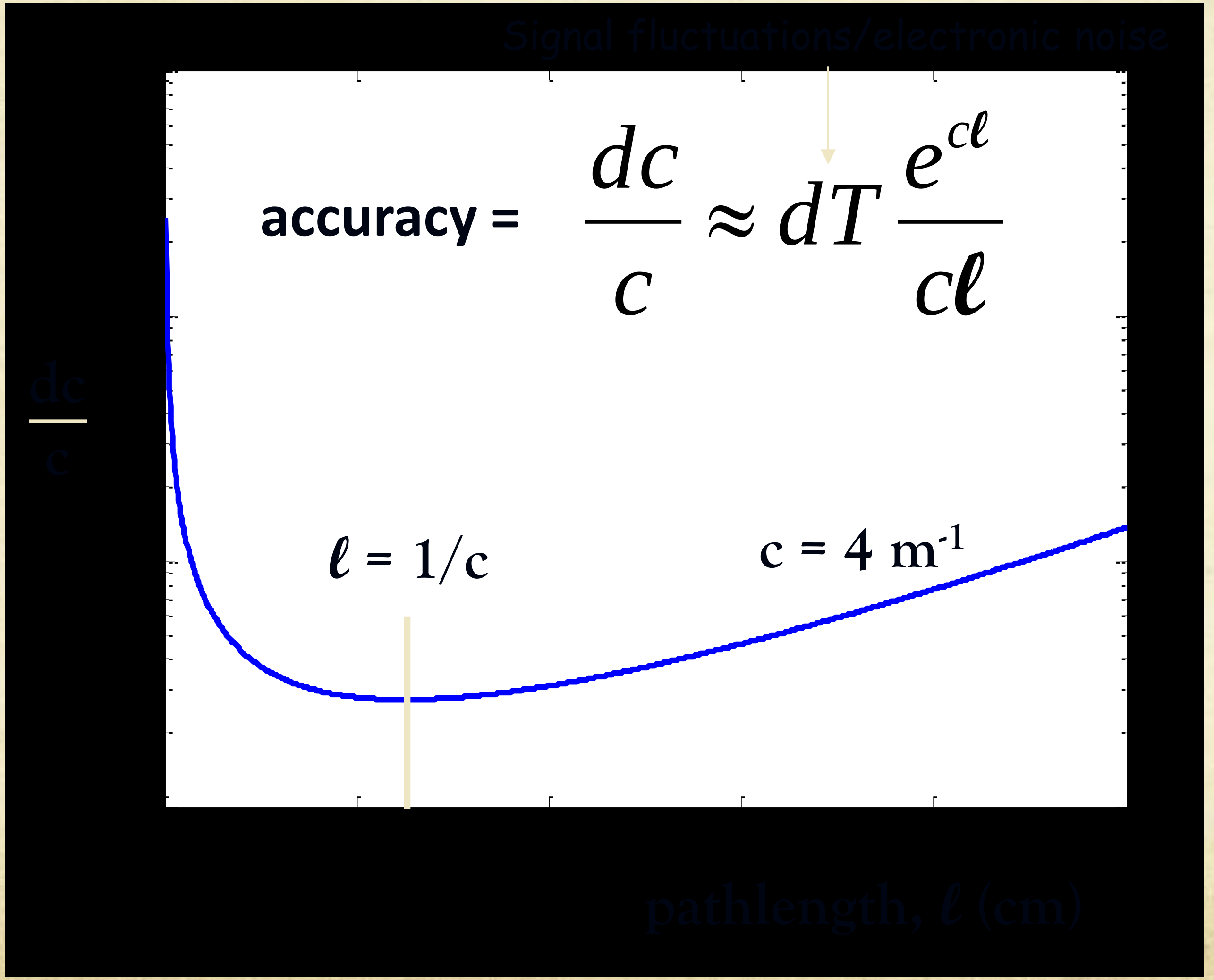

Accuracy is optimized when dc/c is minimized

Minimum occurs when $c\ell \approx 1$

Choose pathlength accordingly…

What is refractive index?

The refractive index n (or index of refraction) of a medium is a measure of how much the velocity of a wave is reduced inside that medium.

$$n = \frac{c}{v_P} = \frac{\lambda_{vacuum}}{\lambda_{medium}}$$

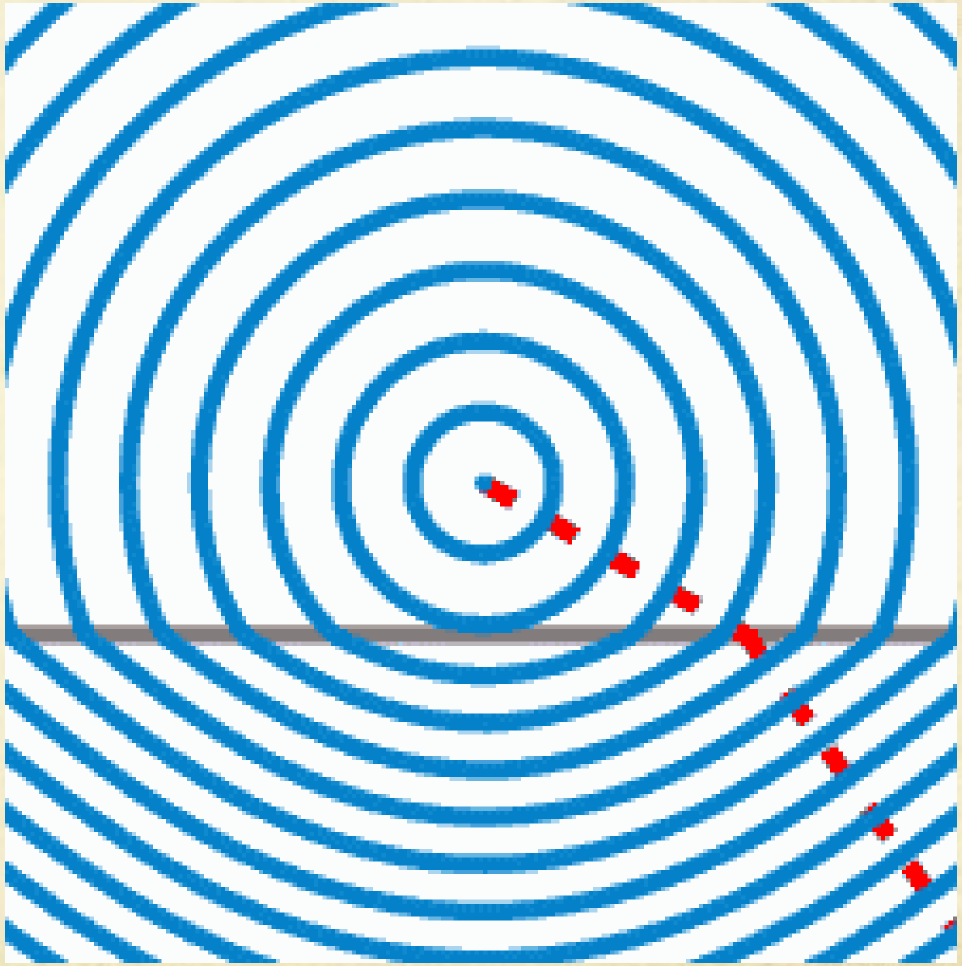

Wavefronts from a point source in the context of Snell's law. The region below the gray line has a higher index of refraction and proportionally lower wave velocity than the region above it.

Birefringent materials like CaCO3 have different *n* for different polarization elements and light directions….

Snell's Law

$$n_1 \sin\theta_1 = n_2 \sin\theta_2$$

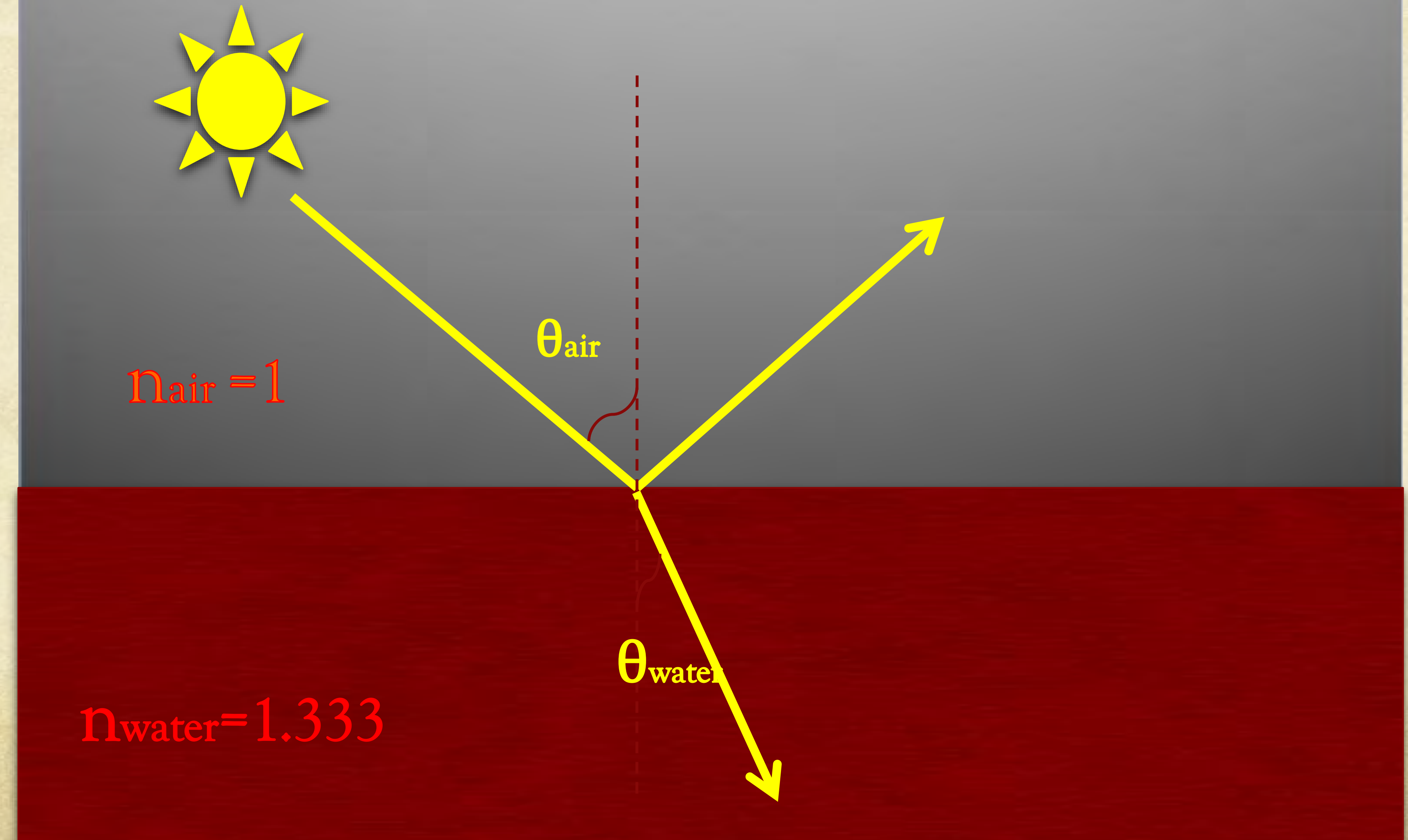

Snell's Window

Polarized scattering: effects of bubbles

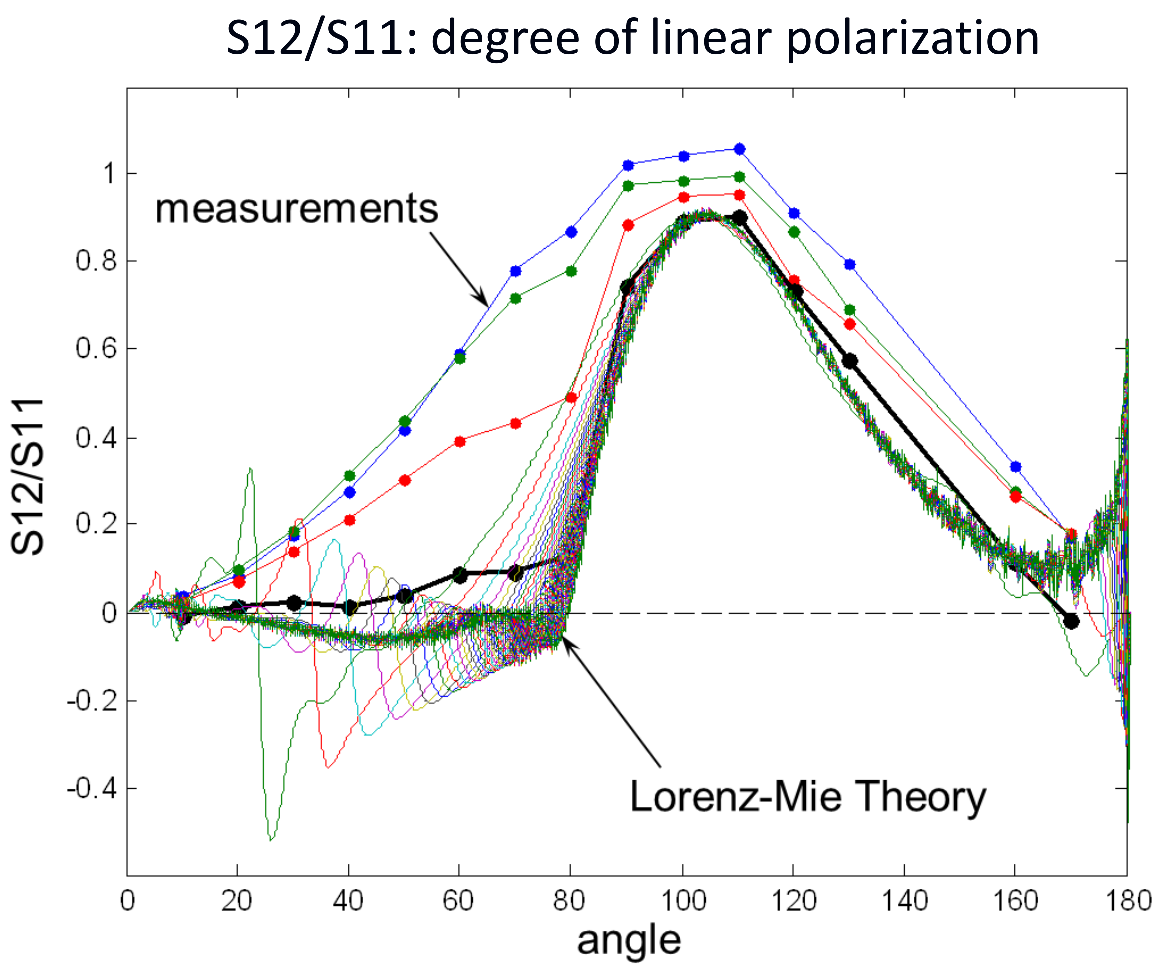

Twardowski et al. (unpubl)